The effects of medicinal cannabis on the sensitivity of glioblastoma cell lines to chemotherapy

Research Thesis

In Partial Fulfilment of the Requirements for the Degree of

Master of Biotechnology

CHINONSO KENNETH IBEAGWA

Submitted to the College of Medicine and Public Health

Flinders University, South Australia

November 3rd, 2025

Table of Contents

Abstract

Glioblastoma is the most lethal primary brain tumour in adults and remains a major challenge in neuro-oncology. Despite multimodal treatment involving maximal surgical resection, radiotherapy and temozolomide (TMZ) chemotherapy, GBM clinical outcomes remain poor due to extensive tumour heterogeneity, rapid proliferation, high invasiveness and acquired drug resistance. Therefore, there is a critical need to identify novel therapeutic agents capable of enhancing chemotherapy response and overcoming drug resistance mechanisms. Emerging evidence suggests that cannabinoids, including cannabidiol (CBD), cannabigerol (CBG), and Δ^9-tetrahydrocannabinol (THC), may reduce tumour cell viability and enhance sensitivity to chemotherapeutic agents through endocannabinoidome-mediated signalling.

This study investigated the cytotoxic and chemosensitizing potential of seven purified cannabinoids and phytocannabinoid extracts obtained from ten cannabis strains in three established human GBM cell lines (U87, U251 and TMZ-resistant T98G). Phytochemical profiling using HPLC-MS/MS confirmed that the cannabis extracts differed significantly in their cannabinoid composition. Cell viability assays (Hoechst staining) revealed that both purified cannabinoids and extracts induced cytotoxicity in all three cell lines, with T98G showing notable sensitivity despite its TMZ-resistant phenotype. Among the purified cannabinoids tested, CBD and CBG demonstrated the greatest potency based on CC_{50} values, while the *Poddy Mouth* and *The Wife* extracts showed the strongest cytotoxic effects among the cannabis extract treatments. Annexin-V/PI flow cytometry assay was further used to confirm that cannabinoid-induced cell death occurred primarily through apoptosis.

Differential responses between cell lines prompted analysis of key endocannabinoid-associated genes via RT-qPCR. All three cell lines exhibited low to undetectable *CNR2* (CB2 receptor) expression, while *CNR1* (CB1 receptor) was undetectable in T98G, potentially contributing to its altered drug sensitivity profile. Combination assays of the cannabinoids and extracts with TMZ demonstrated an increase in cytotoxicity across all cell lines, with the most pronounced enhancements observed in TMZ-resistant T98G cells, suggesting an additive chemosensitisation effect.

In conclusion, this study provides evidence that the purified cannabinoids and the phytocannabinoid-rich extracts exert anti-GBM activity and may enhance the cytotoxic effects of

TMZ, including in TMZ-resistant models. Future research should focus on elucidating the precise mechanism of action of these cannabinoids down to the receptor level and also include pre-clinical models that take into consideration the complexity of the tumour microenvironment.

Signed Declaration

This research was conducted under the supervision of **Prof. Simon Conn and Dr. Ganessan Kichenadasse** at the College of Medicine and Public Health, Flinders University.

I hereby declare that the work presented in this thesis is my own and is the result of the original research carried out by me. The collection, processing, and presentation of data, as well as the analysis, comparison with previous data, and interpretation of findings, were all performed honestly and in accordance with the ethical and academic standards expected of scientific research.

Furthermore, I certify that this thesis does not incorporate without acknowledgment any material previously submitted for a degree or diploma in any university and the research within will not be submitted for any other future degree or diploma without the permission of Flinders University; and to the best of my knowledge and belief, does not contain any material previously published or written by another person except where due reference is made in the text.

Name: …CHINONSO IBEAGWA……

Signature: ……

Date: …3/11/2025……

Acknowledgements

I want to express my deepest gratitude to my supervisors, **Professor Simon Conn and Dr. Ganessan Kichenadasse**, for their invaluable guidance, mentorship, and continuous support throughout the course of this research. Their expertise and encouragement have been instrumental in shaping this work and my growth as a student.

I am sincerely thankful to **Dr. Gustavo Bracho Granado** at Cell Screen SA, where most of the high-throughput cell screening was carried out, for his guidance, time, patience, and technical expertise, which were vital to the success of this work.

I would also like to acknowledge the Omics Laboratory at the Health and Medical Research building for performing the quantification and mass spectrometry analysis of cannabinoids in the extracts.

Special thanks to **Dr. Vanessa Conn** for providing and validating all the primers used for the real-time PCR experiments, as well as supplying the RNA sequencing data for the cell lines investigated in this thesis.

I would also like to acknowledge the members of the Circular RNA in Cancer Laboratory – **Stephen Johnson, Will Plewa, Helen Lin, and Ryan Liu** – for their contributions, advice, and constant support. Their suggestions during the lab meetings and willingness to assist whenever I had challenges were greatly appreciated.

I would like to thank Dirk Beelen and Allanna Lean (MedTec Pharma) for providing all of the cannabis flowers for this work. I would also like to thank Matthew Soliman (Cann Compounding Pharmacy) for providing all of the purified cannabinoids for this project.

Finally, I wish to thank everyone who, in one way or another, contributed to the success of this research, but whose names may not have been mentioned here. Your help and encouragement are deeply appreciated.

Above all, I am profoundly grateful to God, to my family, and loved ones for their unwavering love, patience, and belief in me. Your support has been my greatest source of strength and motivation throughout this journey. This achievement is as much yours as it is mine.

List of Abbreviations

2-AG -2-Arachidonoylglycerol

AEA- Anandamide

AMS- Amsterdam Amnesia

BBB- Blood-brain barrier

BSA- Bovine serum albumin

CB1- Cannabinoid receptor 1

CB2- Cannabinoid receptor 2

CBD- Cannabidiol

CBDA- Cannabidiolic acid

CBDV- Cannabidivarin

CBG- Cannabigerol

CBGA- Cannabigerolic acid

CBN- Cannabinol

CNR1- Cannabinoid receptor 1 gene

CT- Cycle threshold

DAPI- 4',6'-diamidino-2-phenylindole

DAGLA/B- Diacylglycerol lipase alpha/beta

DMEM- Dulbecco's Modified Eagle Medium

DMTS- DNA methyltransferases

DMSO- Dimethyl sulfoxide

ECS- Endocannabinoid system

EDTA- Ethylenediamine tetraacetic acid

EGFR- Epidermal growth factor receptor

FAAH- Fatty acid amide hydrolase

FBS- Fetal Bovine Serum

FGS- Fluorescence guided signal

GBM- Glioblastoma

GPCR- G protein-coupled receptor

GSCs- Glioma stem cells

HPLC- High-performance liquid chromatography

HPLC-MS/MS- High-performance liquid chromatography tandem mass spectrometry

IDH- Isocitrate dehydrogenase

MAGL- Monoacylglycerol Lipase

MAPK- Mitogen-activated protein kinase

MIM- Mimosa x Orange punch

MNG- Meringue

MGMT- O-6-methylguanine-DNA

MMPs- Metalloproteinases

MS- Mass spectrometry

MTT- 3- (4,5-dimethylthiazol-2-yl)-2,5-diphenyltetrazolium bromide

NAPEPLD- N-Acylphosphatidylethanolamine-specific phospholipase D

NAT- N-actyltransferases

NF-kB- Nuclear Factor kB

PBS- Phosphate Buffer Saline

PCR- Polymerase Chain Reaction

PFA- Paraformaldehyde

PI- Propidium Iodide

P13K – Phosphoinositide 3-Kinase

PPARs- Peroxisome proliferator-activated receptors

PPI- Protease Phosphatase Inhibitor

PTEN- Phosphatase and Tensin homolog

qPCR- Real-time PCR

RNAseq- RNA sequence analysis

RCK- Royal Cookies

STB- Strawberry cookies

TBP- TATA box binding protein

TERT- Telomerase reverse transcriptase gene

THC- Delta 9 tetrahydrocannabinol

TTF- Tumour treating field

THCA- Delta 9 tetrahydrocannabinol Acid

TMZ- Temozolomide

TRPV- Transient Receptor Potential cation channel, subfamily V

UV- Ultraviolet

VC- Vehicle control

VEGF- Vascular endothelial growth factor

WAM- Watermelon cookies

Introduction

Glioblastoma Brain Tumour

Glioblastoma (GBM) is the most aggressive primary brain tumour in adults and presents a major challenge in neuro-oncology (Arthurs et al., 2020; Dasram et al., 2024; Louis et al., 2021). It is classified as a grade IV astrocytoma and is also the most commonly diagnosed malignant brain tumour in adults (Dasram et al., 2024; Louis et al., 2021). The incidence in adults ranges from about 0.60 to 3.70 per 100,000 person-years and accounts for roughly 15% of all brain tumours (Dumitru et al., 2018). Despite aggressive therapy protocols, the prognosis for GBM patients remains poor, with a median survival of 14 to 15 months after diagnosis. In the long term, less than 5% of patients typically survive more than five years after their first diagnosis, and this has not improved over the past 30 years (Grochans et al., 2022). Without treatment, GBM can rapidly lead to death, typically within 5 to 6 months. The minimal improvement in prognosis over the past three decades underscores the urgent need for better therapies and interventions.

Biology and Pathophysiology of GBM

GBM can occur in two forms: either as a *de novo* primary tumour that arises in glial cells or as a secondary GBM that develops from low-grade gliomas (Jovčevska et al., 2013). Primary GBM is more common in men, and the median age at presentation is 62 years, whereas secondary GBM occurs more often in females and young adults, with the median age at presentation being 45 years (Dumitru et al., 2018; Tamimi & Juweid, 2017). The 2016 WHO classification further divides GBM based on the presence or absence of isocitrate dehydrogenase (IDH) gene mutation into IDH-wildtype and IDH-mutant GBM, showing distinct clinicopathological features (**Table 1**), including poorer survival for IDH-wildtype GBM (Louis et al., 2021; Zhang et al., 2020). At the cellular level, GBM usually starts with normal glial cells, which pass through a multi-step and very complex oncogenic process (Walker et al., 2024). This difference in origin and patient

demographics aligns with primary and secondary GBMs being entirely different biological conditions, each caused by various underlying molecular alterations (Perus & Walsh, 2019).

TABLE 1. *The 2016 WHO classification of the tumours of the central nervous system, based on the presence and absence of the IDH mutation, and other mutations. This image was adapted from (Louis et al., 2016)*

Figure removed due to copyright restriction.

The malignant nature of GBM is characterized by rapid growth with extensive cell proliferation and division, as well as the formation of new blood vessels, leading to tumour angiogenesis, which counter-intuitively results in cell death (necrosis) within the tumour (Grech et al., 2020; Scherma et al., 2020). GBM cells have the ability to migrate and invade the surrounding normal brain tissue (metastasis), forming secondary tumours, known as metachronous lesions (Dumitru et al., 2018; Seker-Polat et al., 2022). The invasiveness of GBM is promoted by the activity of matrix

metalloproteinases (MMPs), which break down the extracellular matrix to help tumour spread (Walker et al., 2024). Furthermore, even within GBM tumours, there are small but clinically important subpopulations of glioma stem cells (GSCs) that are considered critical in making the tumour highly resistant to treatment and contributing to its recurrence after therapy (Auffinger et al., 2015; Eckerdt & Platanias, 2023). It is this combination of aggressive growth, invasiveness, and the presence of resistant GSCs that creates an insurmountable barrier to achieving complete and long-term tumour control.

GBM development involves a multifactorial interplay of genetic and epigenetic changes. Dysregulation of the G1/S cell cycle phase and numerous genetic abnormalities in glioma cells are characteristic of GBM (Torrisi et al., 2022; Walker et al., 2024). Genetic diversity is inter-tumoural and intra-tumoural and reflects the pathognomonic characteristic of the disease (Shergalis et al., 2018). IDH1 and IDH2 gene mutations, which regulate cell metabolism, are most common in secondary GBM and may influence epigenetic modifier enzymes such as histone methyltransferases (HMTs), DNA methyltransferases (DNMTs), and histone deacetylases (HDACs) (Zhang et al., 2020). Epigenetic reprogramming, such as histone modification, chromatin organization, and DNA methylation, is common in gliomas and becomes a characteristic of the tumour microenvironment with long-term effects (Shahani et al., 2025). GBM's intricate epigenetic and genetic profile, with its various subtypes and unique mutations affecting treatment, highlights the need for personalized treatment approaches. The role of epigenetic modifications in treatment resistance further emphasizes epigenetics' potential for future therapies. (Zhu et al., 2023).

Glioblastoma Signalling Pathways

Many GBMs exhibit mutations in key signalling pathways involving cell surface receptors known as receptor tyrosine kinases (RTKs) such as Epidermal growth factor receptor (EGFR), Vascular endothelial growth factor receptor (VEGFR), Platelet-derived growth factor receptor (PDGFR), Fibroblast growth factor (FGFR), and Insulin-like growth factor 1 receptor (IGF-1R) (Cordover & Minden, 2020). When these RTKs are activated by signalling molecules, they usually activate two major pathways inside the cell: Ras-Raf-MEK-ERK and PTEN/PI3K/AKT/mTOR (Hoxhaj & Manning, 2020; Terai & Matsuda, 2005). A common issue in glioblastoma is an excess of EGFR, which can cause the 'grow and divide' ERK pathway to remain constantly active, even after

treatment. This ERK pathway is significant in glioblastoma because it helps the tumour cells move, multiply, and survive (Terai & Matsuda, 2005). Overactivity of this pathway is linked to EGFR, which is responsible for recruiting downstream signalling proteins that help it facilitate tumour growth and survival. About 20% of glioblastoma mutations cause this pathway to be overactive, and most cases have issues in at least one of these two main pathways. Another common problem is the loss of function mutation of the PTEN protein, which normally regulates the 'survive and grow big' PI3K pathway; this ultimately results in this pathway being constantly active (Du et al., 2024). These pathways also support glioblastoma stem cells in maintaining their cancerous traits. Other factors that contribute to glioblastoma include mutations in the P53 gene (which regulates cell growth and division) and overactivity of the JAK/STAT pathway, which can transform normal cells into cancer cells (Liu, 2001; Purohit et al., 2023). The NF-kB protein also aids glioblastoma growth and chemotherapy resistance by being continually activated by factors such as increased EGFR or PI3K activity and/or loss of PTEN protein (Luo, 2005; Soubannier & Stifani, 2017). NF-kB promotes genes that help glioblastoma stem cells renew themselves and genes that help the tumour spread and resist treatment by enhancing DNA repair.

Standards of care for GBM

The overall aim of GBM treatment is to extend the patient's survival and preserve quality. of life as long as possible. The current standard of care usually involves a multimodal approach including surgical removal, radiation therapy, and chemotherapy (**Figure 1**) (Nabian et al., 2024; Stupp et al., 2005). The aim of surgical resection/debulking is to remove as much tumour as possible without causing significant neurological deficits. Gross total resection (GTR), or removal of the visible tumour, is the preferred approach and has been shown to improve patient outcomes (Nabian et al., 2024). Surgery may also reduce intracranial pressure and remove tumour cells that are either resistant to or develop resistance against radiation and chemotherapy. Complete surgical resection is, however, not possible due to the infiltrative nature of GBM, as tumour cells tend to project microscopically into surrounding brain tissue (Shergalis et al., 2018). In most cases, surgery is also the initial procedure used to establish the diagnosis through tissue biopsy. Adjuvant fluorescence-guided surgery (FGS) with 5-aminolevulinic acid (5-ALA) has been described to improve progression-free survival by enhancing visualization and tumour tissue removal (Rodgers et al.,

2024). While surgery is still an important first step, its inherent limitation due to GBM's invasive nature necessitates the need for adjuvant therapy to control the residual tumour cells. Adjuvant radiation therapy is typically indicated after surgery to target and eliminate any remaining cancer cells in the tumour bed (Nabian et al., 2024). Conventional external beam radiation treatment consists of administering a number of sessions, or fractions of radiation, to the tumour bed and a margin around it over a period of weeks; this treatment attempts to damage the DNA of any remaining tumour cells so that they cannot grow and divide.

Figure removed due to copyright restriction.

Figure 1. *The Stupp protocol, which is considered the standard treatment option for GBM. It involves a combination of radiotherapy and adjuvant Temozolomide given together after maximal surgical resection (Stupp et al., 2005). This image was obtained from (Batistella et al., 2021)*

Chemotherapy with the agent Temozolomide (TMZ) is one of the key components of the current standard treatment for GBM (Strobel et al., 2019). The Stupp protocol, initiated in 2005, involves TMZ administered alongside radiation therapy, followed by several cycles of adjuvant TMZ. (Dumitru et al., 2018; Stupp et al., 2005). TMZ is an oral alkylating agent that crosses the blood-brain barrier and is therefore of value for brain tumours. The methylation status of the MGMT gene promoter in tumour cells is an important biomarker used to predict a patient's response to TMZ. Patients with a methylated MGMT gene promoter tend to have a better response. (Rodgers

et al., 2024). Despite the significant improvement in survival provided by the Stupp regimen, recurrence rates for GBM remain high. Recent evidence and research indicate that adding other agents, such as the multi-kinase inhibitor anlotinib, to the Stupp regimen can enhance survival effectiveness (Lai et al., 2024). Alternative TMZ dosing regimens, such as dose-dense extended TMZ, have also been explored for potential advantage (Weller et al., 2013). The Stupp protocol has been a significant advance in GBM therapy, but the low long-term success indicates that combination regimens and the creation of treatments for breaking through treatment resistance need to be explored. The prognostic value of the MGMT status highlights the growing role of biomarkers in the individualization of chemotherapy regimens for GBM patients. The treatment of recurrent GBM, which is, for the most part, unavoidable in most patients, has been the focal therapeutic challenge. The treatment of recurrent GBM is less well defined and depends on many variables, including the patient's initial treatment protocol, the size and location of the recurrent tumour, and the patient's overall clinical status. In a limited number of carefully selected patients, reoperation or reirradiation is a possibility (Weller et al., 2013). Enrolment in clinical trials to evaluate novel therapies can be a possibility for patients with recurrent GBM in order to offer them cutting-edge therapy. Tumour treating field (TTF) therapy can also be a possibility in recurrent GBM patients. It is an interferential electrical field of intermediate frequency and low intensity utilised in inhibiting the growth and cell division of cancer (Kotecha et al., 2023). Limited effectiveness of standard therapies for recurrent GBM highlights the need for developing innovative and new therapeutic alternatives.

Challenges in the Treatment of Glioblastoma

Although knowledge and understanding of GBM have advanced, a number of important hurdles preclude the provision of curative treatments (**Figure 2**). One of the most significant obstacles to GBM treatment is the blood-brain barrier (BBB), which is a junctional permeability barrier that protects the brain against harmful compounds in the blood. It is made up of tightly attached endothelial cells lining the capillaries in the brain and preventing most molecules, including most drugs, from crossing into brain tumour tissue from the bloodstream. Additionally, the BBB secretes efflux transporters such as P-glycoprotein that actively pump foreign chemicals, such as most chemotherapeutic drugs, out of the brain and lower their levels at the tumour. Even though the BBB is usually disrupted in the tumour mass core, where it is permeable, it will probably

remain intact in the tumour margin, where the actively proliferating and invading carcinoma cells are (Shergalis et al., 2018). Interestingly, in some cases, the compromised BBB in the tumour, or so-called blood-tumour barrier (BTB), ironically acts against therapy by enabling the passage of pro-tumoural molecules and preventing the passage of anti-tumoural molecules (Liguori, 2024). BBB is a major hindrance to GBM therapy and significantly decreases the effectiveness of the vast majority of systemically administered drugs. Drawing up tactics on how to overcome or bypass this challenge is therefore crucial in furthering drug delivery to the tumour.

Figure removed due to copyright restriction.

FIGURE 2. *A schematic diagram highlighting the challenges hindering successful GBM treatment, hence the need for novel treatment alternatives. This image was obtained from (Kan et al., 2020)*

As mentioned previously, glioblastoma shows significant intratumoural and intertumoural heterogeneity, with cancer cells within one tumour and across tumours of different patients harbouring a wide set of genetic and molecular differences (Gularyan et al., 2020). This accounts for the differences in susceptibility to therapy among different groups of cells within the same tumour. Because of this, some cells can be effectively killed by a particular therapy, but others will remain, and this can lead to the formation of resistant clones and later tumour relapse, making it extremely difficult to eliminate all the tumour cells with one drug (Kan et al., 2020; Shergalis et al., 2018). Even the presence of molecular subtypes of GBM, each with its own distinct set of genetic mutations and expression profiles, further increases the treatment response gaps.

Additionally, recurrent tumours will also gain new mutations and even switch molecular subtypes due to the selective pressure of the initial treatments (Rodgers et al., 2024). The genetic and cellular heterogeneity in GBM tumours is a main obstacle to effective treatment since treatments designed for the intervention of a particular pathway or mutation will be effective in only a restricted subset of tumour cells. Personalized medicine approaches, in which treatment is tailored to the special molecular characteristics of the tumour in one patient, can help alleviate this intrinsic heterogeneity. The infiltrative nature of GBM is one of the largest problems in its management because the tumour cells infiltrate and protrude into the surrounding healthy brain tissue.

This pattern of aggressive migration allows tumour cells to escape complete surgical resection, as it is impossible to excise all of the tumour cells without risking disastrous neurological damage by resecting overlying normal tissue (Shergalis et al., 2018). Therefore, tumour recurrence is essentially inevitable and typically occurs within a few centimetres of the original site. Further, subsequent to maximum surgical removal of the bulk tumour, residual glioma stem cells (GSCs) remaining behind in the resection cavity have the ability to migrate and result in the regrowth of the entire tumour (Liguori, 2024; Lu et al., 2025). The infiltrative pattern of growth of GBM is the main reason why surgical resection alone is non-curative. Even following the most complete surgical resection (maximal surgical resection), residual microscopic disease still exists and gives rise to the high incidences of tumour recurrence. Glioblastoma tumours contain a subpopulation of cancer stem cells (CSCs), or glioma stem cells, which are responsible for the resistance of the tumour to the treatment and its recurrence; these cells can self-renew and differentiate into numerous cell types in the tumour, resulting in the tumour's varied genetic compositions (Ng et al., 2024).

Compared to the majority of tumour cells, GSCs would possess changed regulatory and metabolic processes that result in them being more resistant to conventional treatments such as radiotherapy and chemotherapy (Liguori, 2024). GSCs also possess low sensitivities towards chemotherapy and radiotherapy, and this may be further increased through several repeated treatments. The existence of GSCs, which are resistant by nature and capable of inducing tumour recurrence, is a particularly difficult feature of GBM treatment (Lu et al., 2025). Their targeting and elimination are regarded as a key aim towards creating more efficient long-term treatments for this disease. Finally, unlike with other organs within the human brain, the limited self-repair mechanism of the brain and

potential neurotoxicity of the chemo itself are also areas of concern when managing GBM. Not only can the tumour itself kill nearby healthy brain tissue, but interventions used for treatment, such as surgery and radiotherapy, have the potential to destroy the healthy brain tissue (Debela et al., 2021).

Moreover, certain therapeutic agents and anticancer drugs are also neurotoxic and affect neurological function further, worsening the quality of life of the patient (Was et al., 2022). Considering the delicate nature of brain tissue and its limited regenerative capacity, GBM therapies and their effects on neurological function and overall quality of life need to be weighed carefully. Treatment has to be optimized to kill as many tumour cells as possible while sparing the surrounding brain tissue as much as possible so that neurological function can be maintained.

Phytocannabinoids and The Endocannabinoid System

There is an ongoing and intensive search for novel therapeutic strategies in light of the significant challenges associated with current GBM treatments. One area of increasing interest is the potential role of cannabinoids in GBM treatment.

Cannabinoids are a diverse group of active chemical compounds found in the Cannabis plant (phytocannabinoids), produced naturally by the body (endocannabinoids), or synthesized in the laboratory (**Figure 3**) (Walker et al., 2024). The endocannabinoid system (ECS) is a complex neuro-modulatory network that plays an important role in regulating a wide range of physiological processes in the body. It is made up of endocannabinoids, such as anandamide (AEA) and 2-arachidonoylglycerol (2-AG), their specific receptors, mainly the cannabinoid receptors type 1 (CB1) and type 2 (CB2), which are G-protein coupled receptors (GPCRs). The enzymes responsible for the synthesis of 2-AG are specifically Diacylglycerol lipase-alpha (DAGLA) and Diacylglycerol lipase-beta (DAGLB), while N-Acetyl transferase (NAT) is responsible for synthesizing AEA (Reisenberg et al., 2012).

The ECS also comprises the enzymes responsible for the degradation of AEA and 2-AG, which are fatty acid amide hydrolase (FAAH) and monoacylglycerol lipase (MAGL), respectively. The CB1 receptors are primarily found on neurons in the nervous system, where they help regulate

neurotransmitter release, while CB2 receptors are mainly located in cells of the immune system but have also been observed in some brain cells, including microglial cells, astrocytes, and glioma cells (Tang et al., 2024). The endocannabinoid system (ECS) is now understood to encompass a broader range of receptors and ion channels, not just the classical cannabinoid receptors (CB1 and CB2), which are G-protein coupled receptors (GPCRs). This expanded view includes members of the transient receptor potential cation channel subfamily V (TRPVs), the peroxisome proliferator-activated receptors (PPARs), and several other GPCRs, such as GPR3, GPR6, and GPR55 (Alves et al., 2020; Dasram et al., 2024).

Figure removed due to copyright restriction.

Figure 3. *The provided figure classifies cannabinoids into three groups based on their source: those made by the body (endocannabinoids like anandamide and 2-AG, involved in processes like pain and mood regulation), those from cannabis plants (phytocannabinoids such as Δ9-THC and CBD, used as treatments for brain-related conditions), and those created in a lab (synthetic cannabinoids like JWH-018 and JWH-073, used in research and for pain management). The illustration depicts how these different types of cannabinoids engage with the body's endocannabinoid system receptors and their roles in medicine and therapy. This image was obtained from (Faiz et al., 2024).*

Understanding the ECS and its different components is of fundamental interest to understanding how cannabinoids might exert therapeutic effects in the context of GBM. The presence of cannabinoid receptors on glioma cells and within the tumour microenvironment suggests a potential direct target for cannabinoid-based therapies. The ECS plays important roles concerning the regulation of cell growth, differentiation, and survival, all of which malfunction in cancer. Therefore, if this system is targeted with cannabinoids, it could potentially help in treatment or have anti-tumour effects.

Cannabinoid signalling in cancer and Glioblastoma

In addition to their antipsychotic, antidepressant, anxiolytic, and precognitive effects (Scherma et al., 2020). Cannabinoids also possess significant anti-cancer activity on glioma cell lines and GBM preclinical models. The cannabinoids demonstrate validated antiangiogenic activity by inhibiting angiogenesis and antimetastatic activity, with the potential to halt the growth of tumour dissemination (Dasram et al., 2024).

Cannabinoids have been found to possess antiproliferative activity, with the potential to inhibit tumour growth by suppressing tumour cell proliferation and inducing tumour cell apoptosis (Dumitru et al., 2018). Preclinical studies also indicate that cannabinoids can reduce the aggressiveness of GBM cells, thereby limiting their invasion into surrounding brain tissue and targeting the stem cell-like activity of GBM tumours (Dumitru et al., 2018; Torres et al., 2011). This substantial body of preclinical data strongly highlights the therapeutic potential of cannabinoids as anti-GBM agents through multiple mechanisms, providing compelling reasons to explore their use in future cancer therapy. Various mechanisms are involved in how cannabinoids exert their effects on GBM cells **(Figure 4**). They are reported to induce apoptosis, or programmed cell death, via the p8 protein and ceramide pathways (Carracedo et al., 2006). However, these processes are not specific to GBM and are shared by other types of cancer cells as well (Massi et al., 2010; Michalski et al., 2008). Additionally, cannabinoids influence the tumour microenvironment and immune response, helping to balance the tumour-host immune system (Faiz et al., 2024; Kyriakou et al., 2021). Furthermore, CB1 and CB2 cannabinoid receptors suppress the PI3K/Akt/mTOR pathway through activation by cannabinoids, a common pathway that promotes cell survival and growth. This suppression subsequently inhibits cell growth, apoptosis, and autophagy—a form of cell death (Dasram et al., 2024; Held-Feindt et al., 2006). The inhibition

occurs via modulation of the PI3K/Akt/mTOR pathway, and notably, tetrahydrocannabinol (THC) can trigger apoptosis in GBM cells by stimulating CB1 and CB2 receptors, which stimulates pro-apoptotic ceramide sphingolipid biosynthesis. Additionally, THC may modulate sphingolipid metabolism by increasing intracellular ceramide levels (McAllister et al., 2021).

Figure removed due to copyright restriction.

Figure 4. *The diagram outlines the molecular mechanisms through which cannabinoid receptors (CB1R, CB2R) and transient receptor potential (TRP) channels (TRPV1, TRPV2, TRPM8) mediate the effects of cannabinoids in cancer cells. When cannabinoids like THC and CBD bind to CB1R and CB2R, they can modulate the ERK1/2 pathway, leading to cell cycle arrest by inhibiting pRb phosphorylation or activating the PI3K/AKT pathway, influencing proliferation and autophagy, but potentially causing ER stress and apoptosis with prolonged activation. In contrast, CBG interaction with TRPV1, TRPV2, and TRPM8 triggers the production of reactive oxygen species (ROS), which in turn promote apoptosis in cancer cells. The illustration highlights the diverse ways in which different cannabinoids can impact cancer cell fate through specific receptor interactions and downstream signalling cascades. This image was obtained from (Faiz et al., 2024)*

In addition, their cytotoxic effects directly, cannabinoids have also been shown to inhibit tumour angiogenesis, the process by which tumours cause the formation of new blood vessels to feed their growth. They have also been shown to inhibit GBM tumour invasiveness, reducing their ability to invade into the surrounding brain tissue (Dumitru et al., 2018). For example, THC has been shown to downregulate MMP-2 expression, an enzyme employed in the breakdown of the extracellular matrix when cancer is invading the tissue, by which they can reduce glioma cells' invasiveness (Nahler, 2023). These findings show that, besides directly killing cancer cells, cannabinoids can also, to some extent, suppress tumour development by cutting off its supply of blood and decreasing its ability to metastasize, further proving their efficacy as drugs used to treat GBM.

One of the most promising avenues of cannabinoid research in GBM is their ability to target glioma stem cells (GSCs). Some indication has been seen from some preclinical models that cannabinoids can suppress the stem cell-like behaviour of GBM tumours (Dumitru et al., 2018; Torres et al., 2011). As there is a strong belief that GSCs are a major underlying cause of resistance to treatment and tumour recurrence in GBM, the ability of cannabinoids to target these cells is clinically relevant. Eliminating GSCs can be considered important for the achievement of long-term disease suppression, and whether cannabinoids can do this is interesting. Different cannabinoids have been studied for potential therapeutic use in GBM to date. Δ9-Tetrahydrocannabinol (THC) is the psychoactive component of cannabis and has been reported in glioma animal models to inhibit tumour development (Velasco et al., 2007). Its mechanism is by inducing autophagy-mediated tumour cell apoptosis.

Another main cannabinoid found in cannabis is cannabidiol (CBD), but as opposed to THC, it is non-psychoactive (Reblin et al., 2019). Earlier studies have already proven that CBD has also inhibited the growth of GBM cells and caused death (BOC, 2022). The mechanism whereby CBD generates its anti-tumour effect is also distinct from that of THC; this includes the induction of higher levels of ROS generation in the tumour cell (**Figure 4**). When co-administered with THC, CBD has been reported to reduce glioma xenograft growth to an amazing extent (Torres et al., 2011). In some preclinical models, even CBD has been reported to be more effective at suppressing tumour growth than THC (Guzmán et al., 2006). Since it is not psychoactive and has already demonstrated anti-GBM activity, there is considerable potential for CBD as a therapeutic agent, especially when used in conjunction with other cannabinoids or with standard GBM treatment. Its

distinctive mechanism of action relative to THC suggests synergistic effects are possible when paired.

Apart from THC and CBD, other cannabinoids have been examined for their use in treating GBM. However, another non-psychotic cannabinoid, which is called Cannabigerol (CBG), has also shown activity in inhibiting the viability of GBM tumours and triggering apoptosis in preclinical models (BOC, 2022). Synthetic cannabinoids, such as WIN-55,212-2, have also indicated antiproliferative activity against glioma cells in vitro (Velasco et al., 2007). This increasing inquiry into other cannabinoids and their synthetic analogues highlights that more therapeutic options may be available for GBM than THC and CBD. The promising preclinical data observed with CBG, for example, mirror the need for additional studies to determine whether it has any clinical promise.

Research Motivation

With respect to existing GBM treatment limitations, investigating novel or adjuvant therapies, such as cannabinoids, has the potential to improve outcomes. Antitumoural synergistic effects have been demonstrated when THC and CBD are given with temozolomide according to preclinical studies (Torres et al., 2011). This suggests that the inclusion of cannabinoids with existing treatment regimens may be able to make existing treatments more effective. Moreover, research has also established that the combination of cannabinoids with chemotherapy might be a more effective treatment for recurrent GBM. Interestingly, one preclinical study by MGC Pharmaceuticals using 18 patient-derived biopsy samples and 5800 cell tests shows that cannabinoid therapies, such as Cannabidiol (CBD) and Cannabigerol (CBG), can be effective even without the use of chemotherapy (BOC, 2022). In addition, CBD can potentially improve the effectiveness of radiation treatment in preclinical models (Ivanov et al., 2017). The potential use of cannabinoids synergistically with standard therapies like chemotherapy and radiation therapy ranks among the most significant research interests. Such combinations could lead to more effective treatment regimens and perhaps reduce reliance on vastly toxic substances, finally maximizing GBM patient survival and quality of life.

Despite preclinical research having been performed using cannabinoids in GBM, molecular evidence still does not exist regarding who could benefit from such therapy. More research should be devoted to elucidating the whole pharmacological effectiveness and the particular molecular

mechanisms of cannabinoids on the endocannabinoid system against the backdrop of GBM pathophysiology.

With GBM heterogeneity, personalized therapeutic strategies that calibrate cannabinoid-based treatments to a patient's distinct molecular characteristics in their tumour are most likely to yield the most promising pathways towards improvement in treatment outcomes (Zhang et al., 2020). Additional studies on combinatorial therapies that pair cannabinoids with standard GBM treatment, such as chemotherapy and radiation, are also required to clarify potential synergistic benefits and optimize therapeutic efficacy (Torres et al., 2011). Additional research in these areas is needed to fully realize the potential of cannabinoid therapy for improving the lives of patients with this devastating disease.

We have 10 different cannabis flower strains of different cannabinoid concentrations in our lab. We can isolate and quantify more than 100 cannabinoids from the flowers. We also possess purified cannabinoids, which can be combined at different concentrations and tested against a panel of different GBM cell lines. Studies have proven that certain cannabinoid mixtures may have different pharmacological effects (Baram et al., 2019). Their actions also vary depending on receptor diversity since different types of receptors are expressed differently in various glioblastoma tumours. Understanding all these will help us establish cannabinoid combinations and concentrations that would be effective for glioblastoma tumour types.

Hypothesis

Treatment with Cannabinoids will increase the sensitivity of GBM cell lines to chemotherapy.

Research objectives

The objectives of this study are to isolate whole phytocannabinoids from the cannabis plant and procure commercially available temozolomide (TMZ), cannabinoids, and their derivative acids for this research. Different concentrations and combinations of these compounds will be tested on GBM cell lines: TMZ-sensitive (U87, U251), TMZ-resistant T98G (S. Lee, 2016), and 12 patient-derived GBM cell lines with known mutational profiles. Employing a high-throughput strategy, using proliferation and apoptosis as a readout, the study will establish the impact of cannabis extracts, purified cannabinoids, and their derivative acids by themselves and in possible synergy with TMZ on GBM cells. Following this primary screen, more focused research will investigate

cellular invasiveness, viability, apoptosis, and cell cycle distribution, along with the impact on gene expression within the ECS of GBM cell lines. Given the known mutational profiles of these patient-derived lines, this project may illuminate the ability to tailor treatments to specific patients, so-called precision medicine.

Aims

The objectives of this research will be accomplished through the following specific aims:

- To investigate whether the viability and proliferation of GBM cell lines would be affected by treatment with phytocannabinoids/or the TMZ-cannabinoid combination.

- To assess the endocannabinoid system(ECS) within GBM cell lines

Materials and methods

Materials and Reagents

Drugs and Cannabinoids: CBD, CBDV, CBDA, CBGA, CBG, CBN, THC were obtained from Cann Compounding as 1 mg/mL stock solutions in 100% dimethylsulfoxide (DMSO) in amber glass vials. Cannabis flowers (*The Wife*, *Poddy Mouth*, Mimosa, *Meringue*, oyal cookies, *Jack Herer*, Watermelon cookies, Strawberry diesel cookies, *Amsterdam Amnesia*, *Café Racer*) were obtained from MedTecPharma as the 2025 harvest from plantations in Riverland, South Australia. CB1 and CB2 agonist and antagonist were obtained from SelleckChem as lyophilised powder.

Cell lines

Human glioblastoma cell liens -U251, U87, T98G

Reagents:

Bovine serum albumin (BSA, Sigma Aldrich), Dimethyl sulfoxide DMSO (Merck Millipore), DMEM, Ethanol, Glycerol, Ampicillin, Isopropanol, methanol, Maxima kit, gelatin, Optimem, paraformaldehyde, SYBR fast green master mix, SYBR PCR master mix, Tri-reagent (Sigma-Aldrich), Triton X-100, ultra-pure water (Thermo-scientific), TrypLE (Gibco, Denmark), Apotox Triplex Kit (Promega), MTT, Zymo RNA miniprep Kit, Quantinova DNA kit, Nucleobond midi/maxi kit, Isolate II plasmid mini kit (Meridian), Annexin V stain, Propidium Iodide, Hoechst stain, PBS, Fetal bovine serum, Glycine, DAPI stain.

Primers and Plasmids

Plasmids: CNR1-Tango, CNR2-Tango, gpr55-Tango, gpr3-Tango, gpr12-Tango, gpr119-Tango, gpr18-Tango, gpr6-Tango (Roth Lab PRESTO-Tango GPCR Kit -**addgene).**

Primers: CNR1, TBP, FAAH, DAGLA, DAGLB, GPR119, TRPV4, GPR55, TERT, NAPE-PLD, EGR1

Preparation of Cannabis Extracts

Air-dried female inflorescences of medical cannabis (~5 grams) were weighed into a disposable weigh boat, and the weight was recorded in our database. The samples were ground into a fine powder using an electric grinder (such as a spice or coffee grinder), pulsing on and off to prevent overheating. Grinding was performed in a fume hood to minimize exposure to fine cannabis dust. The powder was then transferred into a 50-250 mL plastic container with a lid using a brush, with 50 mL of absolute (undenatured) ethanol added. The cannabis-to-solvent ratio was 1:10. The samples were sonicated in an ultrasonic bath for 30 minutes and then agitated on an orbital shaker at room temperature (~25°C) for 15 minutes. The slurry was then gravity-filtered through Whatman filter paper (#4), and the ethanol was evaporated under reduced pressure at 38°C using the rotary evaporator (Rotavap, Heidolph).

Phytocannabinoid Quantification by Reversed-Phase HPLC Coupled with Triple Quadrupole Mass Spectrometry (HPLC-MS/MS, SRM Mode)

Phytocannabinoids were analyzed using reversed-phase liquid chromatography coupled with tandem mass spectrometry (HPLC-MS/MS) on a Thermo Vanquish HPLC system (Thermo Scientific, Bremen, Germany) equipped with a binary pump and split autosampler. This system was connected to a TSQ Altis Plus Triple Quadrupole mass spectrometer (Thermo Scientific, Bremen, Germany). The chromatographic separation was carried out on a Symmetry C18 analytical column (100 x 4.6 mm i.d., 3.5 µm particle size, Waters, Milford, MA, USA) without a pre-column. Mobile phases consisted of: Solvent A, water with 2 mM ammonium acetate and 0.1% formic acid (Fluka Analytical, P/N: 94318); and solvent B, methanol with 5% water, 2 mM ammonium acetate, and 0.1% formic acid (Fluka Analytical, P/N 94318). The flow rate was

maintained at 0.25 mL/min, and the column temperature was set to 30 °C. The injection volume was 1 µL. Gradient elution was programmed for a total run time of 28 minutes. The initial conditions were optimized to separate five cannabinoids of interest: cannabidiol (CBD), cannabidivarin (CBDV), cannabigerol (CBG), cannabinol (CBN), and Δ9-tetrahydrocannabinol (Δ9-THC).

Mass spectrometric detection was performed using an OptaMax NG APCI ion source (Thermo Scientific) operated in positive ion mode. Compound-specific selected reaction monitoring (SRM) transitions were optimized for each analyte. Data acquisition was carried out with the Thermo Scientific Chromeleon™ 7.3.2 Chromatography Data System, and quantification was based on calibration curves generated from serial dilutions of mixed standards. Cannabinoid reference standards (≥98% purity; 1 µg/µl stock solutions, Medtech Pharma) were serially diluted in 70% methanol with 0.1% formic acid. A mixed calibration standard was prepared containing CBD (20 ng/µl), CBDV (4 ng/µl), CBG (20 ng/µl), CBN (20 ng/µl), and THC (6.66 µg/µl), with subsequent serial dilutions to generate calibration levels. Final calibration concentrations ranged from 0.1-20 ng/µl for CBD, CBG, and CBN; 0.002–4 ng/µl for CBDV; and 0.033–6.66 µg/µl for THC. All standards were transferred into low-bind microcentrifuge tubes (Axygen, 1.7 mL) and subsequently into short-thread ND9 autosampler vials (Thermo Scientific).

10 cannabis flower extracts were diluted by combining 1 µL of extract with 199 µL of 70% methanol containing 0.1% formic acid. Diluted samples were transferred into autosampler vials and stored at 4°C until injection. Data acquisition was performed in SRM mode, monitoring specific mass transitions for each cannabinoid. Quantitative analysis was conducted by comparing the integrated peak areas of analytes in the cannabis samples to the calibration curves. Data processing and reporting were carried out using Chromeleon™ 7.

Cell culture

Human Glioblastoma cell lines (U87, U251, and T98G) at early passage numbers were retrieved from the liquid nitrogen, thawed, and grown in DMEM supplemented with 10% heat-inactivated foetal bovine serum in 5% CO_2 humidified incubator at 37°C. Cells were passaged accordingly by removing media and washing with 1X PBS. 1mL TrypLE Express (Gibco) was then added and allowed for 2 minutes at 37°c. TryPLE was then neutralized with 9mL complete media. Cells were

counted with a cell count or haemocytometer (passage max 1:10). During experimental procedures, cells were washed with 1x PBS and resuspended with Trypsin B-EDTA and treated accordingly.

RNA Isolation and cDNA Preparation

Total RNA was purified and isolated using the Zymo RNA miniprep kit. The cells were suspended and lysed in TRI reagent. An equal volume of 100% ethanol was added to the lysed samples and mixed thoroughly. The mixture was transferred into a Zymo spin column inserted into a collection tube and centrifuged at 13,000*g* for 30 seconds. The spin column was transferred into a new collection tube, and the flow-through was discarded. 400µL of RNA wash buffer was added to the column and centrifuged. 5µL of DNase I and 75µL of DNA digestion buffer were added to an RNase-free tube and mixed gently by inversion and then added to the spin column. The column was then incubated at room temperature for 15 minutes. 400µL of RNA Prewash was added to the column and centrifuged. This step was repeated twice, and the flow-through was discarded. Afterwards, 700µL of the RNA Wash buffer was added to the column and centrifuged for 1 minute (twice) to ensure complete removal of wash buffer. The column was then transferred into an RNase-free tube. To elute the RNA, 50µL of DNase/RNase-free water was added directly to the column and centrifuged. The eluted RNA was used immediately to prepare the cDNA.

The QuantiNova kit was used to prepare the cDNA. The template RNA, gDNA removal mix, and the reverse transcriptase enzyme were thawed on ice. Each solution was mixed properly by flicking the tubes. The genomic DNA removal reaction (template RNA, gDNA removal mix, and RNase-free water) was prepared according to specifications and left on ice. This was incubated for 2 minutes at 45°C, then placed immediately on ice. The reverse transcription mix was prepared according to QuantiNova specifications. Freshly prepared reverse transcription mix was then added to each tube containing template RNA and stored on ice. The tubes were then placed into a thermal PCR cycler and incubated for 3 minutes at 25°C, 10 minutes at 45°C, and finally for 5 minutes at 85°C to inactivate the RT enzyme. The prepared cDNA was stored at 4°C and used for real-time PCR. Analysis was done by Quantitative PCR using SYBR-green self-designed primers (see materials). Each PCR reaction sample was done in replicate. The PCR running protocol was created and executed in Qiagen's Rotor-Gene Q series software. ΔCt and ΔΔCt values for targets examined were obtained using the Rotor Gene Q series software.

Measurement of viability, cytotoxicity, and apoptosis using the Apotox triplex assay

Cells were plated on 384-well plates (U87 at 1500 cells/well, U251 at 1000 cells/well, and T98G at 5000 cells/well) with complete DMEM and allowed to settle overnight. Cells were then treated with selected concentrations of agents for the required exposure time and incubated at 37 °C. After the exposure, 2.5µL of viability/cytotoxicity reagent was added to each well. The mixture was gently shaken by orbital shaking for 30 seconds and incubated for 30 minutes at 37 °C. Fluorescence was measured at two wavelengths: 400ex/505em (viability) and 485ex/520em (cytotoxicity). Next, 12.5µL of caspase-GLO reagent was added to each well, briefly mixed by orbital shaking (300-500 rpm) for 30 seconds, and incubated at room temperature for 30 minutes. Luminescence was then measured to assess caspase activation, which is a hallmark of apoptosis.

Measurement of viability and cytotoxicity using fluorescence microscopy (Hoechst Staining)

Cells were harvested in 5 mL media and counted in the automatic counter and adjusted to the required seeding density. 100µL of cells/well was dispensed to a 384-well plate. The plates were allowed to incubate overnight. Treatments were delivered to the cells by a 1µL transfer from cannabinoids 100x dilutions in DMSO. The plates were then incubated at 37oc for 48 hours. A 1:100 Hoechst stain was prepared in PBS, and 6% PFA was also prepared in PBS from a 10% stock solution. The content of each well was aspirated, leaving only 45µL, and then 5µL of Hoechst was transferred to each well. The plates were incubated for 30 minutes at 37Oc. After incubation, the contents of the well were aspirated, leaving 25µL behind. 25µL of 6% PFA was transferred to each well, leaving a final concentration of 3% PFA. The plates were incubated for 30 minutes at room temperature. After incubation, the cells were washed twice with PBS. Plates were processed automatically in a Cell::Explorer workstation (Revvity). Treatments were delivered by a JANUS liquid handler (Revvity) while staining, fixation and cell washes were carried out in an automatic Biotek plate washer and dispenser (Millenium Science). Imaging was performed on an Operetta

1261 automated microscope with Harmony (v4.1) image acquisition and analysis software (Revvity Inc.). Plates were handled by a Plate::Handler robotic arm (Revvity)

Apoptosis Assay via Annexin V/PI staining.

Cells were plated on the required well plates and grown until 80% confluency with complete DMEM. Cells were treated with the indicated treatments for the time of exposure needed. Cells were detached and collected using TrypLE (Trypsin B-EDTA), centrifuged at 1000g for 5 minutes, and washed with PBS. Cell samples were resuspended in Annexin V binding buffer and centrifuged for 5 minutes. The binding buffer was removed, and cells were then stained with 5µL of Annexin V-FITC for 15 minutes at room temperature in the dark. Cells were then treated with 10µL of PI staining. Apoptotic cell death was determined by measuring the percentage of positive Annexin V and/or double-stained PI cells out of the total cells counted over 10,000 events by a Cytoflex S flow cytometer and analyzed using CytExpert software.

Isolation, sequencing, and extraction of Presto-Tango GPCR constructs

Selected GPCR constructs were obtained from the library plate provided by the Janovjak lab and streaked onto agar plates containing ampicillin. The plates were incubated at 37°C overnight. The next day, single colonies were picked from each plate and cultured overnight in liquid broth with 100 µg/mL ampicillin at 37°C in a shaker incubator. Plasmid DNA was extracted using the Meridian Isolate II plasmid mini kit following the manufacturer's instructions. The plasmid DNA was then sent for sequencing to confirm identity. After confirmation, the same colonies were re-isolated and cultured overnight in 100 mL flasks. Finally, plasmid DNA was extracted using the Nucleobond Xtra midi/mini kit according to the manufacturer's protocol.

Preparation and Validation of GPCR Constructs for the Presto-Tango Assay

Circular glass coverslips (13 mm diameter) were coated with poly-L-lysine (PLL) to promote cell adhesion. Coverslips were placed individually into the wells of a 24-well tissue culture plate (one coverslip per well) and incubated with 10% (v/v) PLL solution in 1X PBS. Excess PLL was removed, and coverslips were washed twice in 1X PBS, then in 80% (v/v) ethanol in water and allowed to air dry under sterile conditions, or kept in 80% ethanol at room temperature for later use. U251 cells (or specify cell line) were seeded onto the PLL-coated coverslips at a density sufficient to achieve 60–70% confluence after 24 h. Cells were maintained in complete growth medium at 37 °C in a humidified atmosphere containing 5% CO_2. The following day, cells were transfected with the GPCR-encoding plasmid using Lipofectamine (Thermo Fisher Scientific, USA) following the manufacturer's protocol. Two control conditions were included: a negative control, where cells were seeded on coated coverslips without GPCR plasmid transfection, and a no-primary-antibody control, where cells were transfected with the GPCR plasmid but incubated only with the secondary antibody during staining. At 24 h post-transfection, cells were fixed with freshly prepared 4% (w/v) paraformaldehyde (PFA) in PBS for 10 min at room temperature. Following fixation, cells were washed three times with PBS to remove residual fixative. Cells were permeabilized with 0.1% Triton X-100 in PBS for 10 min at room temperature to allow antibody access to intracellular epitopes, followed by three PBS washes. Non-specific antibody binding sites were blocked by incubating cells in blocking buffer consisting of 3% (w/v) bovine serum albumin (BSA) in PBS for 30 min at room temperature. The GPCR construct contained a FLAG tag, confirmed by plasmid sequence analysis, which determined the choice of primary antibody. The primary antibody was rabbit anti-Flag antibody; it was diluted in blocking buffer at a 1:1000 concentration and applied to cells overnight at room temperature in a humidified chamber. The host species of the primary antibody (rabbit) was noted to ensure compatibility with the chosen secondary antibody. Cells were washed three times with PBS (5 min per wash) to remove unbound primary antibody. Cells were incubated with the appropriate species-specific secondary antibody conjugated to Alexa Fluor® 488 (Thermo Fisher Scientific, USA) diluted in blocking buffer, for 1 h at room temperature in the dark. Following incubation, cells were washed three times with PBS to remove excess antibody. Coverslips were carefully removed from the 24-well plate using

fine forceps and mounted cell-side down onto glass microscope slides with an anti-fade mounting medium containing DAPI (for nuclear staining). Mounted samples were sealed with nail polish to prevent drying and stored at 4 °C in the dark until imaging. Fluorescence images were acquired using the laboratory's widefield fluorescence microscope equipped with appropriate filter sets for DAPI and Alexa Fluor® 488 detection.

Data and statistical analysis

Images were transferred to a dedicated local server and analysed using Columbus (v2.5) data storage and image analysis software running on an Omero (v4.0) and Acapella (v3.2) server (all from Revvity). Raw image data was then compiled using a Python (v13.1) script and imported into Spotfire Desktop (v10.8.0, TIBCO Software Inc) for further analysis and data visualization. General data exploration was carried out for quality control purposes. Dose-response curves were adjusted using a four-parameter logistic regression model, and ICC50 were calculated from the equations of the adjusted curves. Results from the analysis were visualized using tables, bar and scatter plots. Statistical analyses were performed in SPSS Statistics software (v30, IBM), using the Kruskal-Wallis ANOVA test with multiple sample comparisons. The level of significance was 0.05.

Results

The human glioblastoma cell lines (U87, U251, and T98G) differ in their expression of cannabinoid targets, metabolic enzymes, and GBM-associated genes.

To determine the expression levels of key endocannabinoid targets and glioblastoma (GBM)-related genes, real-time RT-PCR analysis was performed on three established human cell lines: U87, U251, and T98G, which are to be used for cannabinoid drug response experiments. The genes selected for this analysis represent crucial components of the endocannabinoid system. They include genes for receptors (CNR1, CNR2, GPCR55, GPCR119, TRPV1, TRPV4), metabolic enzymes (FAAH, NAPE-PLD, DAGLA, DAGLB), and transcriptional regulators (EGR1 and TERT). The expression levels of these genes are summarised in the heatmap shown in FIGURE 2, where the colour code indicates absence (red), low (yellow), and presence (green) of gene expression.

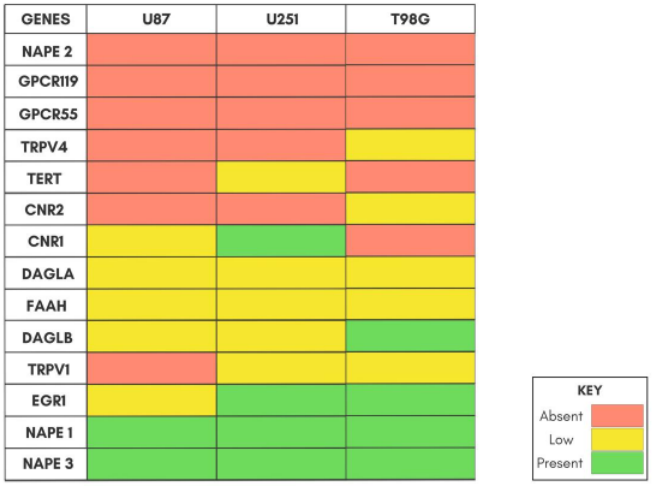

***Figure 5**: Heatmap of gene expression profiles across Human glioblastoma cell lines (U87, T98G, U251). CDNA prepared from each cell line was stored 4°c and used for real-time PCR. The reactions were performed in triplicate using SYBR green and primers designed by the lab (Vanessa Conn). Amplification was carried out using the Rotagen Q (Qiagen), and relative expression levels were calculated using the ΔCT and ΔΔCT method, normalized to TATA-box binding protein (TBP) as a reference gene. The heat map shows expression levels of CB1 (Cannabinoid receptor type 1, CNR1), CB2 (Cannabinoid receptor type 2, CNR2), GPR55 (G protein-coupled receptor 55), FAAH (Fatty acid amide hydrolase), MAGL (Monoacylglycerol lipase), NAPEPLD (N-acyl phosphatidylethanolamine phospholipase D), TRPV1 (Transient receptor potential vanilloid 1), TERT (Telomerase reverse transcriptase), and EGR1 (Early*

growth response 1). Expression levels are shown relative to TBP with red indicating low expression levels, Yellow indicating moderate expression, and green indicating high expression levels across all cell lines.

Across all three cell lines, *NAPE-PLD* showed reliable and strong expression, suggesting that the cell lines have an active capacity to synthesize anandamide. There were cell-line-specific differences in the expression of cannabinoid receptors. *CNR1* was strongly expressed in U251, weakly expressed in U87, and absent in T98G. However, *CNR2* was absent in U87 and U251 but detectable at low levels in T98G. *GPCR 119* and *GPCR 55* were all absent in the three cell lines. There was also variation in the TRP ion channels; *TRPV1* was absent in U87, but low in U251 and T98G, while *TRPV4* was detectable only in T98G. When it comes to the metabolic enzymes, *DAGLA* and *DAGLB* were expressed at low levels in U87 and U251, but were highly expressed in T98G, while *FAAH* was weakly expressed across all cell lines. This suggests that GBM cells may maintain partial capacity for 2-AG turnover, although at reduced frequency.

TERT, a gene involved in maintaining the length of telomerases, important for GBM proliferation and survival, was detected in U251 but was mostly absent in the other two cell lines. Finally, EGR1 was found to be high in U251 and low in U87 and T98G, suggesting that U251 has a stronger immediate-early response capacity that could enhance CBD-triggered signaling changes. Due to these differences in gene expression, we expect these cell lines to respond differently to cannabinoid treatment. These results confirm the RNA sequencing studies carried out on these cell lines by Vanessa Conn.

The Purified cannabinoids differ in their ability to induce glioblastoma cell death

Our research aims to understand how cannabinoids exert their effects on GBM cells and whether they can sensitize these cells to TMZ treatment. Other studies have explored this using only THC and CBD, which are the most popular cannabinoids. However, since we know that cannabis extracts vary in their CBD and THC concentrations and also contain other cannabinoids, we decided to screen seven different cannabinoids (CBD, CBG, CBDA, CBGA, CBN, THC, CBDV) against three human glioblastoma cell lines. There is no preliminary data on the concentrations to use against these cell lines, so we conducted initial screening with high concentrations of these

cannabinoids. We found that at high concentrations, the cannabinoids were lethal for all cells at concentrations of 10 µg/mL and above. Subsequently, we performed dose-response screening of the seven cannabinoids against U251 using the Hoechst assay, with concentrations ranging from 4.7 ng/mL to 10 µg/mL (**Figure 6**). In the Hoechst assay, only cells with intact DNA retain the stain and are then counted. The live cells are compared to the untreated control to determine cytotoxicity. The dose-response curves were reliable, with R^2 values above 0.90 in all cases. The calculated CC50 values (concentration at which cytotoxicity is 50%) fell well within the statistical 95% confidence intervals and proved to be accurate. The individual curves for each cannabinoid and other data can be found in **Supplementary Figure 1.** For most cannabinoids, the effective cytotoxic range was between 0.05 and 0.3 µg/mL, except for THC, which exhibited a broader range from 0.05 to 2.4 µg/mL. Although these values are more precise, it was recognized they could differ for other cell lines; therefore, the dose-response tests were repeated on two additional cell lines, U251 and T98G. Based on the dose-response results across all three cell lines, it was observed that the CC50 of six cannabinoids ranged from 80 ng/mL to 170 ng/mL **(Figure 6).** However, THC had a CC50 between 1.08 µg/mL and 3.43 µg/mL, making it the least effective cannabinoid against these cells. U251 appeared particularly sensitive to CBN and CGBA, U87 was more sensitive to CBD, while T98G showed similar responses to the other cannabinoids.

Dose Response Curves

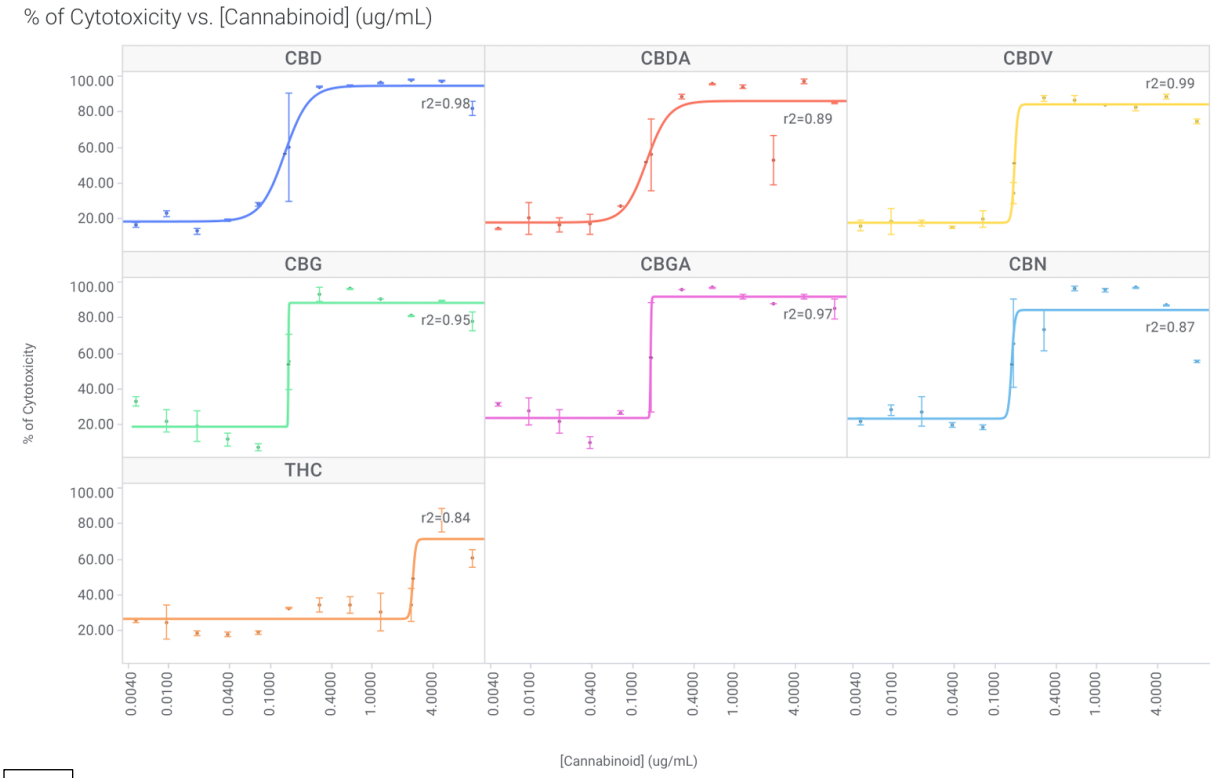

A

Dose Response Curves

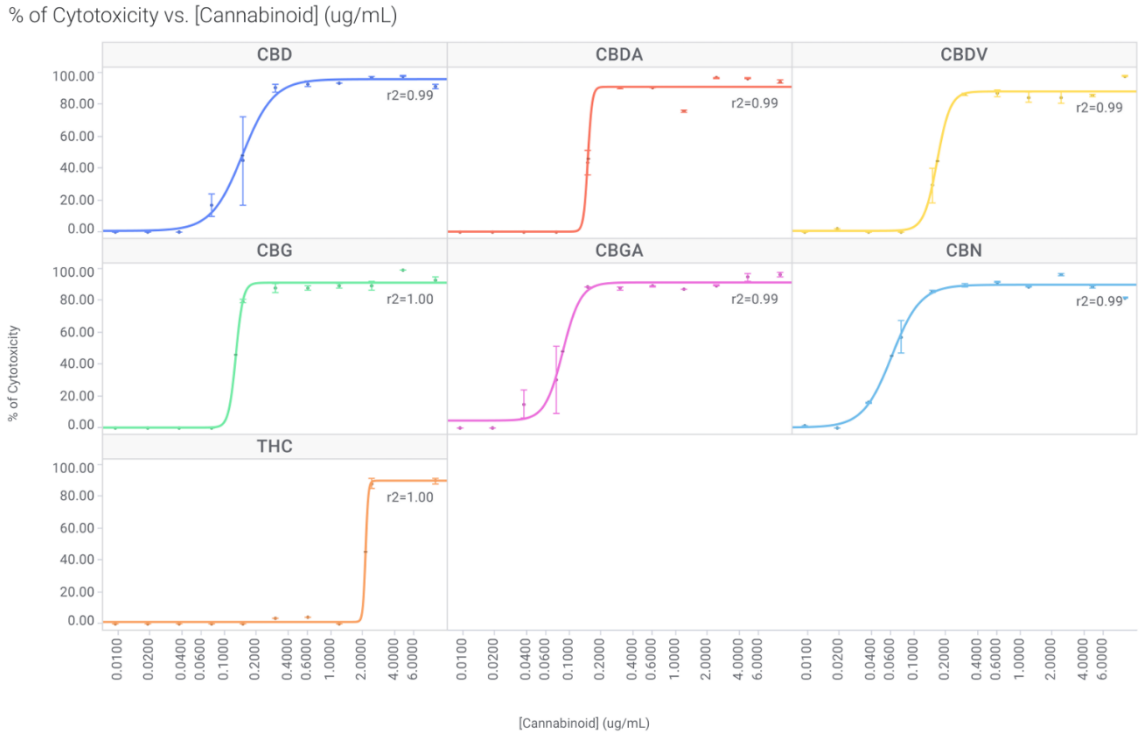

B

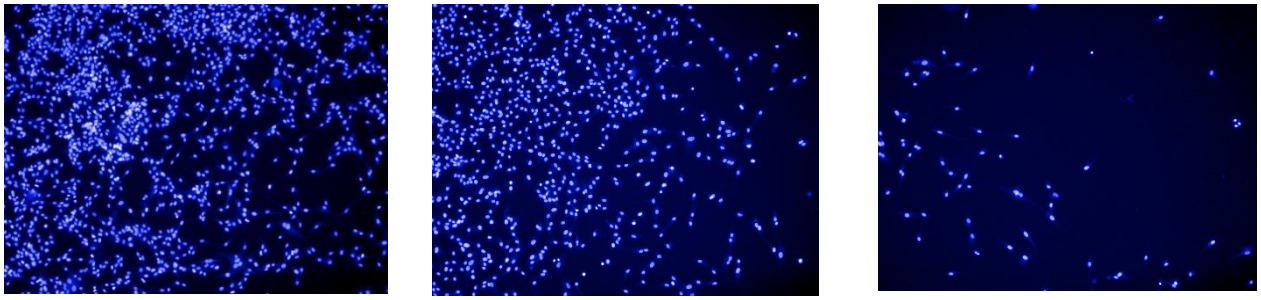

C

Cell Line	Treatment	[CC50] (ug/mL)	Valid
U251	CBD	0.148407035	TRUE
U251	CBDA	0.150618101	TRUE
U251	CBDV	0.166164528	TRUE
U251	CBG	0.128800069	TRUE
U251	CBGA	0.087567074	TRUE
U251	CBN	0.062211012	TRUE
U251	THC	2.145358753	TRUE
U87	CBD	0.108021151	TRUE
U87	CBDA	0.153640073	TRUE
U87	CBDV	0.148067689	TRUE
U87	CBG	0.148346418	TRUE
U87	CBGA	0.160815348	TRUE
U87	CBN	0.146520698	TRUE
U87	THC	1.087416412	TRUE
T98G	CBD	0.144854858	TRUE
T98G	CBDA	0.134381456	FALSE
T98G	CBDV	0.154458424	TRUE
T98G	CBG	0.147839642	TRUE
T98G	CBGA	0.144579006	TRUE
T98G	CBN	0.146768242	TRUE
T98G	THC	3.434166974	TRUE

***Figure 7**: **The purified cannabinoids differ in their ability to induce glioblastoma cell death A).** U251 (bottom) and U251 (Top) cell lines were plated in a 384-well plate at 1500, 1000, and 500 cells/well, respectively, and treated with concentrations of each cannabinoid ranging from 10 µg/mL to 4.68 ng/mL for 48 hours. The plates were stained with Hoechst (500 ng/mL), and four fields in each well were imaged and analysed using the Operetta high-content imaging and analysis system. Percentage cytotoxicity was calculated by dividing the number of dead cells by the total number of cells and multiplying by 100. To account for background cell death, cytotoxicity in each treated well was normalized to the untreated control (no-treatment well). Specifically, baseline death observed in untreated wells was subtracted from treated wells before statistical comparison. Results were averaged across biological replicates. Each sample was also compared to the vehicle control (0.5% DMSO) in the same concentration. The dose-response curves for the cannabinoids against T98G cells are presented in the Appendix**. B.)** Cell images of U251 cells at no treatment (left), CBD at CC50, and at a higher concentration of CBD**. C**). The cells/well logistic regression curve fits show the **CC50** values of each cannabinoid against the cell lines U87 (top), U251 (middle), and T98G (bottom). The R^2 values were above 0.90 in all cases. The calculated CC50 values fell well within the statistical 95% confidence intervals.*

Cannabis strains differ in the amount of extracts and in their phytocannabinoid profile

As part of the goal to determine how cannabinoids exert a cytotoxic effect on GBM cell lines, we considered the fact that cannabinoids can work synergistically to achieve a more effective outcome. However, with over 100 identified cannabinoids, the number of possible combinations and concentration ratios is extremely high, making the identification of a perfect mix a resource-intensive and complex task. Therefore, phytocannabinoids were extracted from 10 different cannabis strains, knowing that each strain would have a unique phytocannabinoid fingerprint and, in essence, provide a biologically relevant way to combine these cannabinoids. After extraction, the different strains yielded varying amounts of extract (equal weights of each strain were used). Table 1 shows the list of cannabis strains and the weights of the extracts obtained from them. To facilitate efficient analysis using mass spectrometry, all the extracts were adjusted to 50 mg/mL with 100% DMSO.

***Table 2**. Table showing the weight of the flower extracts after extraction and evaporation in the rotary evaporator. The extracts were then suspended in 100% DMSO to a concentration of 50mg/mL.*

Strain	Weight of extract (g)
Amsterdam Amnesia	1.2
Poddy Mouth	1.3
Watermelon Zkittles	1
The Wife	1.6
Mimosa x Orange punch	1.3
café Racer	1.2
Meringue	0.8
Jack Herer	1.4
Strawberry diesel cookies	1.7

After extraction, we proceeded to quantify the phytocannabinoid profile of each cannabis strain. Figure 8 details the analysis of 10 different strains of cannabis as determined by mass spectrometry. The analysis focused on key cannabinoids including cannabidiol (CBD), 9-tetrahydrocannabinol (THC), cannabinol (CBN), cannabidivarin (CBDV), and Cannabigerol (CBG). The acidic forms of these cannabinoids were not detected because the flowers were heat-decarboxylated before extraction. The results indicate significant differences in the cannabinoid profile between the strains (Figure 6). THC was the most predominant cannabinoid in each strain; it was present at

µg/µl, while other cannabinoids were detected in µg/µl range. *The Poddy Mouth* strain demonstrated the highest THC concentration; in contrast, *The Wife* strain had the lowest THC concentration (~25-fold less). *The Mimosa x Orange punch* strain had the highest CBD concentration, while the *Jack Herer* had the lowest CBD concentration. *The Amsterdam Amnesia* had the highest CBG concentration, while *the Poddy Mouth* strain had the lowest CBG concentration. The Mimosa and Wife strain had the highest concentration of CBN and CBDV, respectively.

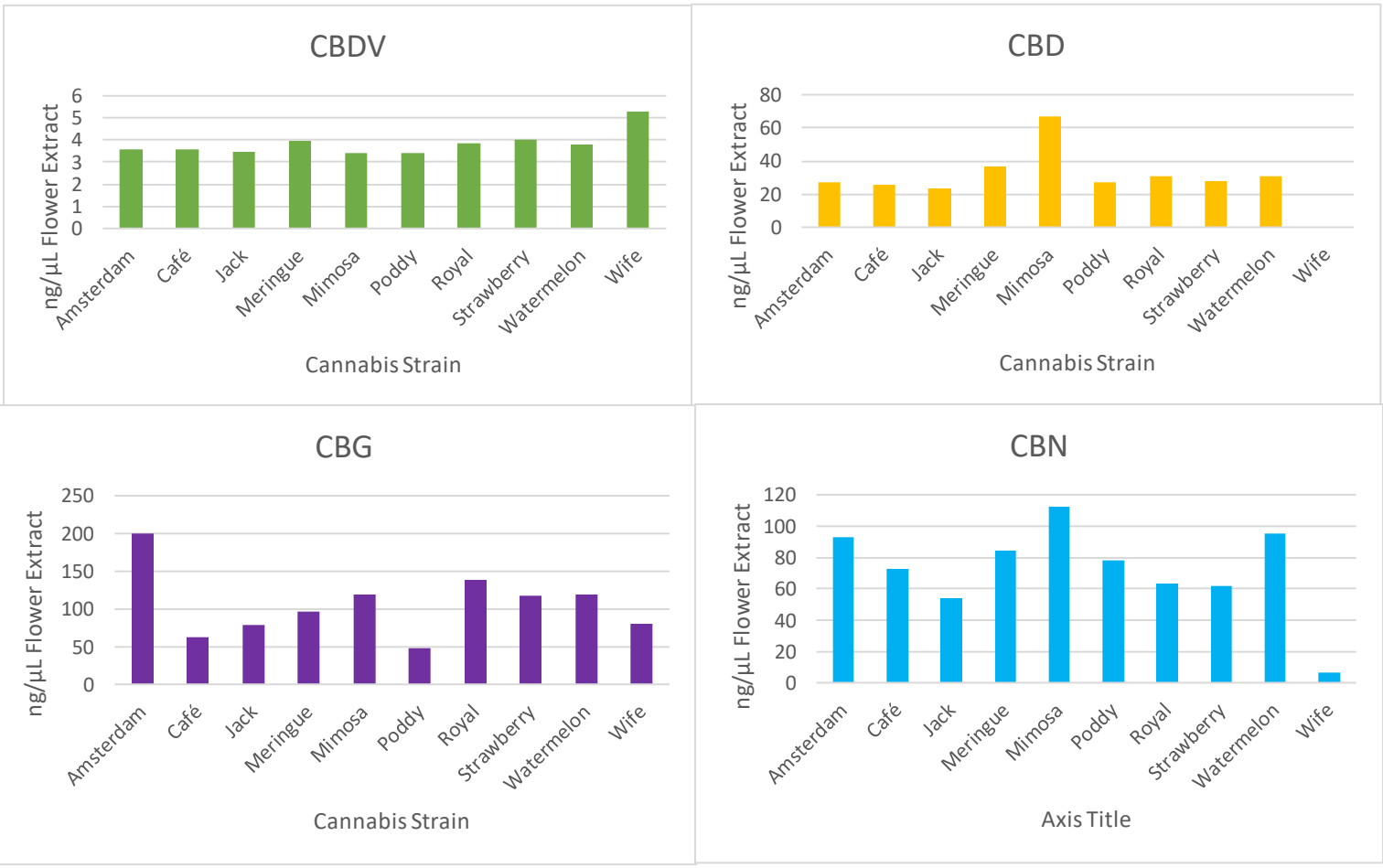

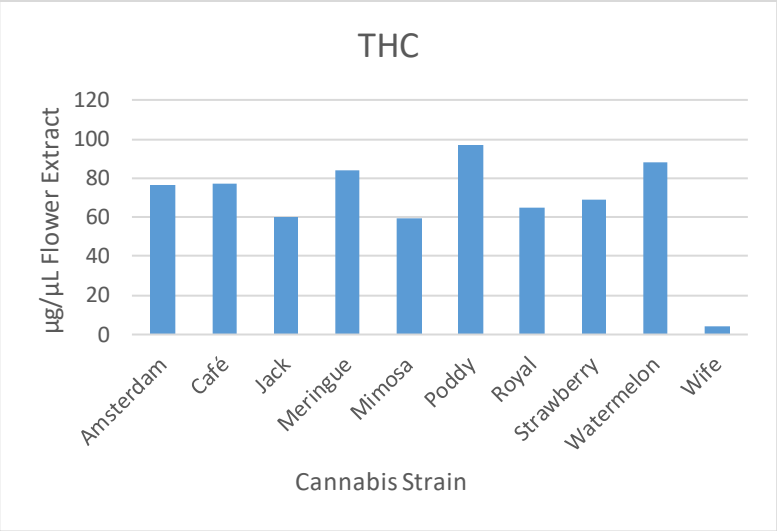

FIGURE 8. The different cannabis strains differ in their phytocannabinoid content. *The phytocannabinoid profile of 10 different strains of cannabis was analyzed after extraction using Reverse-phase liquid chromatography coupled to tandem mass spectrometry (HPLC-MS/MS). The bar charts show individual cannabinoids and their relative amount in each strain. Five key cannabinoids of interest were the main focus of this analysis*

Cannabinoid Abundance Per 2.5 Micrograms of Flower Extract

	Amsterdam	Café	Jack	Meringue	Mimosa	Poddy	Royal	Strawberry	Watermelon	Wife
CBDV (ng)	8.9239	9.0058	8.6664	9.8503	8.5346	8.5538	9.6152	10.0733	9.5130	13.1549
CBD (ng)	67.5279	64.7379	59.0861	92.2788	167.8573	67.1448	76.3610	69.5552	76.2970	n.a.
CBG (ng)	499.3891	156.9133	196.9903	240.4990	297.5708	119.8845	344.8947	293.5631	295.9091	199.6056
CBN (ng)	233.1155	181.2111	135.1050	210.9038	281.4467	194.7609	158.7182	153.6575	237.4858	16.1531
THC (µg)	190.5498	193.2483	149.4346	210.3606	148.5354	242.5170	162.0887	171.7226	219.5449	9.7672

Cannabinoid Abundance Per Microgram of Flower Extract

	Amsterdam	Café	Jack	Meringue	Mimosa	Poddy	Royal	Strawberry	Watermelon	Wife
CBDV (ng)	3.5696	3.6023	3.4665	3.9401	3.4138	3.4215	3.8461	4.0293	3.8052	5.2620
CBD (ng)	27.0111	25.8952	23.6344	36.9115	67.1429	26.8579	30.5444	27.8221	30.5188	n.a.
CBG (ng)	199.7557	62.7653	78.7961	96.1996	119.0283	47.9538	137.9579	117.4253	118.3636	79.8422
CBN (ng)	93.2462	72.4844	54.0420	84.3615	112.5787	77.9044	63.4873	61.4630	94.9943	6.4612
THC (µg)	76.2199	77.2993	59.7739	84.1442	59.4141	97.0068	64.8355	68.6891	87.8180	3.9069

Table 3*: This table shows the concentration of each phytocannabinoid in 2.5µg and 1*µg *of cannabis extracts, respectively. This table shows the different strains of cannabis and their phytocannabinoid content.*

The Cannabis extracts differ in their ability to cause glioblastoma cell death

To evaluate the effect of different extracts on glioblastoma cell death, the extracts were used to treat U251, U87, and T98G cell lines. When determining the appropriate extract concentrations, we considered the CC50 of the purified cannabinoids and the levels of phytocannabinoids present in the extracts. Consequently, the cells were treated with extracts at concentrations ranging from 1 µg/mL to 10 µg/mL. All extracts demonstrated cytotoxic activity against the three cell lines. The dose-response curves in FIGURE 8 were reliable, with R^2 values exceeding 0.90 in all cases. The calculated CC50 values were within the 95% confidence intervals, indicating greater accuracy. The response curves in figure X display the average percentage of cytotoxicity normalized to the untreated control. The CC50 ranged from 1.66 µg/mL to 3.65 µg/mL for T98G, 1.49 µg/mL to 4.70 µg/mL for U251, and 1.71 µg/mL to 3.64 µg/mL for U87.

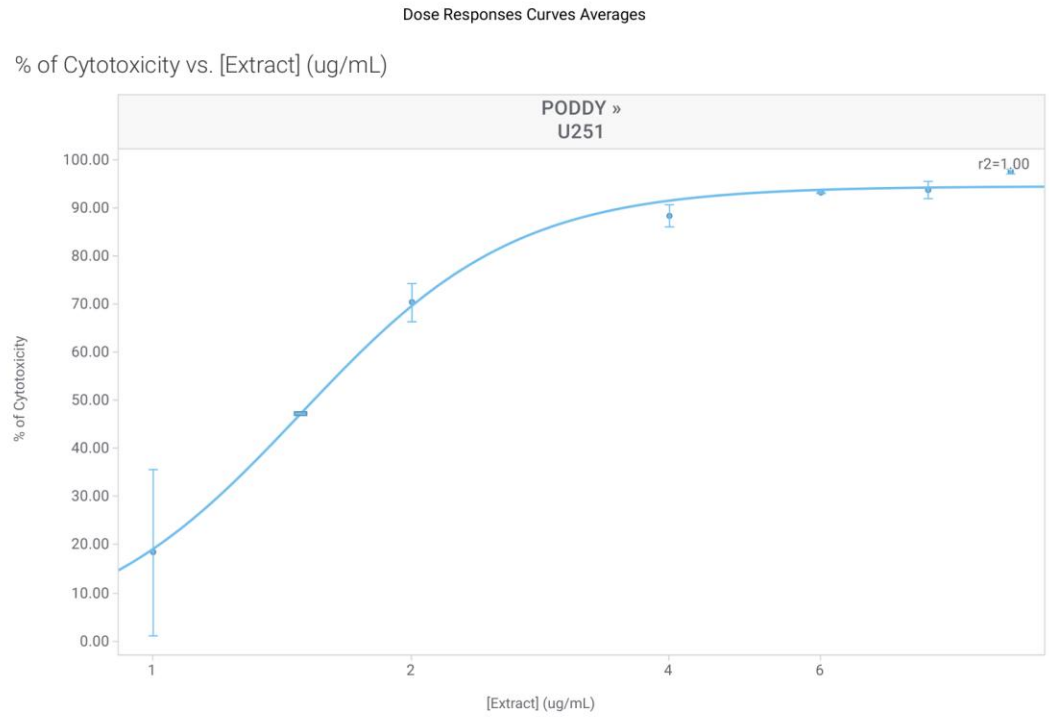

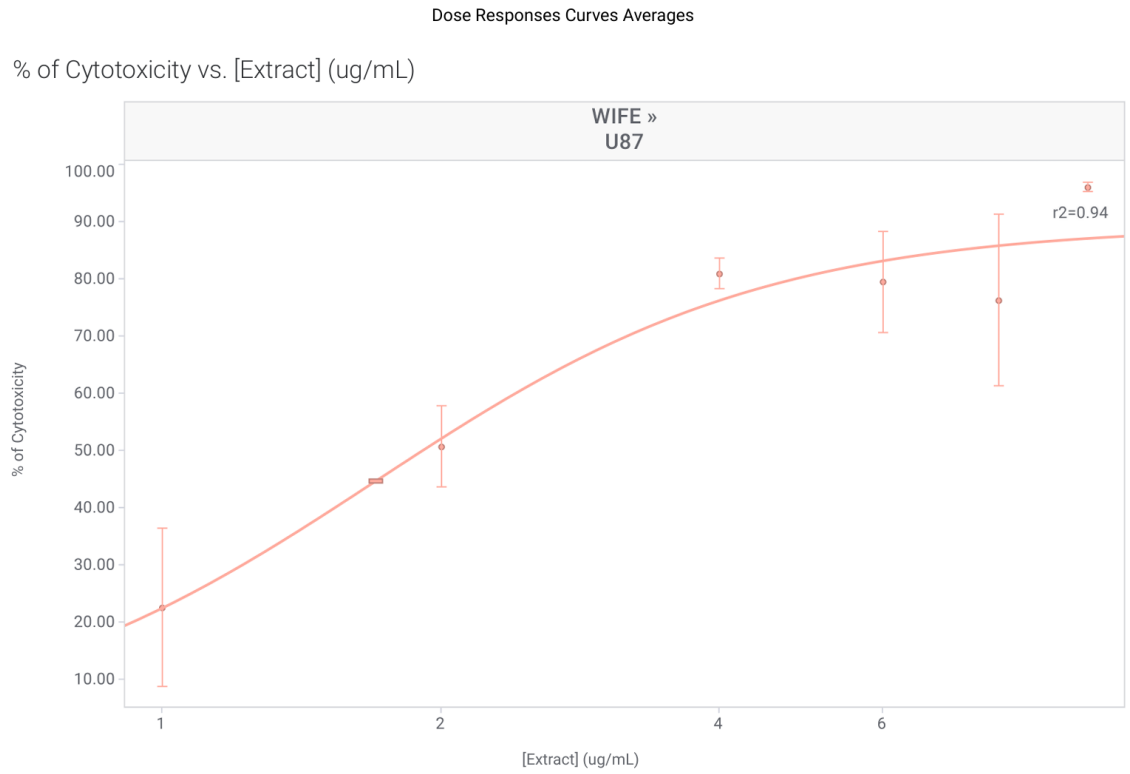

***Figure 9**: **Phytocannabinoid extracts differ in their ability to induce Glioblastoma cell death**. These figures show the dose response curves of the Poddy Mouth strain and The Wife strain against U251 and U87 Cell lines, respectively. U251, U87, and T98G cells were plated in 384 well plates (1x10^4, 1.5x10^4 and 10,000 cells/mL, respectively), and treated with 1, 2, 4,8, and 10µg/mL of indicated extracts for 48 hours. The plates were stained with Hoechst (500ng/mL) and five sites in each well were imaged by the operatta high-performance imaging. The number of detected live and dead cells were counted and analyzed. Percentage cytotoxicity was determined by the number of dead cells divided by the total number of cells multiplied by 100 and presented as a dose response curve. Each treatment was normalized to the untreated and vehicle control (DMSO) in the same concentration. The dose response curves for the other extracts and cell lines can be found in the appendix.*

The extract from the strain *Poddy Mouth* had the best effect against T98G and U251, and also on U87 but the extract from the strain WIFE had the highest potency against U87 (Figure X2). From the results, the two strains PODDY and WIFE had the highest potency against all the three lines. The analysis of the CC50s also shows that T98G is more sensitive to treatments with these extracts compared to the other cell lines (**Figure 10**).

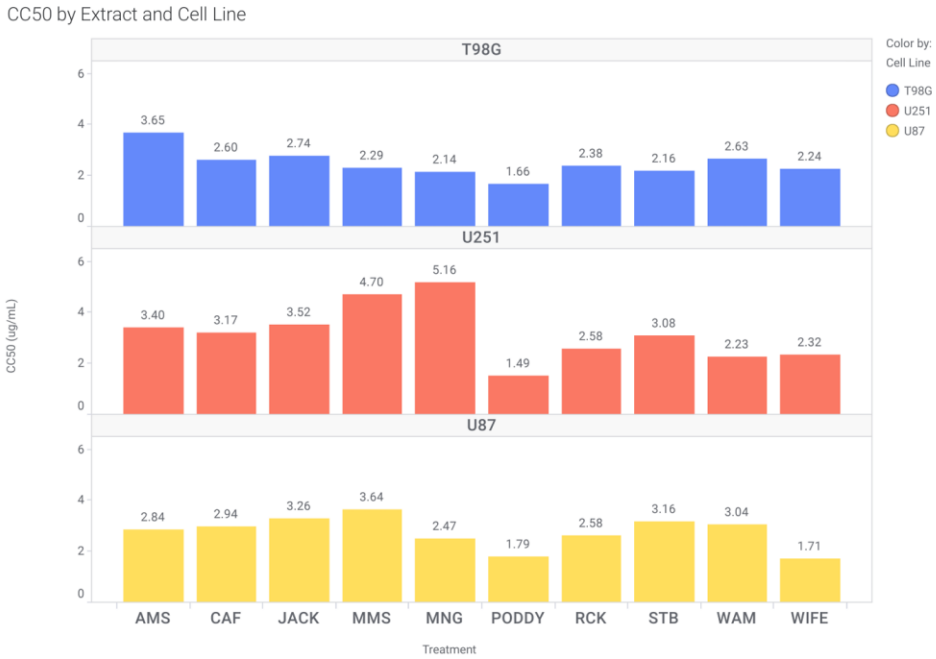

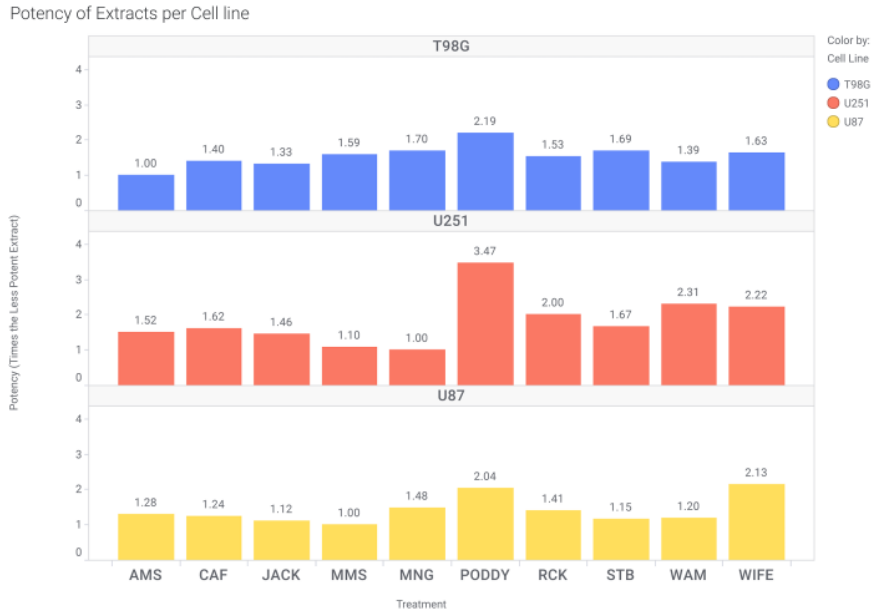

***Figure 10**: Shows the comparison between the different treatments against the three cell lines T98G (Blue), U251 (orange), and U87 (Yellow). The images show the CC50 of each extract on each cell line (top), it also shows the relative potency of each extract on the three cell lines, and finally the average responsiveness of each cell line to the treatments (Bottom).*

Cannabis extracts induce apoptosis in human glioblastoma cell lines

To understand if apoptosis is part of the cell death caused by the cannabinoids, we used Annexin V/PI assay using flow cytometry as the readout. Annexin V binds to cells in early apoptosis, while propidium iodide (PI) binds to cells in late apoptosis or necrosis, while viable cells are negative for both stains. Staurosporine, a known inducer of apoptosis, was used at two concentrations, 1.25µM and 10µM, to treat U251 cells for 7 hours. Cell death due to apoptosis was assessed by the percentage of cells positive for APC Annexin V and/or double-stained with PI out of a total of 10,000 events counted by cytofluorimeter and analyzed with cytoExpert software.

The vehicle control was 3% DMSO, which appeared to have a toxic effect on the cells. 60.99% of the cells were alive and healthy, while 36% were necrotic. 2.43% were in the late apoptosis phase while less than 1% were in early apoptosis. With 1.25 µM Staurosporine, the number of live cells decreased to 18%, with 74% of the cells in early apoptosis and 6.97% in late apoptosis. The number of live cells further decreased to 6.8% with 10µM Staurosporine and up to 83% being in early apoptosis. However, the number of cells in late apoptosis increased to 8.9% as shown in **Figure11.**

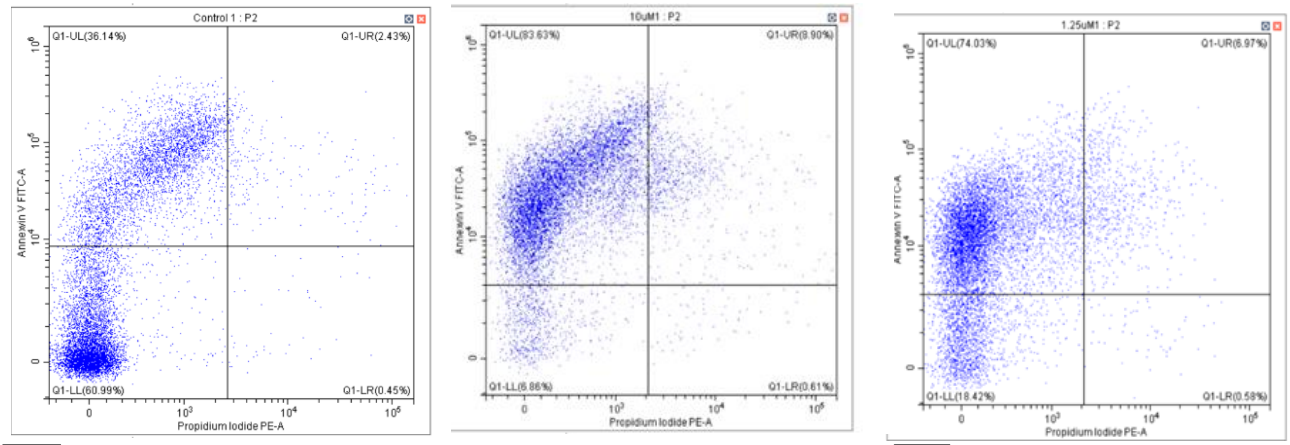

Figure 11: ***Staurosporine induced apoptosis in U251 Cells after 8 hours of treatment.*** *U251 cells were seeded overnight in a 6-well plate at 300,000 cells per well. The wells were treated for 8 hours with 10µM staurosporine, 1.25µM staurosporine, and DMSO (vehicle control) in duplicates. The cells were harvested with trypsin into tubes and suspended in 2 mL of annexin V binding buffer. The cells were spun down, and the buffer was decanted. F of Annexin V FITC were added to each tube and incubated for 15 minutes in the dark. 10 µL of propidium iodide was then added to each well and read immediately on the flow cytometer. Cell death due to apoptosis was assessed by the percentage of cells positive for APC Annexin V and/or double-stained with PI out of a total of 10,000 events counted by the flow cytometer and analysed with CytoExpert software*. The images are labelled as; Vehicle control (Panel A), 1.25*µM aurasperone (Panel C), and 10µM aurasperone (Panel B*

As the next step, after determining the CC50 of the cannabis extracts and the cannabinoids using the Hoechst assay, we proceeded to treat U251 cells with the CC50 of each cannabis extract and the pure cannabinoids and determined the most potent ones using the annexin V/PI assay.

From the results shown in **Figure 12**, the *Poddy Mouth* strain, *The Wife* strain, and THC were the most potent extracts, with 27.42%, 39.51%, and 48.4% apoptosis, respectively, after 24 hours.

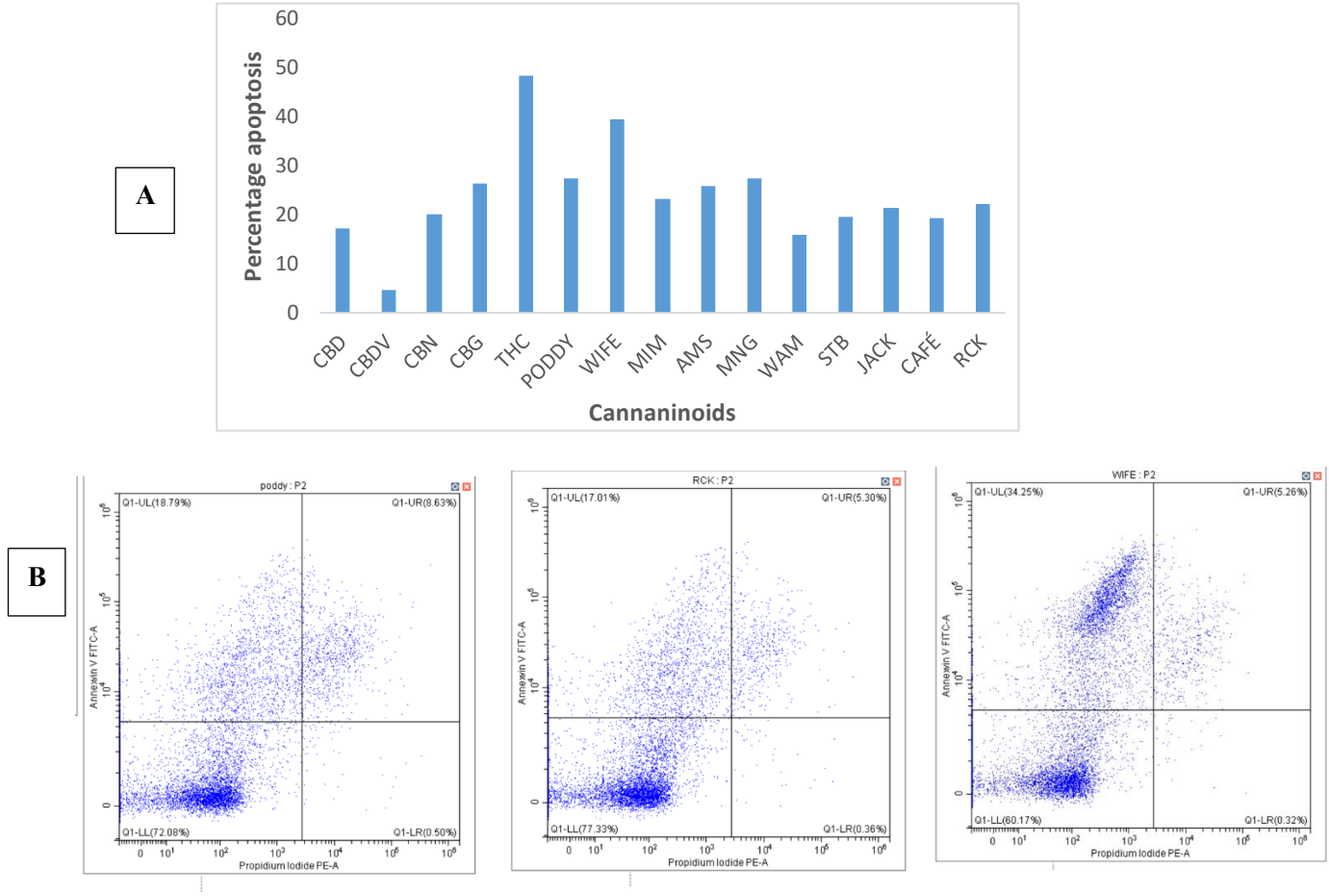

Figure 12: Cannabinoids and cannabis extracts induced apoptosis in U251 Cells after 24 hours of treatment. *U251 cells were seeded overnight in a 6-well plate at a density of 300,000 cells per well. The wells were treated for 8 hours with the CC50 of the cannabinoids and the cannabis extracts, and DMSO (vehicle control) in duplicates. The cells were harvested with trypsin into tubes and suspended in 2 mL of annexin V binding buffer. The cells were spun down, and the buffer was decanted. Five microliters of Annexin V FITC were added to each tube and incubated for 15 minutes in the dark. Ten microliters of propidium iodide were then added to each well and read immediately on the flow cytometer. Cell death due to apoptosis was assessed by the percentage of cells positive for APC Annexin V and/or double-stained with PI out of a total of 10,000 events counted by the flow cytometer and analysed with CytoExpert software.* ***A.)*** *Bar chart showing each treatment and the percentage apoptosis after 24 hours of treatment.* ***B.)*** *Flow cytometry images showing that the cannabis extracts induced apoptosis in the cells after 24 hours (Left -right- Poddy strain, Royal cookie strain, and Wife strain).*

Cannabinoids-TMZ Combination increases Glioblastoma cell death

The exact mechanism of action of cannabinoids inside the cell remains an evolving area of research. One goal of this research is to identify the signaling pathways in which cannabinoids are involved. One approach we chose is to combine cannabinoids with Temozolomide (TMZ), the frontline GBM chemotherapeutic drug with a known mechanism of action. This combination can help to discover new mechanisms or determine whether any synergistic or additive effects could reduce drug tolerance and resistance to TMZ.

First, we needed to determine an effective concentration of TMZ to use in this combination. We performed a kill curve to determine the CC50 of TMZ for the three GBM cell lines. Despite publications reporting on the CC50 of TMZ for some of the cell lines, the values were not consistent (M. T. C. Poon et al., 2021; Soni et al., 2021) We tested TMZ at concentrations ranging from 10 µM to 1M against the three cell lines. As expected from published literature, TMZ showed no effect on T98G, while the other two lines showed a decreasing trend in cell survival with increasing doses of TMZ. Statistically, the results weren't consistent, as we were unable to fit perfect line to the data points (**Figure 13**).

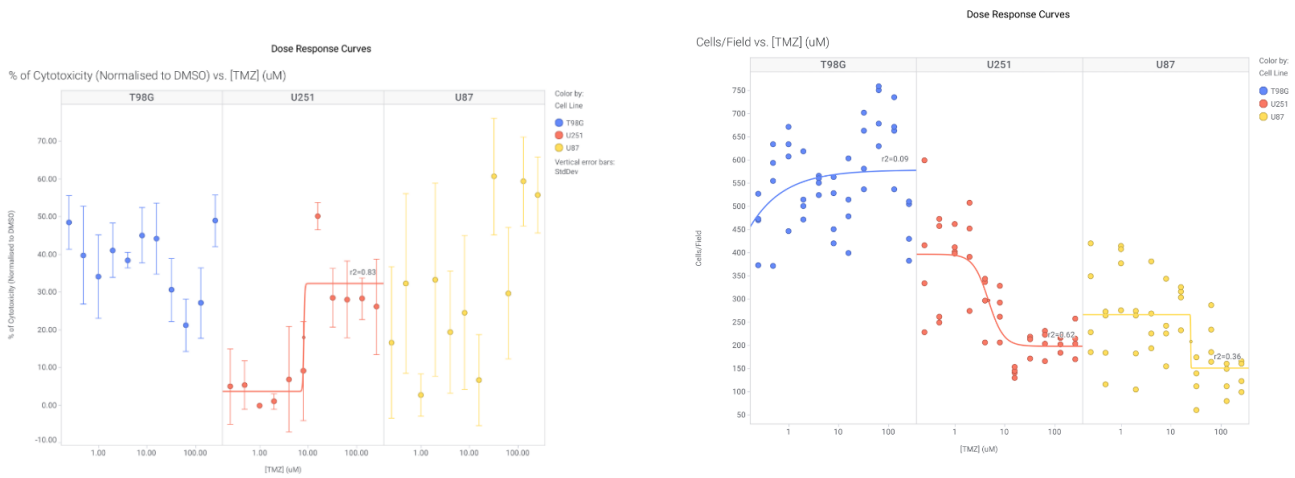

***Figure 13**: **TMZ Dose response curve on the three cell lines (U87, T98G, U251)** U251, U87, and T98G cells were plated in 384 well plates (1x10^4, 1.5x10^4, and 10,000 cells/mL, respectively) and treated with 1M to 10 µM of indicated TMZ for 48 hours. The plates were stained with Hoechst (500ng/mL) and five sites in each well were imaged by the operatta high-performance imaging and analysis. The number of detected live and dead cells were counted and analyzed. Percentage cytotoxicity was determined by the number of dead cells divided by the total number of cells multiplied by 100 and presented as a dose-response curve. Each treatment was normalized to the untreated and vehicle control (DMSO) in the same concentration. The Images show the percentage cytotoxicity (left) and live cells/field counted (right).*

For this reason, we decided to use 50 μM and 200 μM TMZ on the cells as these are widely used in literature. For the purified cannabinoids, we decided to use two concentrations; the CC50 (0.16 µg/mL) and a concentration below the CC50 (0.05µg/mL), that way we would be able to notice any synergism or additivity with TMZ. The cannabinoids had a similar range of CC50; therefore, we chose 0.16 µg/mL to reflect all the pure cannabinoids. For the extracts, we used the average CC50 values for the three cell lines, and a lower concentration (1 µg/mL) that had no significant effect on cell survival by itself. As a control to ensure that the extracts and cannabinoids are killing the cells, we also used a lethal concentration of each cannabinoid (1 µg/mL) and the extracts (5 µg/mL).

We treated the cells with the cannabinoids, extracts, and TMZ individually and then in combination with TMZ to determine if the combination of TMZ and the cannabinoids or extracts would have a higher cytotoxicity as compared to the individual treatments. According to the results shown **(Figure 14** and **Figure S3),** we identified that T98G showed resistance to all the concentrations of THC and combination with TMZ could not increase the effects. For other cannabinoids, T98G was resistant to the smaller concentration (0.05 µg/mL), but showed sensitivity to the CC50 concentrations. There was an observed increase in cytotoxicity with the cannabinoid-TMZ combinations especially with the smaller concentration of the cannabinoids. T98G also showed resistance to the two concentrations of TMZ used with no cytotoxicity recorded, **figure 14A.**

A

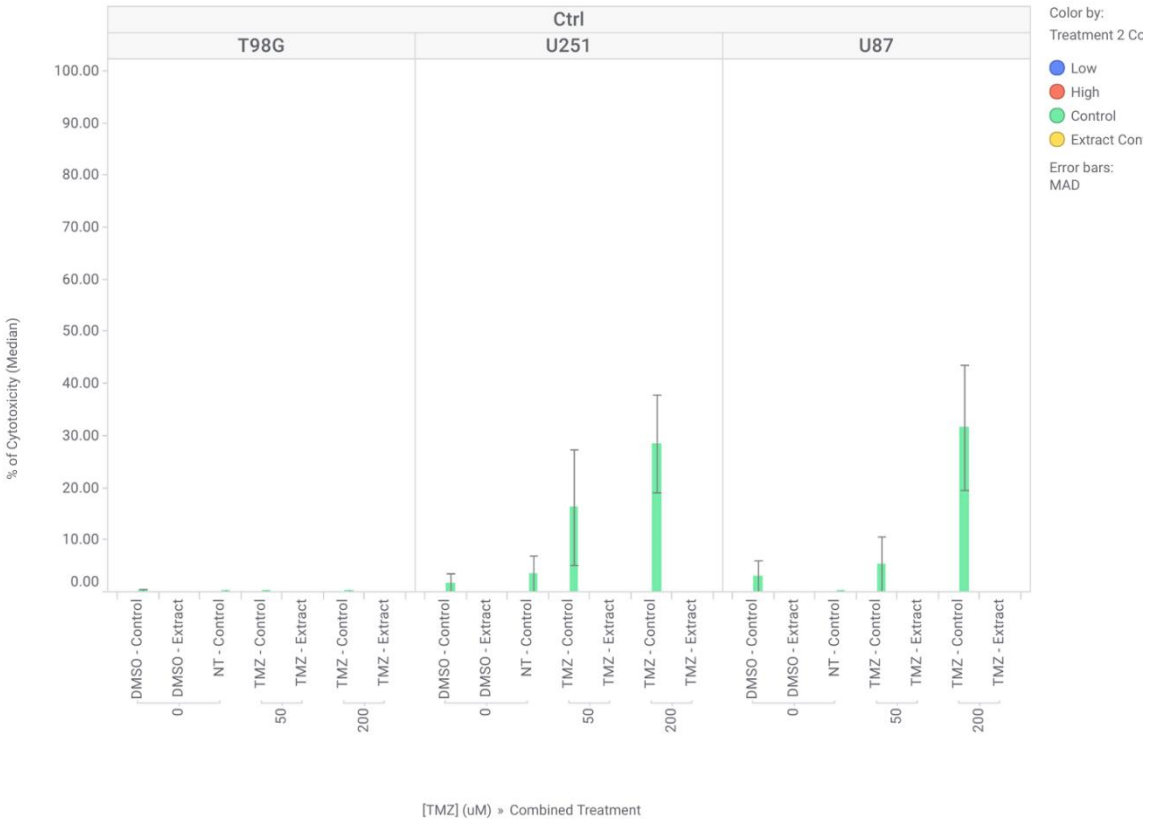

B

Treatment Combinations

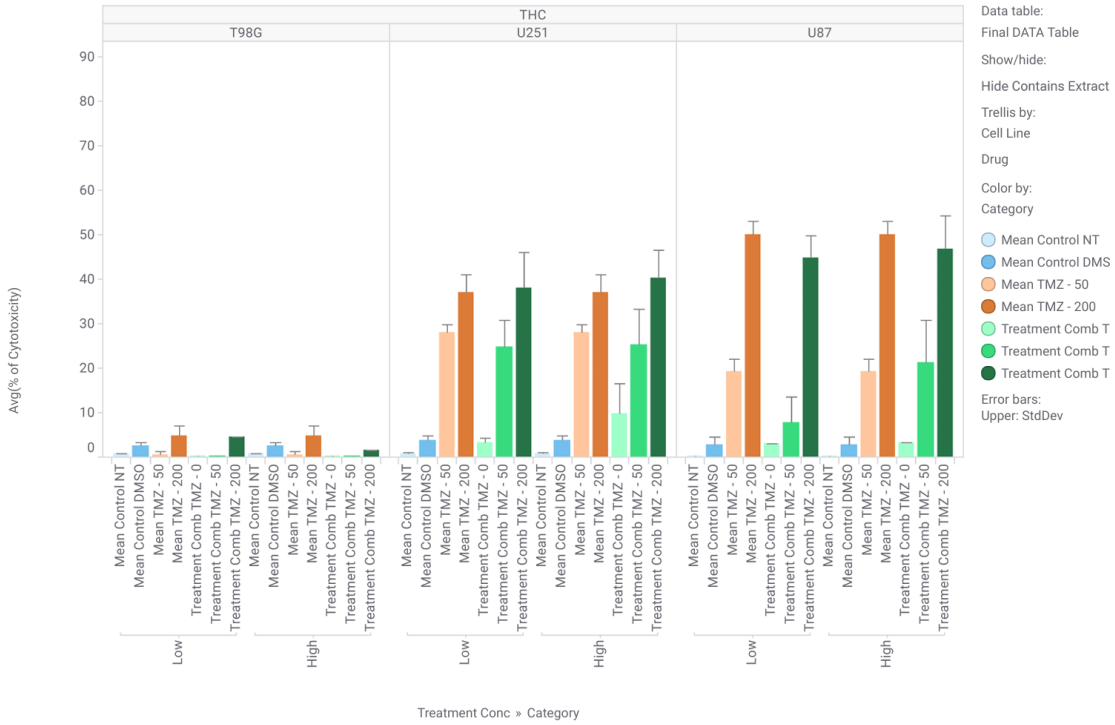

C

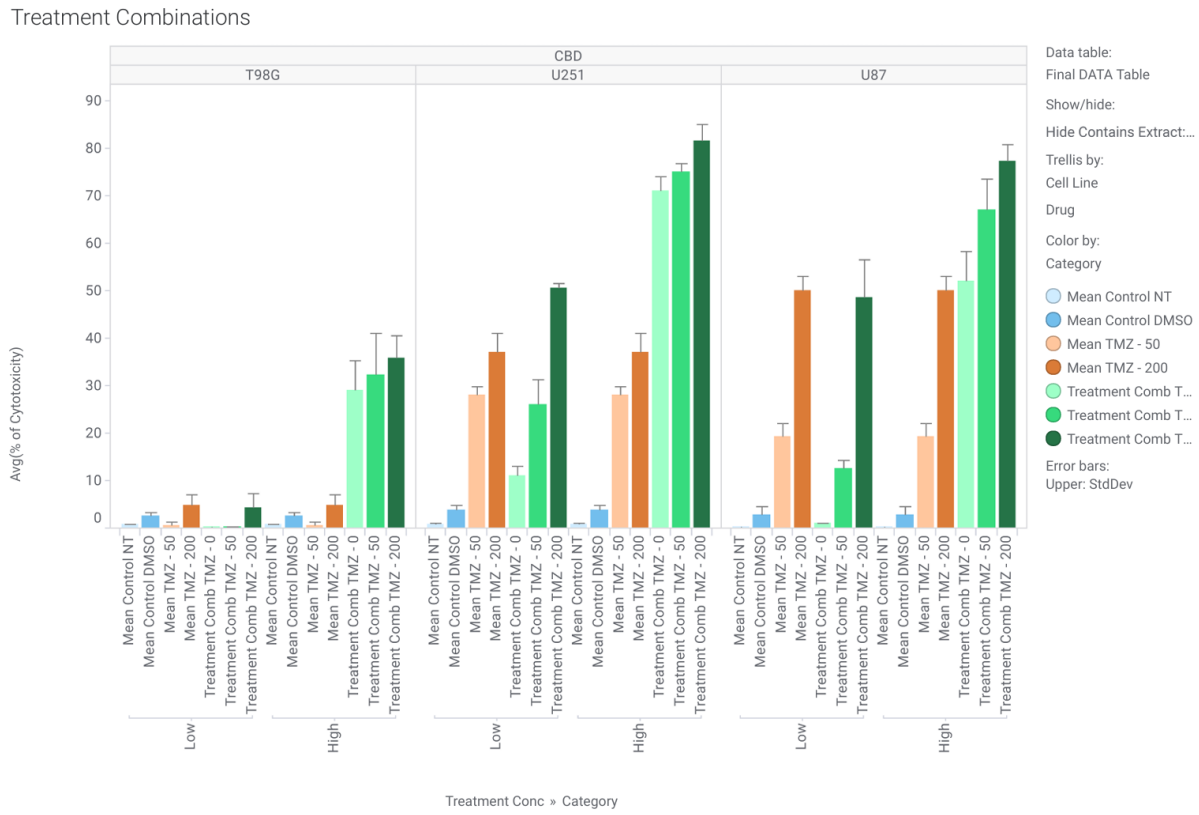

Figure 14: Combining TMZ with the cannabinoids increased glioblastoma cell death. *U251, U87, and T98G cells were plated in 384 well plates (1x10^4, 1.5x10^4, and 10,000 cells/mL, respectively) and treated for 48 hours with 50 µM and 200µM TMZ (Green bars), CC50 cannabinoids, low concentration of cannabinoid (0.05 µg/mL), and cannabinoid concentration with the two TMZ concentrations simultaneously. The plates were stained with Hoechst (500ng/mL) and five sites in each well were imaged by the operetta high-performance imaging and analysis. The number of detected live and dead cells were counted and analysed. Percentage cytotoxicity was determined by the number of dead cells divided by the total number of cells multiplied by 100 and presented as a dose-response curve. Each treatment was normalized to the untreated and vehicle control (DMSO) in the same concentration. The Images show the percentage cytotoxicity (left) and live cells/field counted (right).* ***A.)*** *Bar chart showing TMZ only treatment on the three cell lines.* ***B.)*** *Bar chart showing THC-TMZ combination on the three cell lines.* ***C.)*** *Bar chart showing CBD-TMZ combination on the three cell lines. The dose response-curves for the remaining cannabinoids can be found in the appendix. Results were statistically analysed (n=6) using Kruskal-Wallis ANOVA with multiple sample comparison. The level of significance was 0.05.*

For the extracts, T98G maintained the same pattern of resistance, but for other cell lines, there was some observed increase in cytotoxicity with the combinations, especially for the lower concentrations of the extracts. U87 and U251 appeared to be more sensitive to the cannabinoids, extracts, and TMZ combinations.

Treatment Combinations

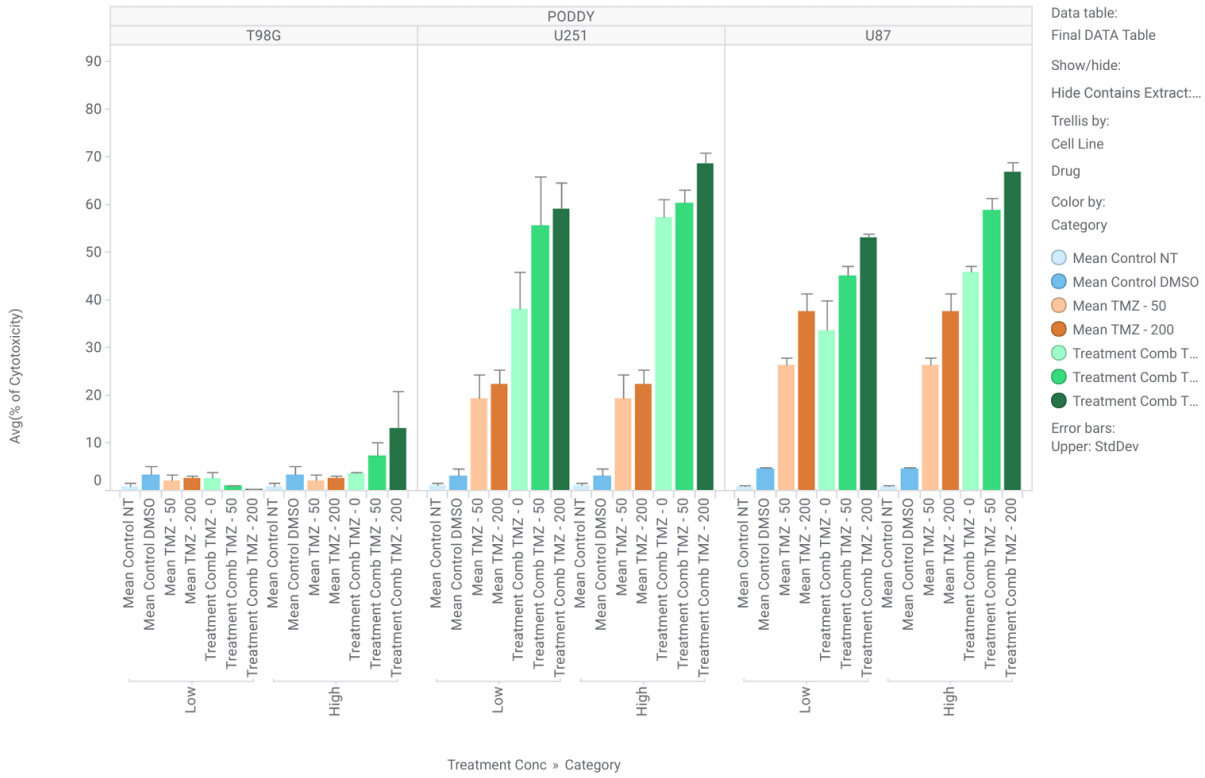

Treatment Combinations

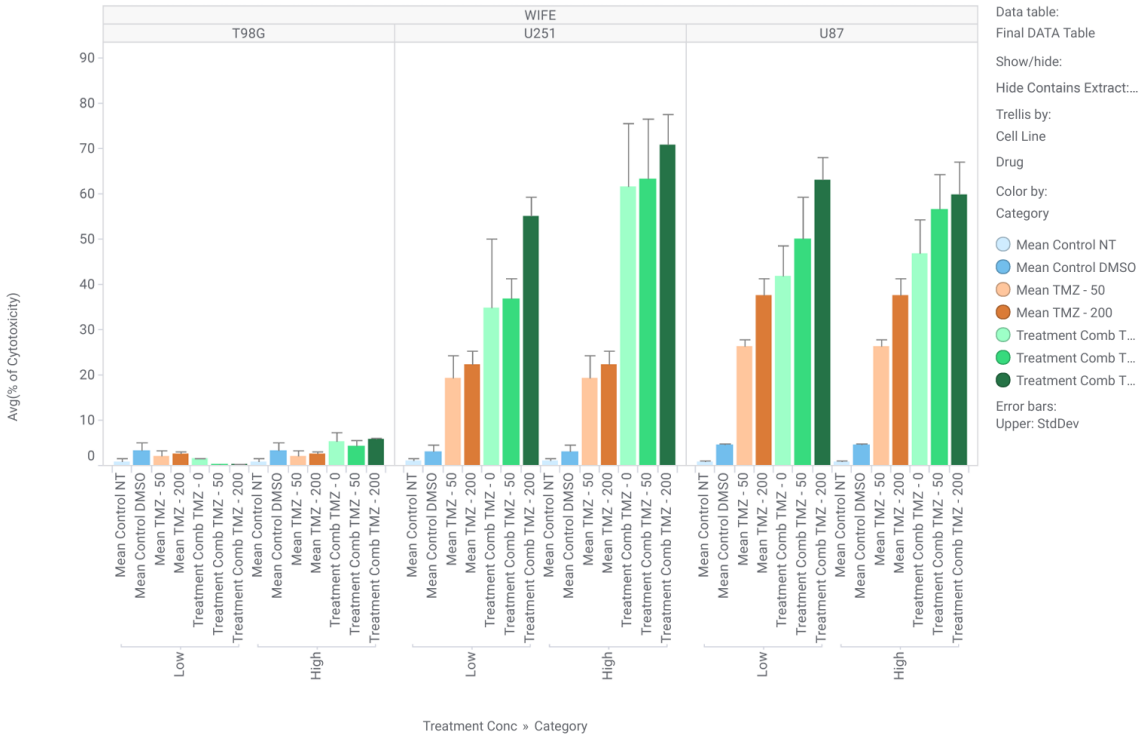

Figure 15: Combining TMZ with the cannabis extracts increased glioblastoma cell death. *U251, U87, and T98G cells were plated in 384 well plates (1x10^4, 1.5x10^4, and 10,000 cells/mL, respectively) and treated for 48 hours with 50 μM and 200 μM TMZ, cc50 of extracts, low concentration of extracts (1 μg/mL), and combination of each extract concentration with the two TMZ concentrations simultaneously. The plates were stained with Hoechst (500ng/mL) and five sites in each well were imaged by the operetta high-performance imaging and analysis. The number of detected live and dead cells were counted and analysed. Percentage cytotoxicity was determined by the number of dead cells divided by the total number of cells multiplied by 100 and presented as a dose-response curve. Each treatment was normalized to the untreated and vehicle control (DMSO) in the same concentration. The Images show the percentage cytotoxicity (left) and live cells/field counted (right). Top (Poddy Mouth-TMZ combination), bottom (Wife-TMZ combination). The dose response-curves for the remaining cannabis extracts can be found in the appendix. Results were statistically analysed (n=6) using Kruskal-Wallis ANOVA with multiple sample comparison. The level of significance was 0.05.*

Statistical analysis

In the statistical analysis, due to a large number of treatments across the three cell lines, an analysis of all the potential combinations of treatments across all cell lines and extracts/cannabinoids was performed. Considering the low number of replicas the Kruskal-Wallis ANOVA method with Multiple sample comparisons was used and the level of significance was 0.05. This is a non-parametric statistical test used to compare median values across more than two independent groups. The data showed that for T98G, there was a little or no significant increase in cytotoxicity for the TMZ only treatments and the low cannabinoid-TMZ and low extract-TMZ treatments. The high combination treatments showed increase in cytotoxicity compared to the TMZ only treatments. However, there were no statistical difference in cytotoxicity between each high combination treatments. **Figure 16** shows a representation of this analysis with CBD, CBG and AMS treatments. The remaining images for the other treatments can be found in the supplementary figures section.

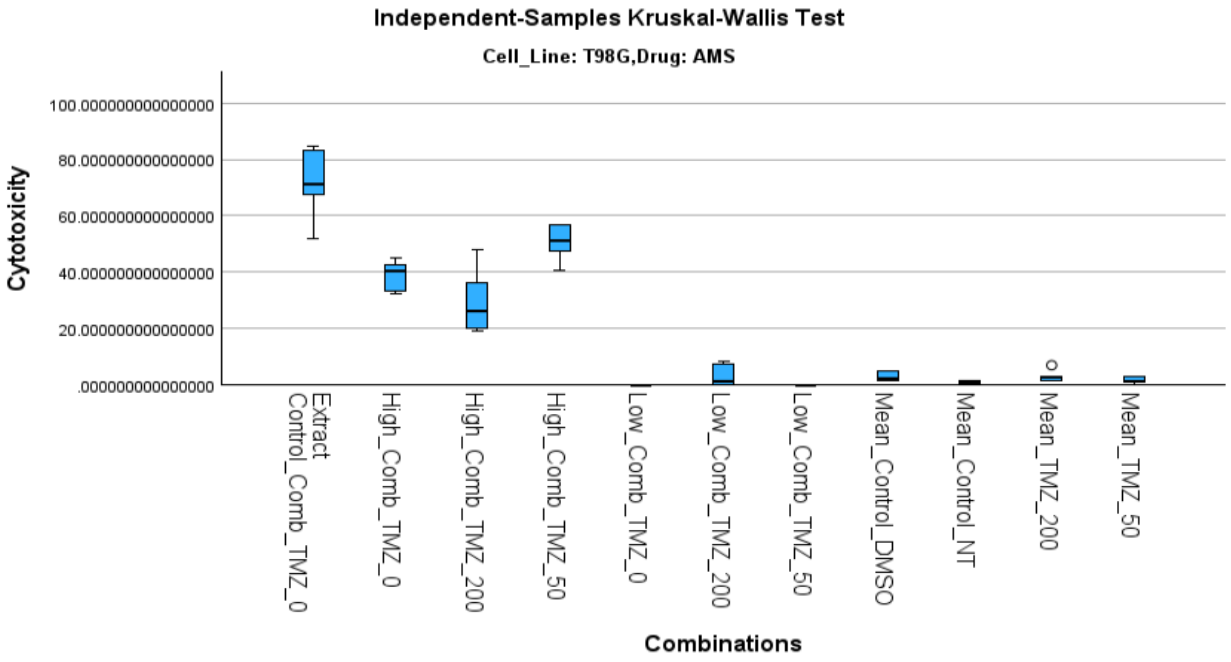
Independent-Samples Kruskal-Wallis Test
Cell_Line: T98G,Drug: AMS
Cytotoxicity
100.000000000000000
80.000000000000000
60.000000000000000
40.000000000000000
20.000000000000000
.000000000000000
Extract Control_Comb_TMZ_0
High_Comb_TMZ_0
High_Comb_TMZ_200
High_Comb_TMZ_50
Low_Comb_TMZ_0
Low_Comb_TMZ_200
Low_Comb_TMZ_50
Mean_Control_DMSO
Mean_Control_NT
Mean_TMZ_200
Mean_TMZ_50
Combinations

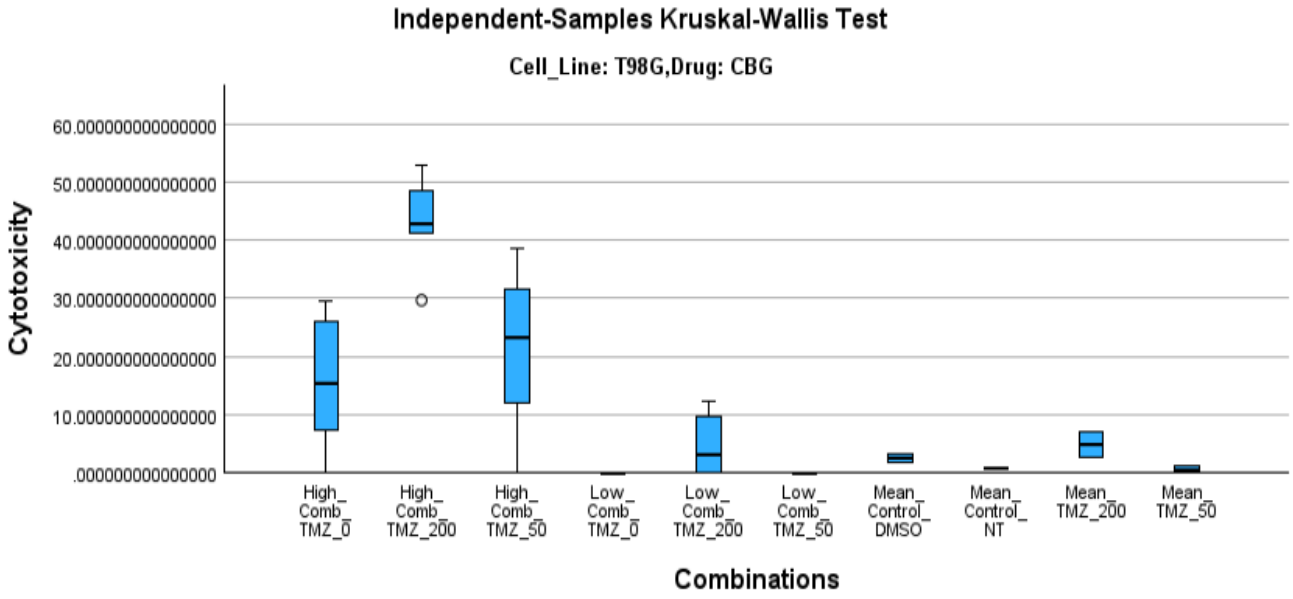
Independent-Samples Kruskal-Wallis Test
Cell_Line: T98G,Drug: CBG
Cytotoxicity
60.000000000000000
50.000000000000000
40.000000000000000
30.000000000000000
20.000000000000000
10.000000000000000
.000000000000000
High_ Comb_ TMZ_0
High_ Comb_ TMZ_200
High_ Comb_ TMZ_50
Low_ Comb_ TMZ_0
Low_ Comb_ TMZ_200
Low_ Comb_ TMZ_50
Mean_ Control_ DMSO
Mean_ Control_ NT
Mean_ TMZ_200
Mean_ TMZ_50
Combinations

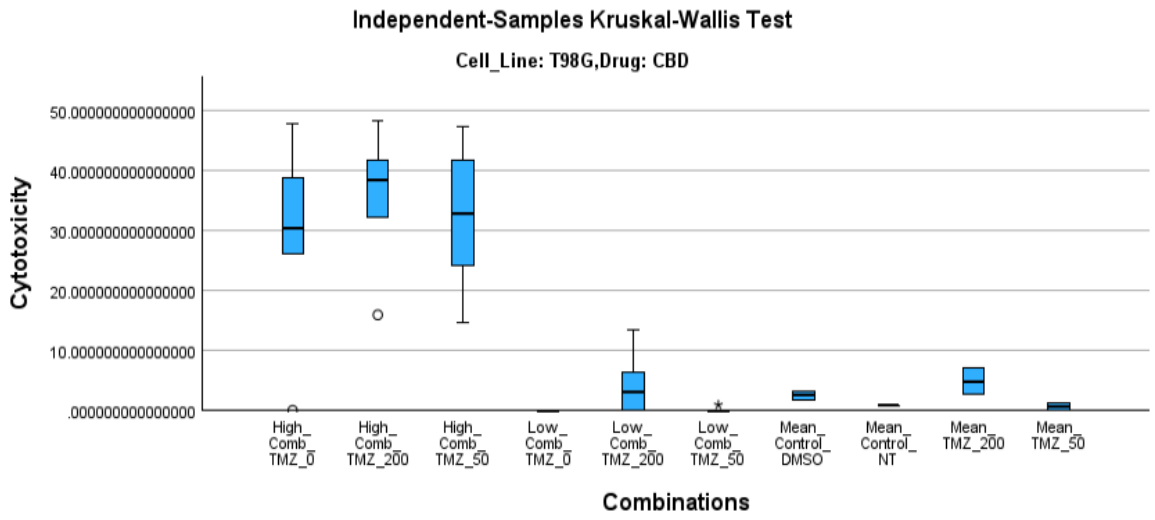

***Figure 16**: **The Independent-samaples Kruskal Walis Test confirms that T98G is resistant to TMZ and that treatment combinations with TMZ increased cytotoxicity.** The bar graphs show the treatment combinations (Top- AMS, middle- CBD, bottom- CBG) and the cytotoxicity levels for T98G from the statistical analysis test (n=6) using Kruskal-Wallis ANOVA with multiple sample comparison. The level of significance was 0.05.*

For the remaining cell lines, the TMZ only treatments showed a level of cytotoxicity lower than the treatment combinations. For some treatments, the lower concentration combinations had a higher cytotoxicity while in some others, the higher concentration combinations showed a higher cytotoxicity. However, there were no statistical difference in the cytotoxicity between the cannabinoids and extracts CC50 only treatments and the TMZ combination treatments, suggesting that the increase in cytotoxicity could be additive rather than synergistic. Representative images from CBD, RCK and WIFE are shown in **figure 17**, the remaining images are shown in the supplementary figures section 4.

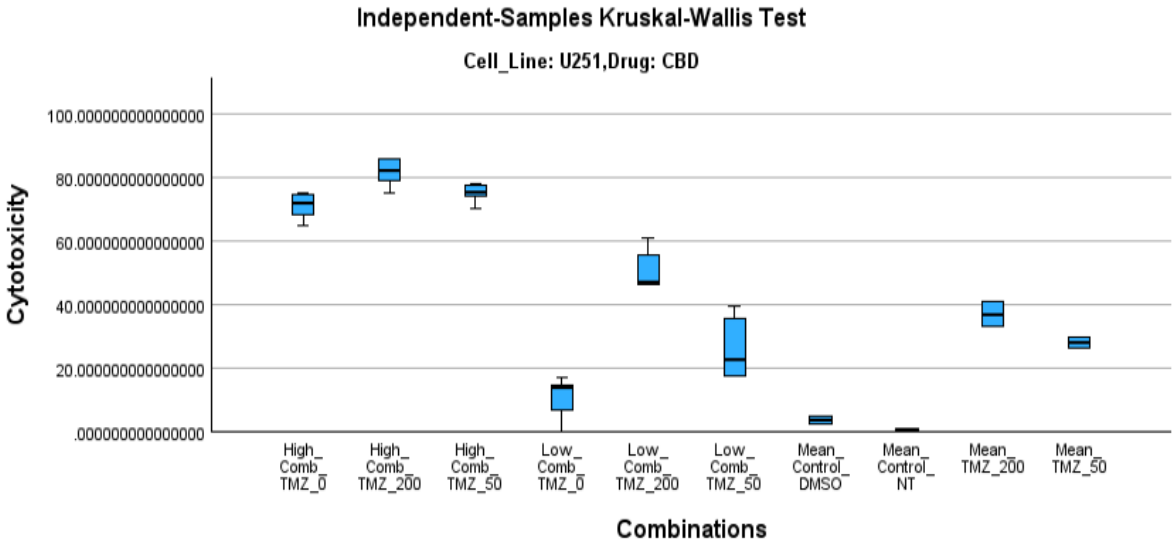
Independent-Samples Kruskal-Wallis Test
Cell_Line: U251,Drug: CBD
Cytotoxicity
100.000000000000000
80.000000000000000
60.000000000000000
40.000000000000000
20.000000000000000
.000000000000000
High_ Comb_ TMZ_0
High_ Comb_ TMZ_200
High_ Comb_ TMZ_50
Low_ Comb_ TMZ_0
Low_ Comb_ TMZ_200
Low_ Comb_ TMZ_50
Mean_ Control_ DMSO
Mean_ Control_ NT
Mean_ TMZ_200
Mean_ TMZ_50
Combinations

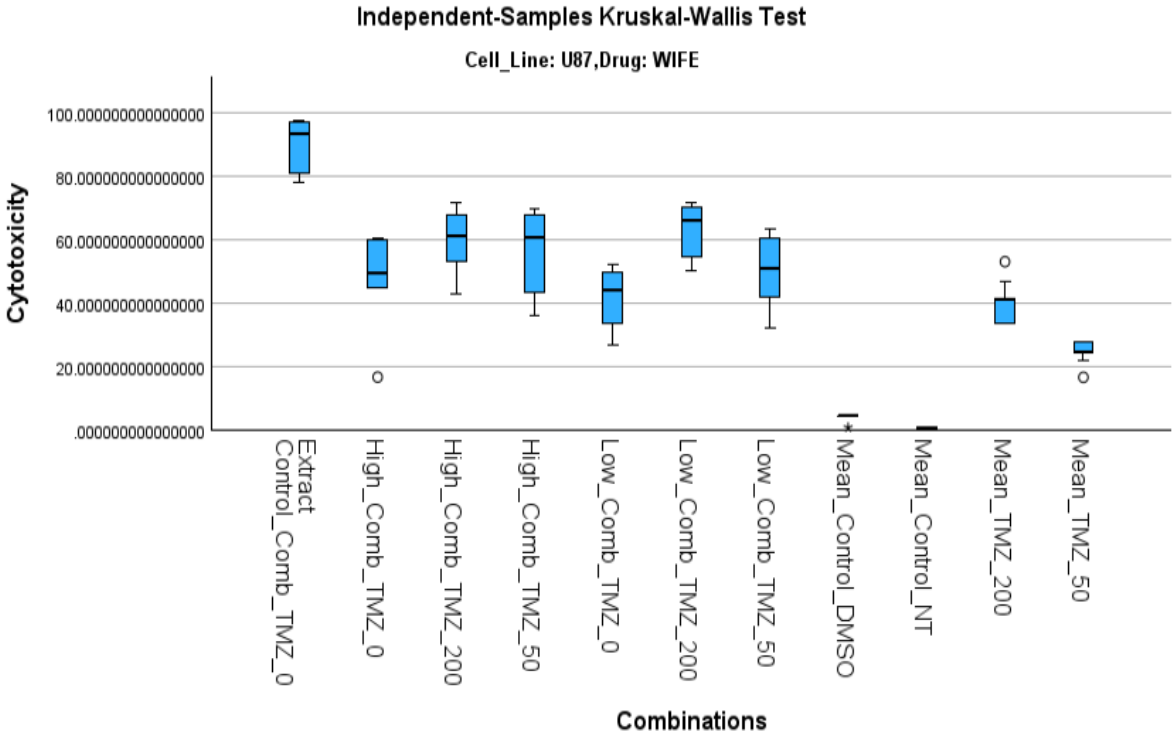
Independent-Samples Kruskal-Wallis Test
Cell_Line: U87,Drug: WIFE
Cytotoxicity
100.000000000000000
80.000000000000000
60.000000000000000
40.000000000000000
20.000000000000000
.000000000000000
Extract Control_Comb_TMZ_0
High_Comb_TMZ_0
High_Comb_TMZ_200
High_Comb_TMZ_50
Low_Comb_TMZ_0
Low_Comb_TMZ_200
Low_Comb_TMZ_50
Mean_Control_DMSO
Mean_Control_NT
Mean_TMZ_200
Mean_TMZ_50
Combinations

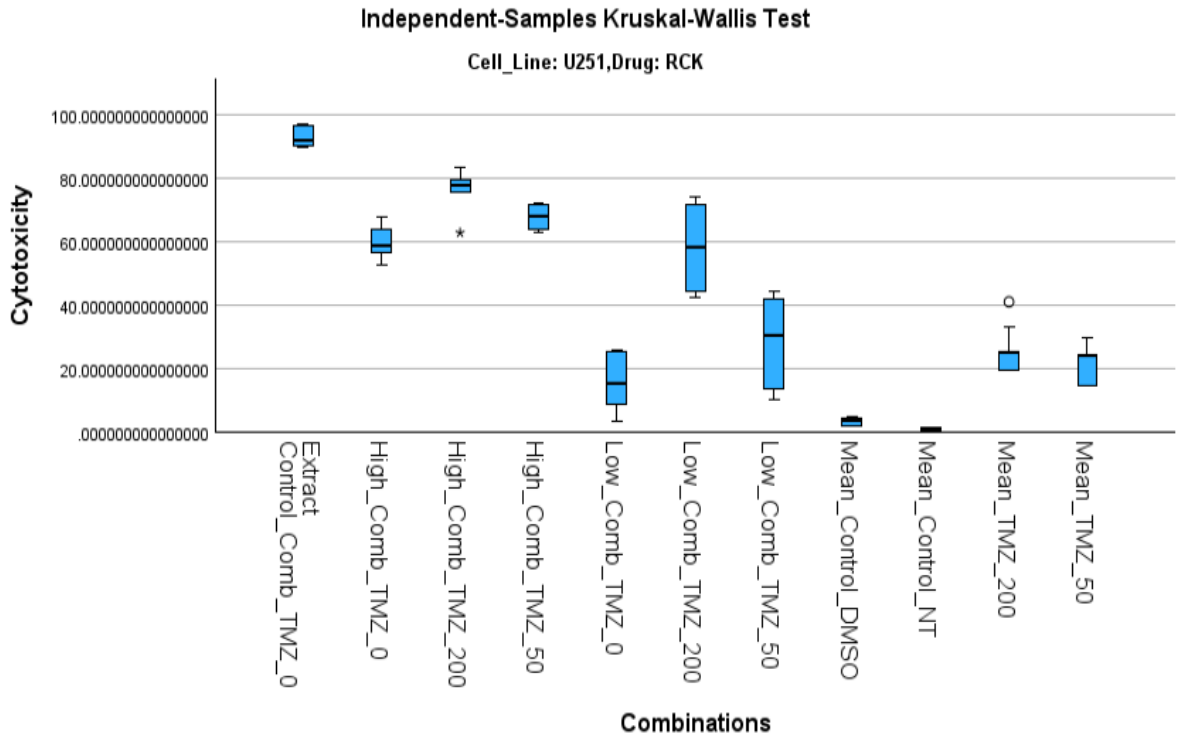

Figure 17: ***Kruskal-Wallis ANOVA with multiple sample comparison.*** *The bar graphs show the treatment combinations (Top- CBD U251, middle- WIFE U87, bottom- CBG U251) and the median cytotoxicity levels for T98G from the statistical analysis test (n=6) using Kruskal-Wallis ANOVA with multiple sample comparison. The level of significance was 0.05. The remaining images for other treatmnent combinations and cell lines can be found in the supplementary figure section 4.*

Preparation and Validation of GPCR Constructs for the Presto-Tango Assay

Steps were taken to test the substrate specificity of cannabinoid receptors, which belong to the family of G-protein coupled receptors (GPCRs). While some integral membrane receptor members of the ECS have been characterized using the Presto-Tango assay system (Kroeze et al., 2015). To study how cannabinoids interact with them, the aim was to test both cannabinoid agonists and antagonists, as well as purified cannabinoids, to see how they might activate or block these receptors. This could also help identify any unknown (orphan) GPCRs that respond to cannabinoids and give a better idea of how these compounds work in the body.

The presto-Tango system works by expressing GPCR constructs that carry a small FLAG tag on their extracellular domain, allowing the confirmation of the presence of the receptor on the cell surface. When a ligand binds to the GPCR and stimulates it, it triggers recruitment of β-arrestin, which is linked to a transcriptional activator. This leads to the transcription of the luciferase gene, producing a measurable fluorescent or luminescent signal. The stronger the signal, the more receptor has been activated. By comparing the signal intensity across receptors and treatments, the cannabinoid compounds that show receptor-specific activity can be determined. **Figure 18A** shows the design and principle of the presto-tango assay.

GPCR-Tango plasmids used in this work were obtained from the Janovjak Lab and included CNR1, CNR2, GPR55, GPR3, GPR12, GPR119, GPR6, and GPR18. They were isolated using the Midi/Maxi Prep Kit, and the plasmids were then sequenced by Dr. Josh Dubwosky using nanopore to confirm their accuracy. The sequencing results were consistent with the reference sequences found in databases, showing that the plasmids were correct and ready to use.

After sequence confirmation, the GPCR-Tango plasmids were transfected into U251 cells by lipofection. Forty-eight hours later, immunohistochemistry to detect the FLAG tag on each GPCR was then performed to check the cellular localization of each receptor. The merged GFP/DAPI images showed that the receptors were found both on the surface of the cells and in the cytosol (**Figure 18B)**. HEK239T cells expressing the luciferase gene were obtained from the Meech's lab, they also provided us with the β-arrestin plasmid for transfection into the HEK293T cells. However, due to time limitations, the Presto-Tango assay itself was not completed. However, all

the preparation steps were successfully done, providing a solid foundation for future experiments to study how cannabinoids may activate or influence GPCR signaling.

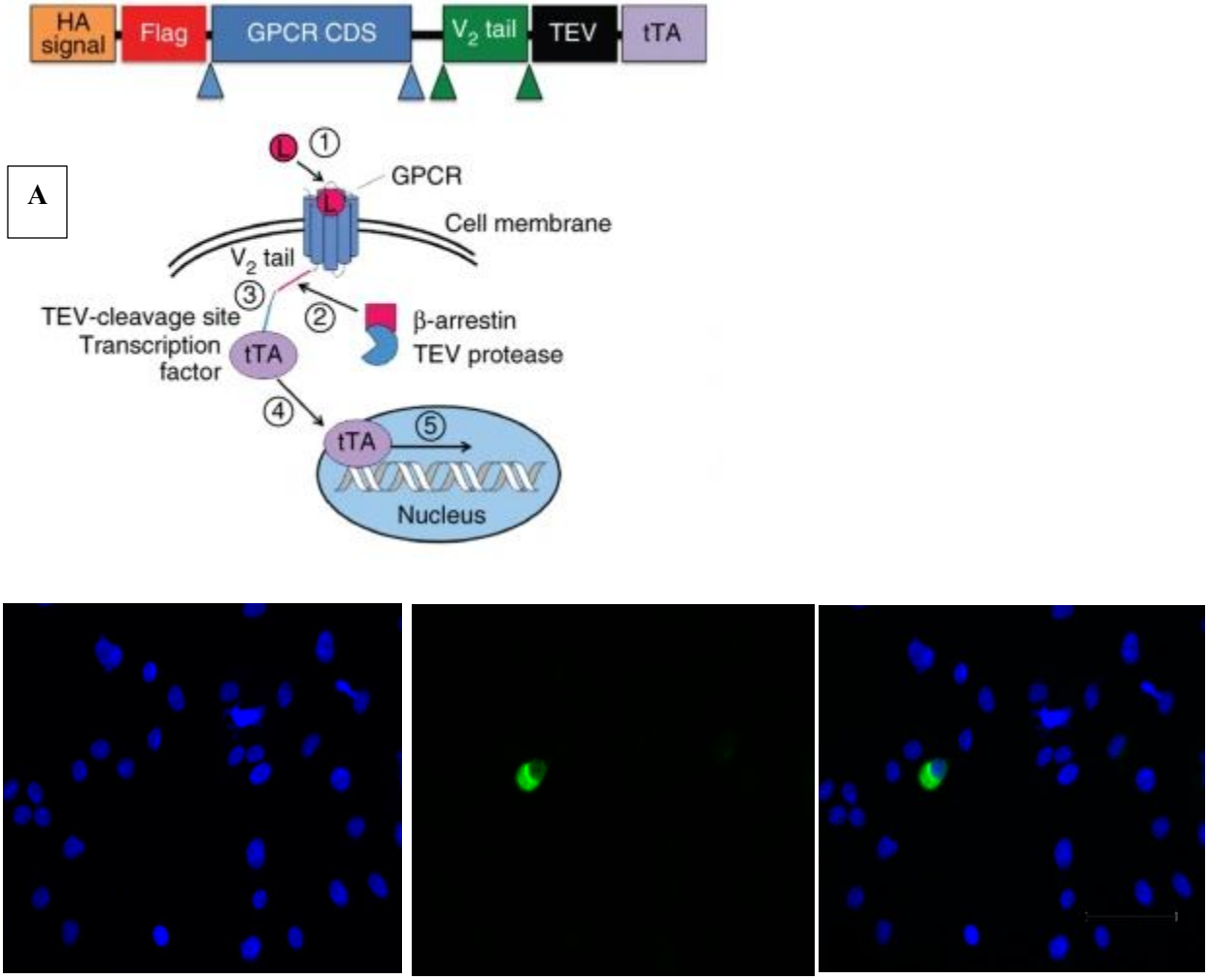

Figure 16: A.) Design and principle of the Presto-Tango assay*. When a ligand binds and stimulates a receptor, the β-arrestin TEV protease is recruited to cleave the TEV-cleavage site, releasing the luciferase transcription factor into the nucleus leading to the transcription of the luciferase gene and then subsequent luminescence.* ***B.) Localization of CNRI-Tango construct in transfected U251 cells.*** *U251 Cells were transfected with CNR1-Tango plasmid and immunolabeled using a rabbit anti-FLAG primary antibody followed by Alexa fluor 488-conjugated anti rabbit secondary antibody to visualize receptor expression (green). Nuclei were counterstained with DAPI (blue). The right panel shows the merged image of DAPI and GFP channels, demonstrating both nuclear and receptor fluorescence. The middle panel shows the Alexa fluor 488 signal corresponding to CNR1-Tango localized predominantly on the cell surface, while the left panel displays DAPI staining of cell nuclei. The remaining GPCR images can be found in the appendix.*

Discussion

In this study, the effects of cannabis extracts from different strains and pure cannabinoids on glioblastoma cells were assessed. It also examined how cannabinoids influence the sensitivity of cell lines to TMZ chemotherapy. The phytocannabinoid profiles of each extract, analyzed through mass spectrometry, showed variability between the different cannabis strains (**Figure 8**). This variability in the phytocannabinoid composition led to differences in the ability to induce glioblastoma cell death (**Fig. 10**). The dose-response assay revealed that the *Poddy Mouth* and *The Wife* strains were more effective against the three cell lines than other strains in causing glioblastoma cell death. However, the CC50 of each extract against each cell line (U251, U87, T98G) was noted for use in the combination assay. Three cell lines were used in this study to reflect the high tumour diversity, which is one of the main challenges in glioblastoma.

To determine the effect of individual cannabinoids on GBM cell death and to find out what cannabinoid combination could be responsible for the cytotoxic effects in the extracts, 7 purified cannabinoids were tested against the three cell lines for 48 hours. The CC50 profiles of the purified cannabinoids across U87, U251, and T98G **(Figure 7C)** revealed distinct patterns of cytotoxic potency, suggesting differential cellular susceptibility to the pure cannabinoids. Among the 7 cannabinoids tested, CBD consistently demonstrated high potency across the three cell lines. This highlights CBD's broad-spectrum cytotoxic potential, which has been seen in other studies on GBM cells (Seltzer et al., 2020). However, the primary psychoactive cannabinoid THC showed the weakest cytotoxicity across all cell lines, evident by its higher CC50 value. Interestingly, the non-psychoactive cannabinoids such as CBD, CBG, CBDV, CBDA, CBGA, and CBN exhibited superior cytotoxicity compared to THC (**Figure 7**). All the cannabinoids had an average CC50 of ≈0.16 μg/mL. Using this concentration, as well as a lower concentration of 0.05 μg/mL, the cannabinoids were combined with 50 μM and 200 μM TMZ to determine if the cannabinoids would sensitise the cells to TMZ, especially in T98G, which was demonstrated to be TMZ-resistant (**Figure 14A**). The treatments were administered simultaneously using the pintool of the Jannus Robot (Heidolph). The cannabis extracts were also combined at their average CC50s (**Figure 10**) and at a lower concentration of 1 μg/mL with TMZ (50 μM and 200 μM) to see the effect of the combination on cytotoxicity. It was determined that T98G was resistant to TMZ in both concentrations used **(Figure 14A)** and lower combination concentrations. However, in the other

cell lines, an increase in cytotoxicity was observed more with the lower concentration combinations compared to the high concentrations. However, from the statistical analysis via the Kruskal-Wallis test, this increase in cytotoxicity appeared to be additive rather than synergistic **(Figure 3S).** Annexin V/PI assay was performed to confirm whether the cannabinoids and extracts induced apoptosis in the cells. The results in Figure 12 show that the cannabinoids and extracts induced apoptosis after 24 hours of treatment.

To account for the variability in response among the cell lines, real-time PCR of key endocannabinoid targets was conducted to determine the relationship between the expression of these genes and drug response. The variability in the expression of these key targets **(Table 1)** suggests that the difference in sensitivity to cannabinoid treatment is related to changes in gene expression. Finally, we intended to use the Presto-Tango assay to determine the cannabinoid-GPCR relationship. The GPCR-Tango receptor plasmids were isolated from the Addgene Library (provided by the Janovjak lab). The plasmids were transfected into U251 cells to determine receptor expression and localization. The immunohistochemistry targeting the FLAG tag on each GPCR after transfecting the receptors into U251 revealed that these receptors are localized on the cell surface and in the cytosol, as expected.

The extraction of phytocannabinoids from 10 cannabis strains produced varying yields **(Table 1).** Such differences in extract mass may reflect diverse resin content, trichome density and cannabinoid potential of each strain. High-performance liquid chromatography coupled with tandem mass spectrometry (HPLC-MS/MS) confirmed the presence of five major neutral cannabinoids – CBD, CBDV, CBN, CBG, and THC in all the extracts, whereas the acidic precursors CBGA and CBDA were not detected. This absence is attributed to the thermal decarboxylation of the cannabis flower before extraction, a process that converts the acidic forms to their neutral components. Studies have shown that extracts with a high concentration of the acidic forms do not affect cell lines; however, the individual acidic forms are not well studied as much as their neutral counterparts, and cancer research has always focused on the neutral forms (Franco et al., 2020; Seo et al., 2022; Velasco et al., 2016). A previous study has also shown that CBGA is the main precursor for other cannabinoids (Fellermeier et al., 2001), suggesting possible cytotoxic effects. It is also worth noting that the cannabinoid composition in cannabis is known to vary with cultivation conditions and seasons of harvest (Crispim Massuela et al., 2022). Thus, to

determine a consistent pattern of cannabinoids in a strain, it is better to use the THC:CBD ratios (Pennypacker et al., 2022). Among the analyzed cannabinoids, THC exhibited the highest abundance overall, with *Poddy Mouth* displaying notably elevated levels compared to other strains. *Mimosa x Orange punch* showed the highest concentration of CBD, whereas the royal strain contained the greatest amount of CBG. Of great interest is the *Poddy Mouth*, which also had the highest CBN, an oxidation product of THC, indicating initial higher THC levels or longer oxidative exposure during processing, according to Sativa University. The CBD: THC ratio is skewed towards THC.

The variation in cannabinoid ratios among strains was particularly relevant for interpreting subsequent cytotoxic results. THC-rich extracts, such as those from *The Wife and Poddy Mouth,* which were more potent*,* were expected to induce more pronounced anti-proliferative and pro-apoptotic effects on GBM cells through CB1receptor activation and downstream modulation of P13K/AKT and MAPK signalling (Marcu et al., 2010). Conversely, CBD-dominant strains like the *Mimosa x Orange punch* may exhibit cytotoxic effects through ROS generation and inhibition of GPR55-mediated signalling (Lah et al., 2022). Additionally, the extracts with elevated CBG level, such as the *Royal Cookies* and watermelon zkittles, may contribute to cytotoxic synergy by targeting TRP channels and inducing apoptosis independent of the CB1 and CB2 receptors. Previous research has also emphasized the ability of CBG to synergize with other cannabinoids like CBD to increase cytotoxic activity (Lah et al., 2021). However, because studies are lacking in some of these strains, we are not certain if the cannabinoid combination in these strains might also lead to antagonism in some of the strains, for example *the mimosa strain* which has a higher CBG content found to be less effective than *The Wife strain* which had undetectable CBD levels, despite its low THC and CBD content, still showed good cytotoxicity, suggesting that its effect could be due to its CBG content. However, information from cannabis-based websites maintains that *The Wife* strain is a CBD-dominant strain, with a 20:1 CBD-THC ratio (Burdherd, 2020). Therefore, the inability to detect CBD in the mass spectrometry analysis could be due to breeding or harvesting conditions, as all the cannabis flower strains used in the study were harvested during the 2024-2025 growing season. CBG has been shown to reduce tumour growth and induce apoptosis in GBM cells via non-psychoactive pathways, especially GPR55 and TRPV receptors (Lah et al., 2022). An important follow-up experiment would be to replicate these cannabinoid combinations in the extracts using the purified cannabinoids to determine any possible synergism

or antagonism. Another important factor to consider when comparing the effects of the purified cannabinoids or their combinations to the whole plant extract is the entourage effect. There could be other bioactive compounds in the extracts that work together to produce a stronger or different biological effect, which the combination of the pure cannabinoids would not be able to recapitulate.

The purified cannabinoids were also tested individually on the three cell lines to determine the level of cytotoxic activity. CBD again proved to be more potent compared to the other cannabinoids, although all the CC50 values were similar except for THC, which proved to be less potent. Previous research has commented on the medical use of CBD for various health conditions like anxiety, pain and inflammation (Wright et al., 2020), and in the management of other types of cancer (O'Brien, 2022). CBD has also been shown to prolong survival in patients with GBM (Likar et al., 2021), and also suggested the effectiveness of the CBD and CBG combination in inducing GBM cell death through apoptosis (Lah et al., 2021). Some cytotoxic effects were also observed from the acidic variants CBDA and CBGA, suggesting that these acidic cannabinoids are also able to induce glioblastoma cell death and should be looked into. Two cell lines, U251 and U87, appeared to be more sensitive to the cannabinoids compared to T98G (Figure S1B), which is notably TMZ resistant.

Hoechst staining, which is a cell-permeable stain, can stain live and dead cells was used for these experiments; this staining is unable to tell the exact mechanism of cell death because, after the staining, only cells with intact nuclei are counted. These live cells are compared to the untreated control to determine the level of cytotoxicity. Hence, it is difficult to distinguish apoptosis from necrosis, autophagy or other death pathways. Therefore, to find out if the mechanism of cell death by these cannabinoids and extracts is a result of apoptosis, as found in the literature (Lah et al., 2021) an annexin v/PI assay was performed, where annexin V binds to phosphatidyl serine found on the outer membrane of cells in early apoptosis, while propidium iodide can only enter cells with a compromised membrane, typically found in late apoptosis or necrosis. This assay allows for simultaneous differentiation of cell death stages. Viable cells are negative for both stains, early apoptotic cells are annexin V positive and PI negative, and late apoptotic/ necrotic cells are positive for both (Lakshmanan & Batra, 2013; Rieger et al., 2011). We treated U251 cells with the CC50 of each cannabinoid and extract, and the results confirmed that these treatments induced apoptosis

after 24 hours of treatment. It was noted that THC induced more apoptosis than any other treatment at its CC50, which was over 2 µg/mL. THC is the known psychoactive cannabinoid, and a high CC50 would rather cause a psychoactive side effect. Results from a previous study suggest that THC induces apoptosis in macrophages and lymphocytes (Zhu et al., 1998). Another study also showed that THC induces glioma cell death through the stimulation of autophagy through a cascade that activated an ER stress response that promoted autophagy via tribbles homolog 3–dependent (TRB3-dependent) inhibition of the Akt/mammalian target of rapamycin complex 1 (mTORC1) axis (Salazar et al., 2009). Additionally, a study by Lah et al (2021) stated that CBD, CBG and THC induce apoptosis in primary GBM cells and GSCs.

Along with the differences in cytotoxic abilities of the different cannabinoids and extracts, differences in sensitivity between the cell lines tested were also noted. As mentioned previously, we used three cell lines with different molecular profiles to account for the heterogeneity normally found in GBM cells. Quantitative real-time RT-PCR was used to check the abundance of key genes in the endocannabinoid system to determine if the difference in the expression of these genes could be a reason why the cells behave differently to the treatments. The three cell lines have a moderate expression of the NAPE-PLD, which is an enzyme involved in producing several N-acylethanolamines, including anandamide (Ayakannu et al., 2019). Higher levels of these lipids can support cell survival by reducing stress and dampening some of the damage signals that chemotherapy normally relies on to kill cancer cells (Petersen et al., 2005). This means that when NAPE-PLD is active, cells may be better able to cope with temozolomide-induced cellular strain, contributing to reduced sensitivity. Interestingly, none of these cell lines show a detectable expression of CNR2 (CB2) receptor, suggesting that the effects of the cannabinoids and the extracts are not through that receptor, and the survival effects driven by these signalling lipids (endocannabinoids) are likely happening through alternative pathways, such as PPAR or TRPV1, rather than the typical cannabinoid receptor route. The three cell lines showed similar expression levels in other targets examined. An outstanding observation is that T98G, which appeared to be more resistant to TMZ and cannabinoid combinations, did not show expression in the CNR1 (CB1) receptor, suggesting that the absence of this receptor could contribute to its resistance to cannabinoid combinations. An unpublished study by Mor Cohn Harrell (Personal communication, 2025) found that CBG targets glioblastoma through the CB1 receptor. Also, loss or down-regulation of CB1 receptors has been reported in some cancer contexts to reduce the ability of

endocannabinoids or exogenous cannabinoids to trigger receptor-mediated death and chemosensitization pathways, and also leads to metastasis and worsening of cancer by impairing anticancer signalling (Cipriano et al., 2013; Tutino et al., 2019; Wang et al., 2008).

The cannabinoids and extracts were combined with TMZ to determine if the cannabinoids/or extracts would sensitize TMZ to chemotherapy. Three cell lines were used, one of which was T98G. T98G is a TMZ-resistant cell line, and previous research has been able to confirm this(S. Y. Lee, 2016; Pinevich et al., 2022). T98G was resistant to 50 μm and 200 μm TMZ, as shown in **Figure 14A**. It was also observed that during the TMZ kill curve in **Figure 13** that it was impossible to fit a dose response curve even when extremely high concentrations of TMZ were used. The remaining cell lines showed sensitivity to TMZ, but the CC50 was inconsistent; this might be due to the dynamic nature of these GBM cell lines or due to the condition of the cells before treatment. No definite CC50 has been recorded in literature for TMZ on these cell lines, only ranges (Michael T. C. Poon et al., 2021), that was why 50 μm 200 μm were selected based on literature for the combination assays. There was an observed increase in cytotoxicity for the T98G cell line with the combination of TMZ and cannabinoids or cannabis extracts; this was highest for the CC50 cannabinoids/ extracts combined with 200 μm of TMZ **(Figure S3 and Figure S4**). However, according to the statistical analysis using the Kruskal-Wallis comparison test, there was no statistical difference between the cytotoxicity caused by CC50 treatments alone and the CC50-TMZ combinations. This suggests that there could be an additive effect between these combinations rather than a synergistic effect. However, for U87 and T98G, the Kruskal-Wallis analysis suggests that combination treatments with TMZ may enhance cytotoxicity compared to TMZ alone, but the level depends on concentration. Previous research, however, stated that a combination of cannabinoids and TMZ can kill cells. For instance, a preclinical study carried out with TMZ-THC combination showed that the combination induced glioma cell death (Torres et al., 2011). Another study found that the administration of THC (or of THC + CBD at a 1:1 ratio) in combination with TMZ, the benchmark agent for the treatment of GBM, synergistically reduces the growth of glioma xenografts (López-Valero et al., 2018). This raises an important question on the combination of cannabinoid mixtures with TMZ. This was one of the aspects elucidated in this experiment because the different cannabis strains had different ratios of CBD and THC. However, since they contained other cannabinoids, it was unclear if these other cannabinoids and terpenes had any antagonistic or inhibitory effects. Another preclinical study

showed that THC/ORAL solution, when combined with TMZ, enhances autophagy and apoptosis in preclinical models of GBM (Sepúlveda et al., 2024). However, this study does not mention the molecular profile of the preclinical models tested, as the heterogeneity of GBM means that some models respond to this combination of treatments while others do not. Our qRT-PCR results indicate there are some links between ECS component expression of cannabinoid sensitivity, which could be further probed. The expression of these components could be tested after treatment exposure to see if they change. This could help to identify potential targets or optimized treatments toward personalized medicine. Use of patient-derived cell lines would assist with this process.

Given the knowledge that drugs bind to receptors to elicit an effect, particularly when using cannabinoids that are known to bind to the traditional CB1 and CB2 receptors, it is essential to establish the connection between these receptors and drug response. From **Figure 2**, it was observed that most of these cell lines do not express CB2 receptors as much as contrary to previous studies, stating that there is an upregulation of the overexpression of CB2R or CB1R (Hashemi et al., 2020; Wu et al., 2012) receptors in human glioma. This alteration in the expression levels of these receptors and other GPCR receptors suggests that they might be a target in finding treatments for glioblastoma. The presto-Tango assay has been validated and used to identify ligands for orphan GPCRS (Kroeze et al., 2015), and knowing that GPCRs are implicated in most other types of cancer, it would be an important assay to determine how these cannabinoids behave with CB1 and CB2 receptors, and how other GPCRS behave with the cannabinoids, and also identify orphan GPCRs for cannabinoids. Eight GPCRs were selected in this work due to their link with the endocannabinoid system and their function in other types of cancer. GPR55, GPR18, GPR119, and orphan receptors like GPR3, GPR6, and GPR12 are all class A GPCRs and are associated with the endocannabinoid system (Andradas et al., 2016; Morales & Reggio, 2017). **Figure 15A** explains the principle of the presto-Tango assay. One of the difficulties in carrying out this assay is creating a stable cell line that would express the luciferase reporter gene and the ß-arrestin gene. Our colleague, Prof. Robyn Meech, attempted to generate this line, but was only able to make a stable line with the luciferase reporter gene. While we obtained the beta-arrestin plasmid, I did not have sufficient time to complete the assay using transient transfection. However, the Presto-Tango GPCR plasmids were each transfected into U251 cells and immunohistochemistry targeting the FLAG tag showed that the receptors are expressed on the cell surface and in the cytosol, which

was a step closer to completing the optimizations needed for this assay. This assay would be invaluable in finding out how these cannabinoids behave at the receptor level.

In conclusion, the cannabinoids and extracts exerted cytotoxic effects on these cell lines, and the combination of these treatments with TMZ showed a potential to sensitize the cell lines to chemotherapy, especially in T98G, which was resistant to TMZ. However, some limitations to this study need to be addressed, and future research should conduct more optimizations to better fine-tune the results from the experiments. These limitations and future areas of development are discussed below.

Limitations of this study

Given that this study involves several high-throughput assays, it requires a lot of time to optimize the experimental conditions, including the seeding density, priming and configuring the Janus Robot and determining appropriate treatment volumes. In the beginning stages of this study, it was observed from the DMSO controls that the DMSO solvent for the cannabinoids was toxic to the cells in a concentration as low as 1%. Administering a lower concentration of DMSO required a high concentration of stock cannabinoids, which weren't available and using other dilutions of DMSO in PBS, such as 50% and 10% caused the cannabinoids and extracts to precipitate out. This issue was eventually solved after many trials using the pintool of the Jannus Robot (Heildoph), which was able to deliver 100 nL treatments.

Furthermore, it is not certain if the passage number of the cell lines affected their sensitivity. In the study, only cells in early passages (less than passage 13) were used, but it was not possible to maintain exact passage numbers for each experiment. The three cell lines had different growth rates; U251 grows faster than U87 and T98G (slowest). This meant that different seeding densities were used for these cell lines to compensate for the 48-hour treatment. The different seeding densities might give varying results in terms of sensitivity.

Due to time limitations, it was not possible to replicate the phytocannabinoid composition ratios in the extracts using the purified cannabinoids. These extracts contain other components other than the cannabinoids, which might affect the potency of these extracts (entourage effect). This would have also made it possible to have many data points in the combination experiment, such as testing

a CBD-CBG combination together with TMZ on the cell lines. Additionally, performing the combinations in other various combinations, using some cannabinoid strains from other years, and also testing these on patient-derived cell lines with different expression compared with established cell lines, which do not always recapitulate the GBM tumour, would have given a more robust idea of the ability of the cannabinoid-TMZ combination to induce cytotoxicity.

The Hoechst staining and the Annexin V/PI staining have their limitations. The annexin V assay requires resuspending the cells in TrypLE, which might lead to false-positive results from mechanical stress or improper handling. The assay is also sensitive to calcium concentrations, requiring specific buffering conditions, and annexin V binding is reversible and which may affect signal stability during analysis (Abcam, 2022). The Hoechst stain, albeit useful, has concerns of causing phototoxicity to living cells and interfering with imaging (Bucevičius et al., 2018). Thus, other functional assays and confirmatory assays, such as the TMRE assay, which measures a change in mitochondrial membrane potential, and western blotting, which detects cleaved caspases linked to apoptosis, would be more useful in this study.

Finally, to determine the effect of the treatments on the endocannabinoid system and a molecular level, qRT-PCR needed to be conducted after each treatment on the remaining lives cells to determine changes in expression level of target genes. However, due to time limitations, this was not completed.

Future research directions

One of the future research directions would be to replicate the combination Ratio of the cannabinoids in the extracts and test them on the cell lines, this is because previous research has mentioned the effectiveness of the cannabinoid ratios, especially the THC: CBD ratio. As the cannabinoid composition of each strain can change with season and time of harvest, the ratio will be invaluable in maintaining consistent comparison.

Another future research direction is to try two modes of the TMZ-Cannabinoid combination. Administering TMZ and cannabinoids together at the same time could lead to drug interactions, which might reduce the potency of each drug or cause antagonism; however, administering few hours apart might show a different effect, allowing each drug to elicit its effect through its own mechanism.

Another direction for future research is to try out different test assays. The Hoechst assay is efficient, but inculcating other reliable functional high-throughput assays could produce better readouts and increase the specificity of the results. This could include use of PI as this is only retained in dead cells.

The presto-Tango assay, as mentioned earlier, is an important future direction that should be considered due to the importance of the receptors. Information from the assay can be used to optimise drug-receptor binding and also identify Potential HITS.

Due to the heterogeneity of GBM, more cell lines and human-derived cell lines can be included in the research to account for GBM molecular diversity. Additionally, Real-Time PCR should be carried out after every treatment to determine the effect of treatment on the molecular expression levels in these cell lines.

Due to time limitations, the number of concentrations used in the combinations was reduced; future research should focus on optimizing combination concentrations to have a wider understanding of how concentrations can affect these combinations.

Supplementary figures and tables

Table S1: Primer Sequences Used for RT-qPCR

Gene	Forward Primer (5′→3′)	Reverse Primer (5′→3′)
TRPV1	ACTGGACCACCTGGAACACC	TGACGTCCTCACTTCTCCCC
TRPV4	ACCATCCTGGACATTGAGCG	CCAGTTCACCTCATCCACCC
NAPEPLD	ATGGATGACAACAAGGTGCT	GGGTCTACATGCTGGTATTTCA
GPR55	ACATCTCTCAGCCCTCTCAGC	AAGGTGGGGATGTGGACTGC
GPR119	CCTCTACCTAGTGCTGGAACGG	AAGCATGTTTCTCCTCTGGGC
EGR1	CCTAAGCTGGAGGAGATGATGC	AGTCGAGTGGTTTGGCTGGG
TERT	CCCTCTGCTACTCCATCCTG	CTGAGTGACCCCAGGAGTG
CNR1	ATACCACCTTCCGCACCAT	TCCCGCAGTCATCTTCTCTT
CNR2	TGTTCATCGCCTTCCTCTTT	ACCTCACATCCAGCCTCATT
CNR2-v1	TGCTCTGTGTGTCCCATTGT	GCTGGCTTCAGGTCTCATCT
CNR2-v2	TACTCCCATCCAAGCCTACC	TCTGTCACCCAGCATTCCTC
FAAH	CAGGGGCTACTTTGGGGATA	TTTTCAGGGGTCATCAGTCG
DAGLA	TTCTACATTGACCCTGCCATC	GCGTGTCCTGTGAGTGCTT
DAGLB	CTGCTGCTCTGCTGCTCAC	ACTGGAGACCCCTTGTGCT

Dose Response Curves

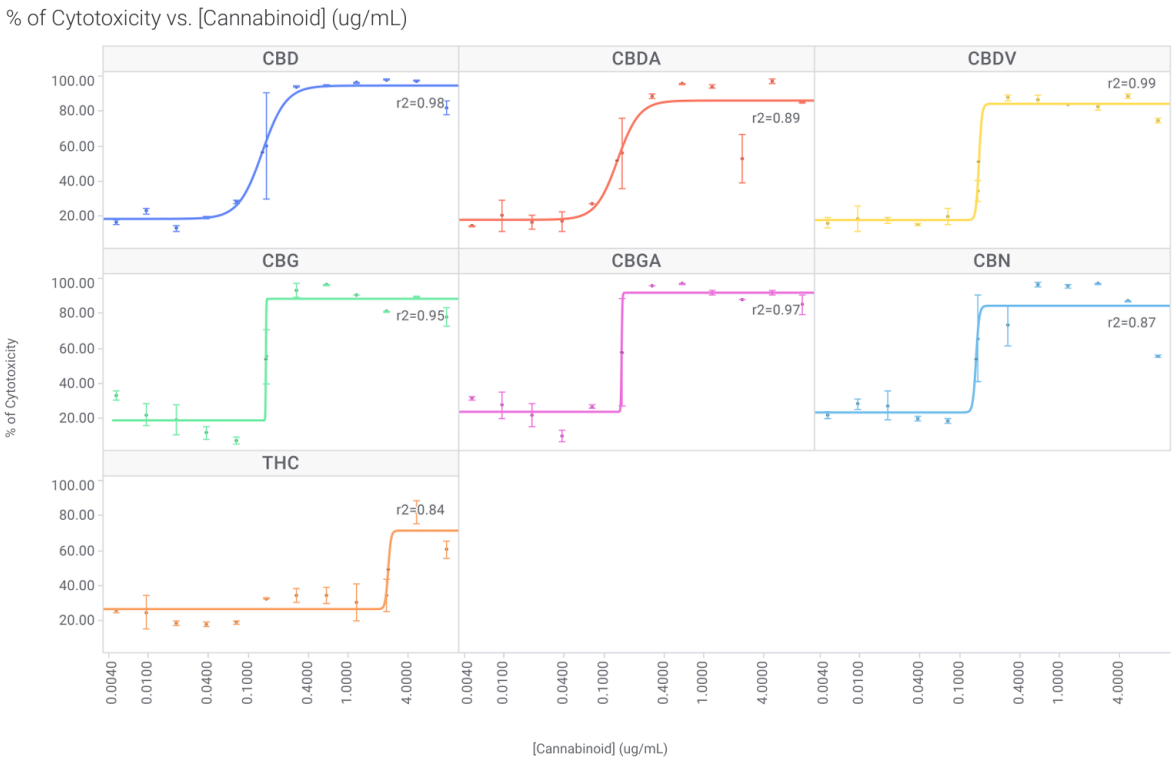

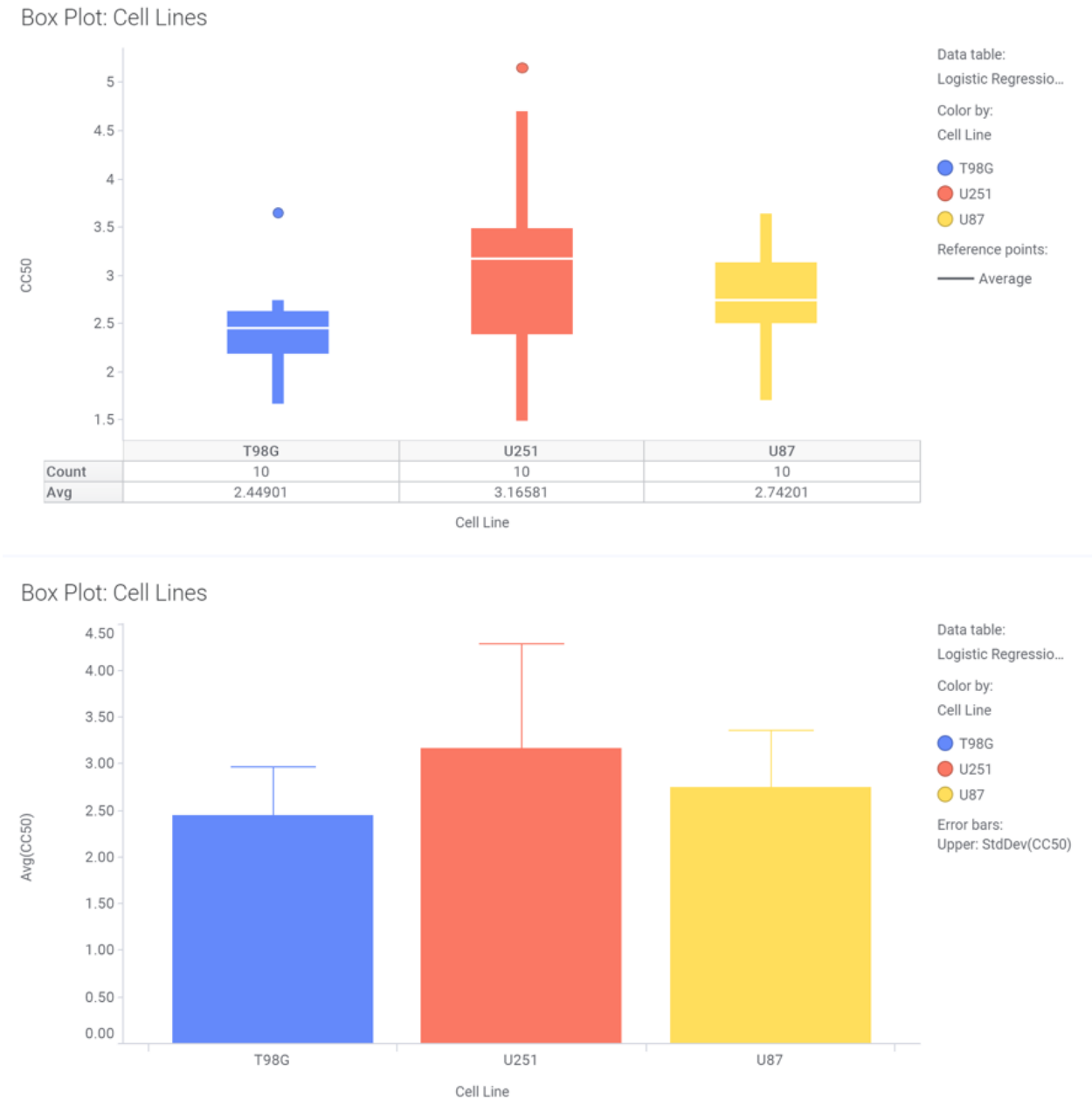

Figure S1*: *The purified cannabinoids differ in their ability to induce glioblastoma cell death. A.) *The figure shows the dose-response curve of the pure cannabinoids against T98G cell line. T98G cell lines were plated in a 384 well plate at 1500, 1000, and 500 cells/well respectively and treated with concentrations of each cannabinoid ranging from 10µg/mL to 4.68ng/mL for 48 hours. The plates were stained with Hoechst (500 ng/mL), and 4 fields in each well were imaged and analyzed using the Operetta high-content imaging and analysis system. Percentage cytotoxicity was calculated by dividing the number of dead cells by the total number of cells and multiplied by 100. To account for background cell death, cytotoxicity in each treated well was normalized to the untreated control (no-treatment well). Specifically, baseline death observed in untreated wells was subtracted from treated wells before statistical comparison. Results were averaged across biological replicates. Each sample was also compared to the vehicle control (0.5% DMSO) in the same concentration. **B.)*** *The bar graph shows the sensitivity of each cell line to treatments with Cannabinoids, T98G was the less sensitive to the cannabinoids.*

% of Cytotoxicity vs. [Extract] (ug/mL)

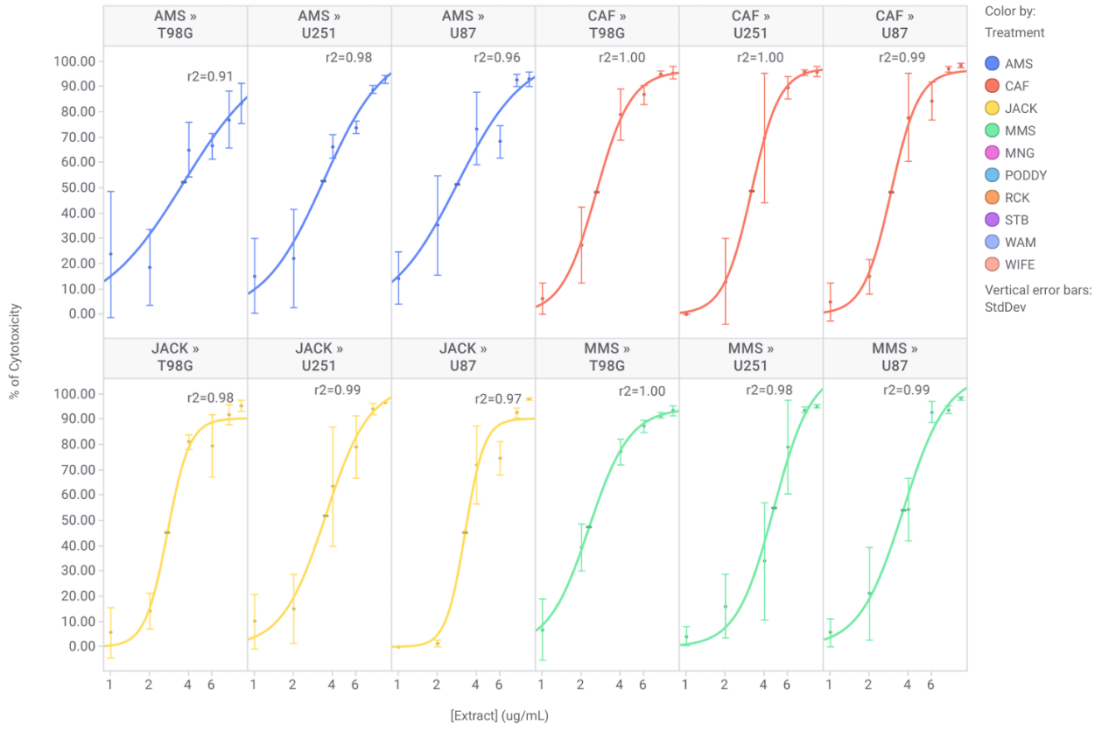

% of Cytotoxicity vs. [Extract] (ug/mL)

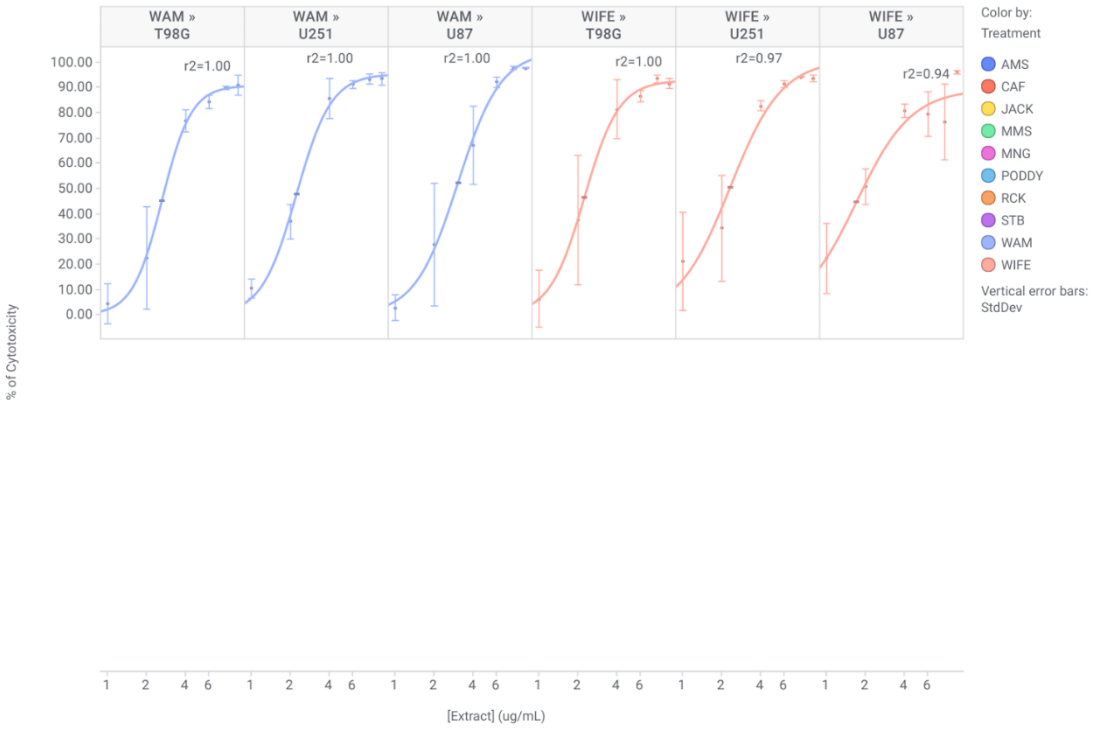

Figure 2S*: *Phytocannabinoid extracts differ in their ability to induce Glioblastoma cell death. *These figures show the dose response curves of the cannabis strain extracts against T98G, U251 and U87 Cell lines. U251, U87, and T98G cells were plated in 384 well plates (1x10^4, 1.5x10^4 and 10,000 cells/mL respectively), and treated with 1, 2, 4,8, and 10µg/mL of indicated extracts for 48 hours. The plates were stained with Hoechst (500ng/mL) and five sites in each well were imaged by the operatta high-performance imaging. The number of detected live and dead cells were counted and analyzed. Percentage cytotoxicity was determined by the number of dead cells divided by the total number of cells multiplied by 100 and presented as a dose response curve. Each treatment was normalized to the untreated and vehicle control (DMSO) in the same concentration. The dose response curves for the other extracts and cell lines can be found in the appendix.*

Supplementary Figures 3

a

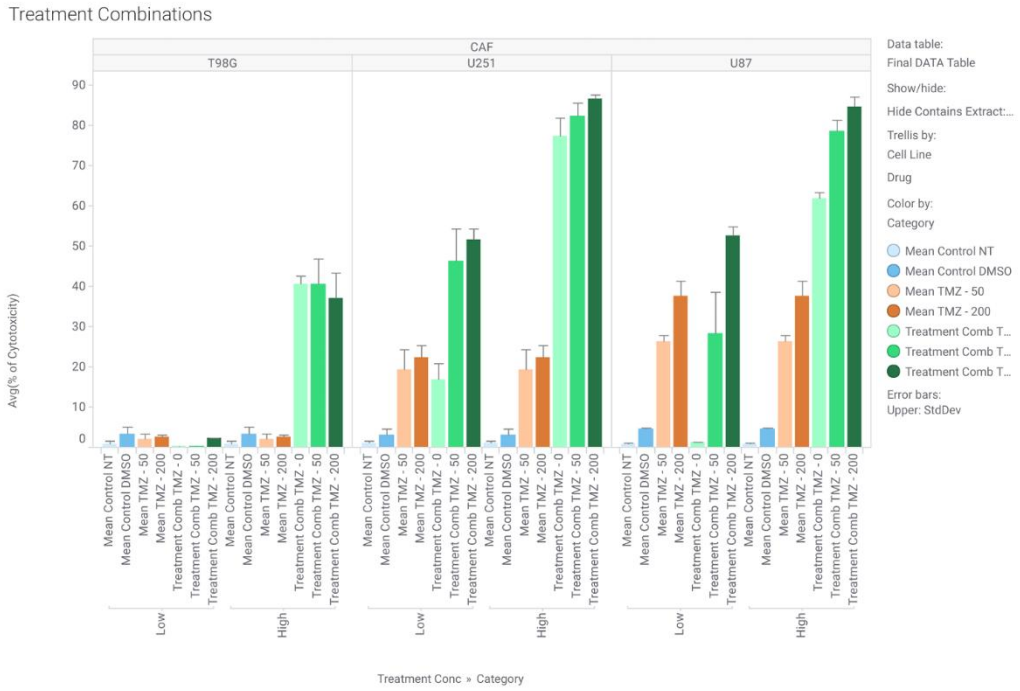

b

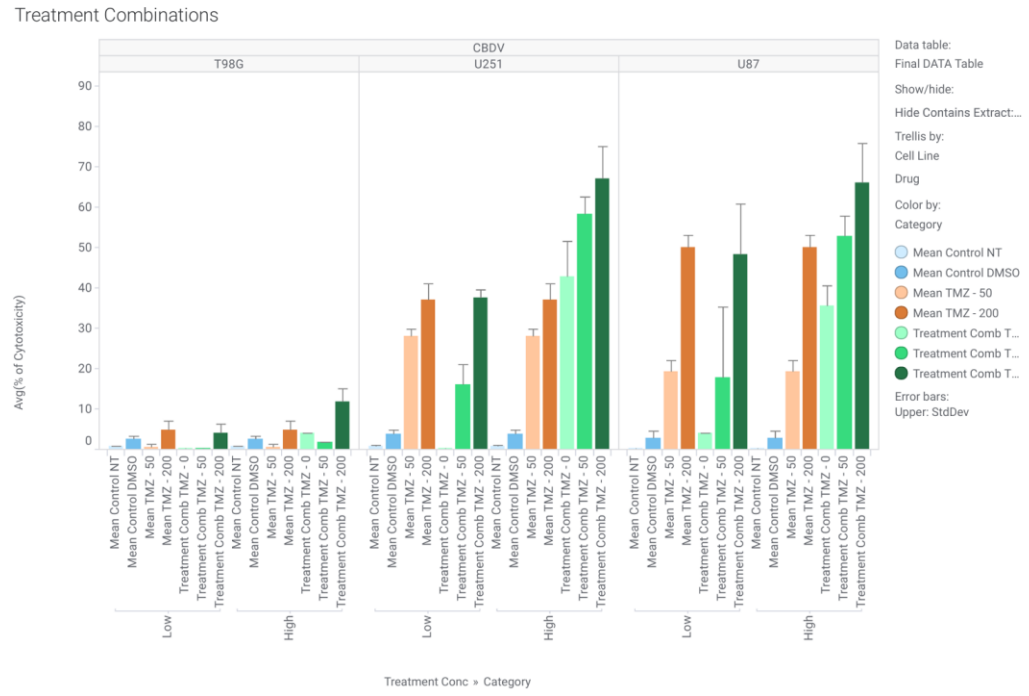
Treatment Combinations
CBDV
T98G
U251
U87
Avg(% of Cytotoxicity)
Mean Control NT
Mean Control DMSO
Mean TMZ - 50
Mean TMZ - 200
Treatment Comb TMZ - 0
Treatment Comb TMZ - 50
Treatment Comb TMZ - 200
Low
High
Treatment Conc » Category
Data table:
Final DATA Table
Show/hide:
Hide Contains Extract:...
Trellis by:
Cell Line
Drug
Color by:
Category
Mean Control NT
Mean Control DMSO
Mean TMZ - 50
Mean TMZ - 200
Treatment Comb T...
Treatment Comb T...
Treatment Comb T...
Error bars:
Upper: StdDev

c

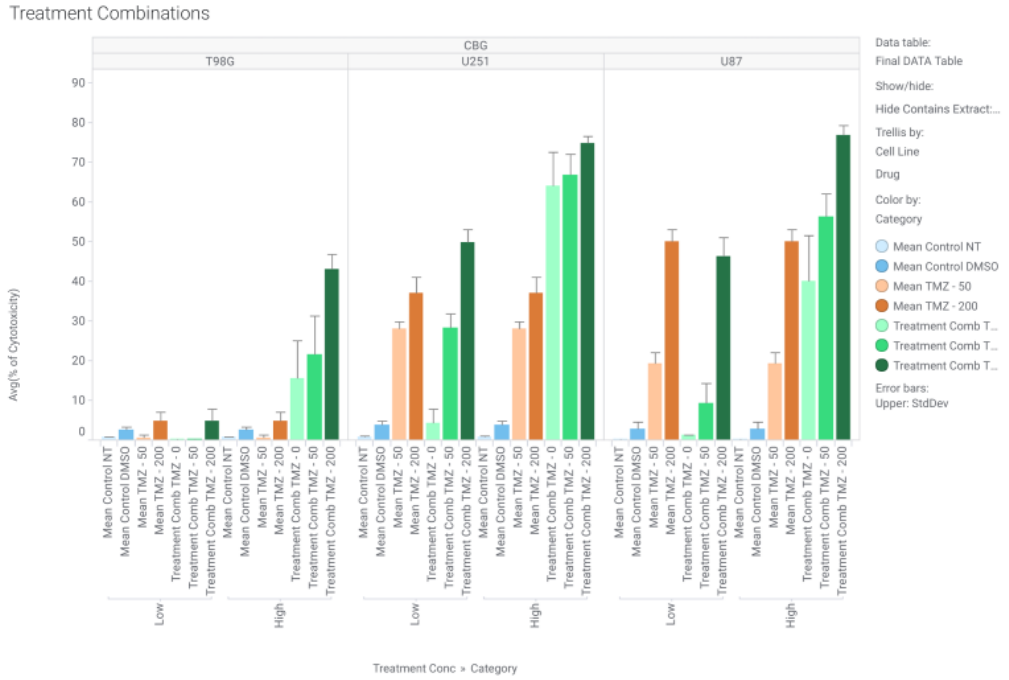
Treatment Combinations
CBG
T98G
U251
U87
Avg(% of Cytotoxicity)
Mean Control NT
Mean Control DMSO
Mean TMZ - 50
Mean TMZ - 200
Treatment Comb TMZ - 0
Treatment Comb TMZ - 50
Treatment Comb TMZ - 200
Low
High
Treatment Conc » Category
Data table:
Final DATA Table
Show/hide:
Hide Contains Extract:...
Trellis by:
Cell Line
Drug
Color by:
Category
Mean Control NT
Mean Control DMSO
Mean TMZ - 50
Mean TMZ - 200
Treatment Comb T...
Treatment Comb T...
Treatment Comb T...
Error bars:
Upper: StdDev

d

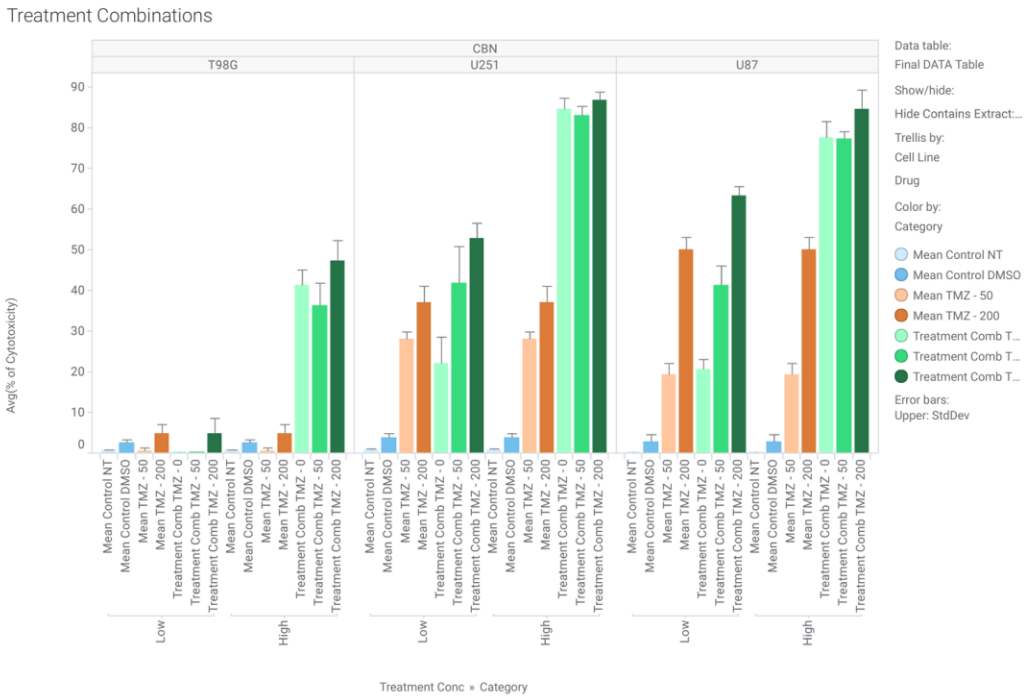
Treatment Combinations
CBN
T98G
U251
U87
Avg(% of Cytotoxicity)
Mean Control NT
Mean Control DMSO
Mean TMZ - 50
Mean TMZ - 200
Treatment Comb TMZ - 0
Treatment Comb TMZ - 50
Treatment Comb TMZ - 200
Low
High
Treatment Conc » Category
Data table:
Final DATA Table
Show/hide:
Hide Contains Extract:...
Trellis by:
Cell Line
Drug
Color by:
Category
Mean Control NT
Mean Control DMSO
Mean TMZ - 50
Mean TMZ - 200
Treatment Comb T...
Treatment Comb T...
Treatment Comb T...
Error bars:
Upper: StdDev

e

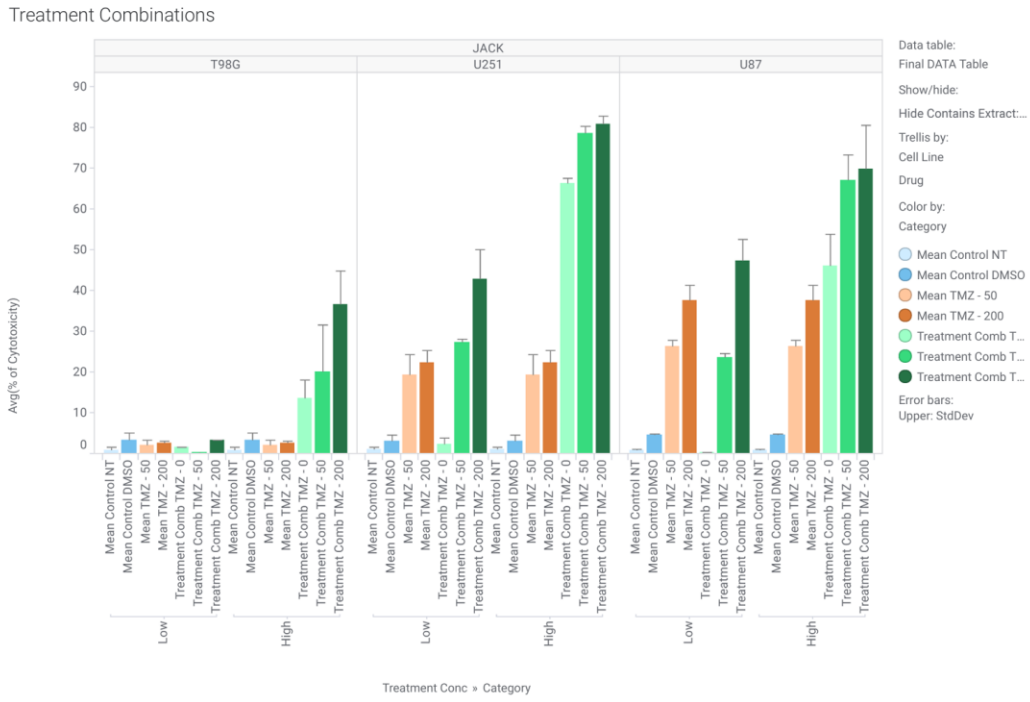
Treatment Combinations
JACK
T98G
U251
U87
Avg(% of Cytotoxicity)
Mean Control NT
Mean Control DMSO
Mean TMZ - 50
Mean TMZ - 200
Treatment Comb TMZ - 0
Treatment Comb TMZ - 50
Treatment Comb TMZ - 200
Low
High
Treatment Conc » Category
Data table:
Final DATA Table
Show/hide:
Hide Contains Extract:...
Trellis by:
Cell Line
Drug
Color by:
Category
Mean Control NT
Mean Control DMSO
Mean TMZ - 50
Mean TMZ - 200
Treatment Comb T...
Treatment Comb T...
Treatment Comb T...
Error bars:
Upper: StdDev

f

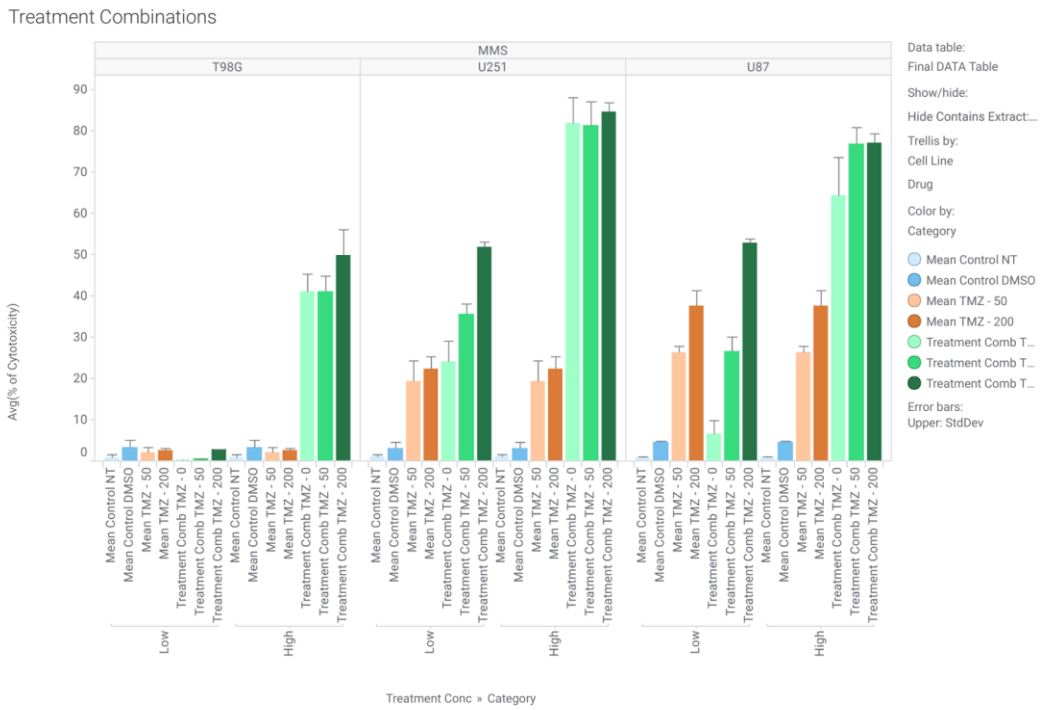
Treatment Combinations
MMS
T98G
U251
U87
Avg(% of Cytotoxicity)
Mean Control NT
Mean Control DMSO
Mean TMZ - 50
Mean TMZ - 200
Treatment Comb TMZ - 0
Treatment Comb TMZ - 50
Treatment Comb TMZ - 200
Low
High
Treatment Conc » Category
Data table:
Final DATA Table
Show/hide:
Hide Contains Extract:...
Trellis by:
Cell Line
Drug
Color by:
Category
Mean Control NT
Mean Control DMSO
Mean TMZ - 50
Mean TMZ - 200
Treatment Comb T...
Treatment Comb T...
Treatment Comb T...
Error bars:
Upper: StdDev

g

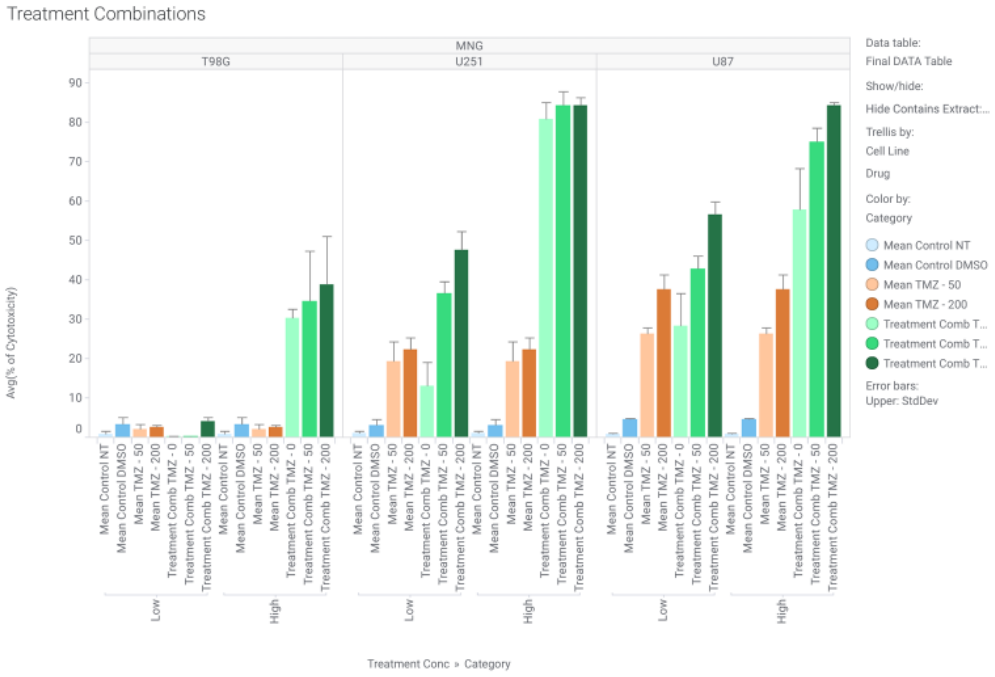
Treatment Combinations
MNG
T98G
U251
U87
Avg(% of Cytotoxicity)
Mean Control NT
Mean Control DMSO
Mean TMZ - 50
Mean TMZ - 200
Treatment Comb TMZ - 0
Treatment Comb TMZ - 50
Treatment Comb TMZ - 200
Low
High
Treatment Conc » Category
Data table:
Final DATA Table
Show/hide:
Hide Contains Extract:...
Trellis by:
Cell Line
Drug
Color by:
Category
Mean Control NT
Mean Control DMSO
Mean TMZ - 50
Mean TMZ - 200
Treatment Comb T...
Treatment Comb T...
Treatment Comb T...
Error bars:
Upper: StdDev

h

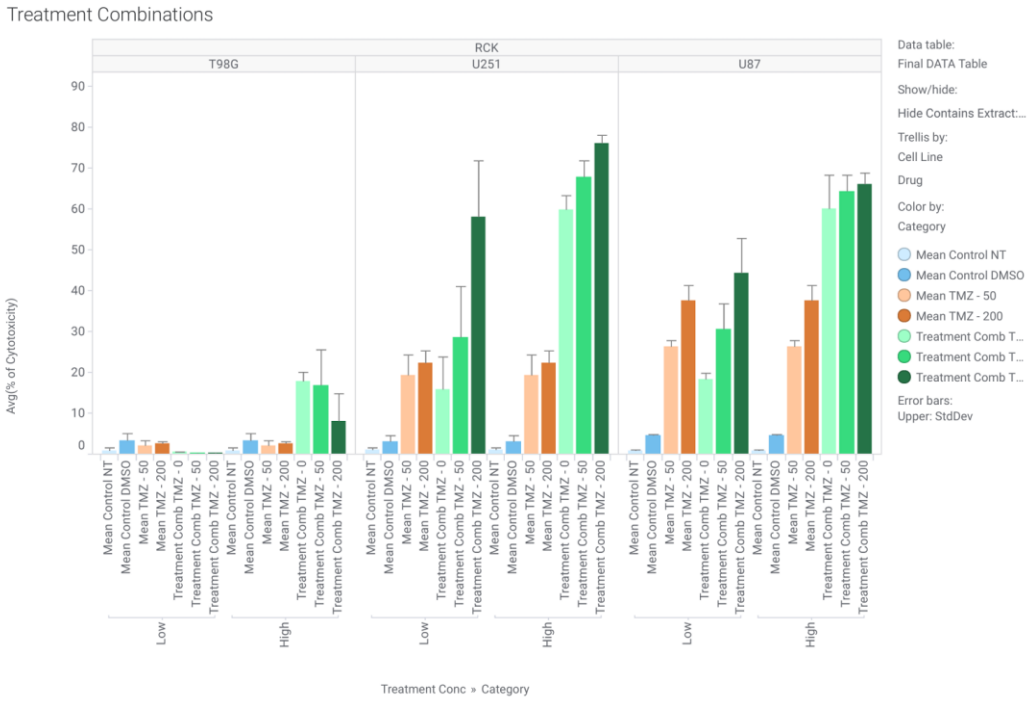
Treatment Combinations
RCK
T98G
U251
U87
Avg(% of Cytotoxicity)
Mean Control NT
Mean Control DMSO
Mean TMZ - 50
Mean TMZ - 200
Treatment Comb TMZ - 0
Treatment Comb TMZ - 50
Treatment Comb TMZ - 200
Low
High
Treatment Conc » Category
Data table:
Final DATA Table
Show/hide:
Hide Contains Extract:...
Trellis by:
Cell Line
Drug
Color by:
Category
Mean Control NT
Mean Control DMSO
Mean TMZ - 50
Mean TMZ - 200
Treatment Comb T...
Treatment Comb T...
Treatment Comb T...
Error bars:
Upper: StdDev

I

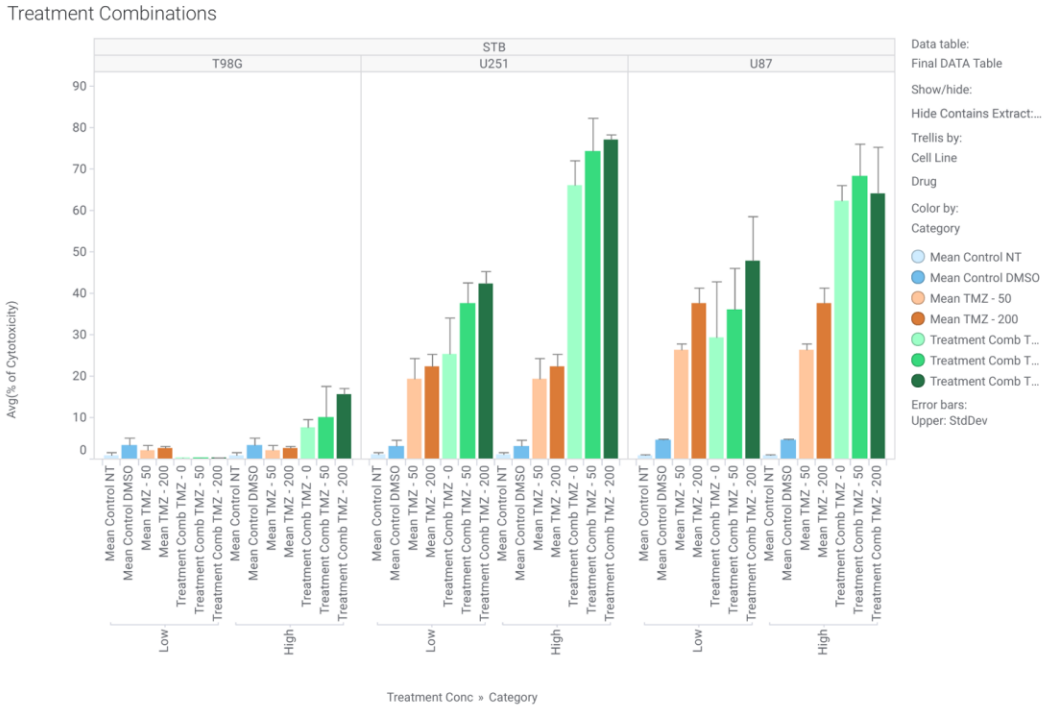
Treatment Combinations
STB
T98G
U251
U87
Avg(% of Cytotoxicity)
Mean Control NT
Mean Control DMSO
Mean TMZ - 50
Mean TMZ - 200
Treatment Comb TMZ - 0
Treatment Comb TMZ - 50
Treatment Comb TMZ - 200
Low
High
Treatment Conc » Category
Data table:
Final DATA Table
Show/hide:
Hide Contains Extract:...
Trellis by:
Cell Line
Drug
Color by:
Category
Mean Control NT
Mean Control DMSO
Mean TMZ - 50
Mean TMZ - 200
Treatment Comb T...
Treatment Comb T...
Treatment Comb T...
Error bars:
Upper: StdDev

j

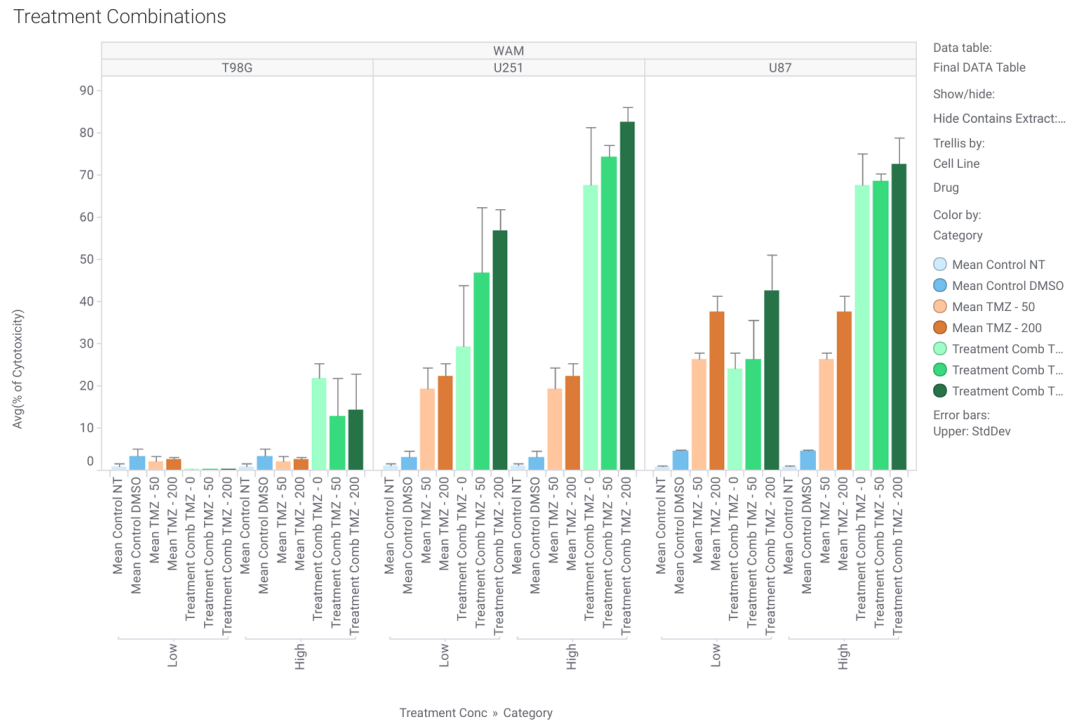

Figure 3S*: *Combining TMZ with the cannabinoids increased glioblastoma cell death. *These figures show the bar charts representing cytotoxicity for the cannabinoids, extracts, and TMZ combination treatments. U251, U87, and T98G cells were plated in 384 well plates (1x10^4, 1.5x10^4, and 10,000 cells/mL, respectively) and treated for 48 hours with 50 µM and 200µM TMZ (Green bars), CC50 cannabinoids, low concentration of cannabinoid (0.05 µg/mL), and cannabinoid concentration with the two TMZ concentrations simultaneously. The plates were stained with Hoechst (500ng/mL) and five sites in each well were imaged by the operetta high-performance imaging and analysis. The number of detected live and dead cells were counted and analyzed. Percentage cytotoxicity was determined by the number of dead cells divided by the total number of cells multiplied by 100 and presented as a dose-response curve. Each treatment was normalized to the untreated and vehicle control (DMSO) in the same concentration. The Images show the percentage cytotoxicity (left) and live cells/field counted (right). Results were statistically analysed (n=6) using Kruskal-Wallis ANOVA with multiple sample comparison. The level of significance was 0.05. The individual images are labelled A-J, the name of the treatments can be found on top of each bar chart corresponding to the following legends- Cannabidiol (CBD), Cannabidivarin (CBDV), Cannabigerol (CBG), cannabinol (CBN), Watermelon zkittles (WAM), Strawberry cookies (STB), Poddy Mouth (PODDY), The Wife (WIFE), Meringue (MNG), Mimosa x Orange punch (MMS), Royal Cookies (RCK), Amsterdam Amnesia (AMS), Jack Herer (JACK), Café Racer (CAF).*

Supplementary figure 4

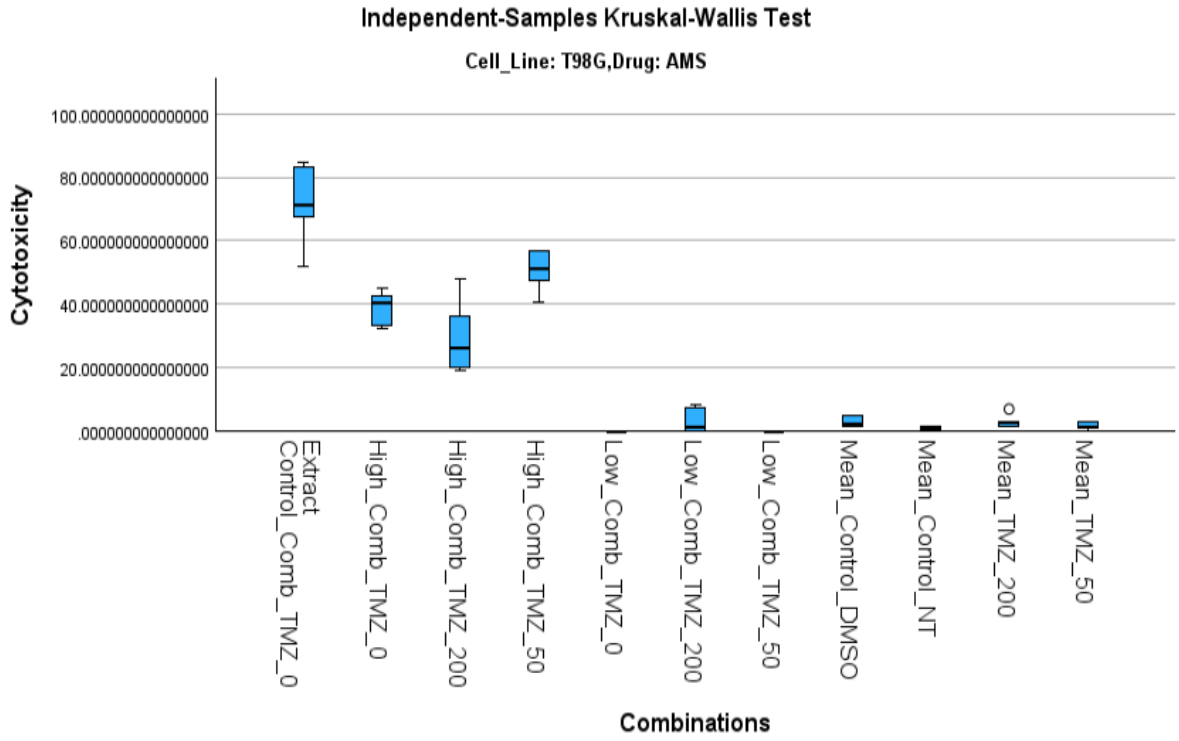

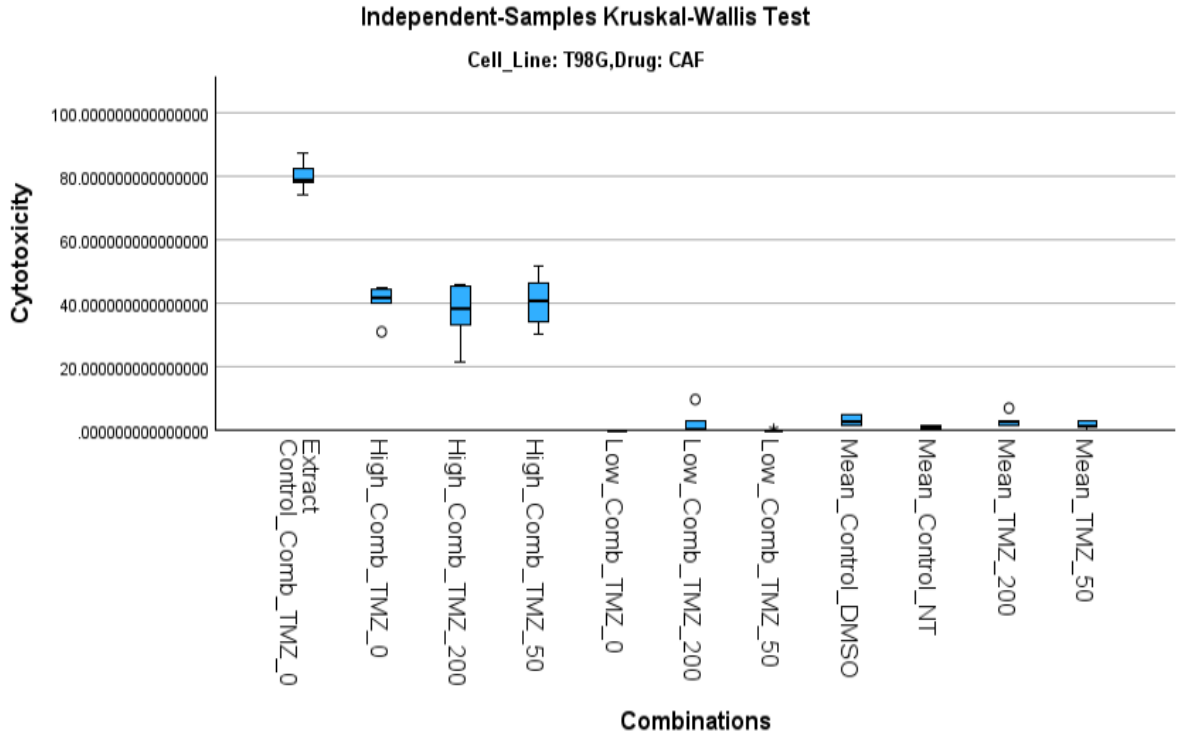

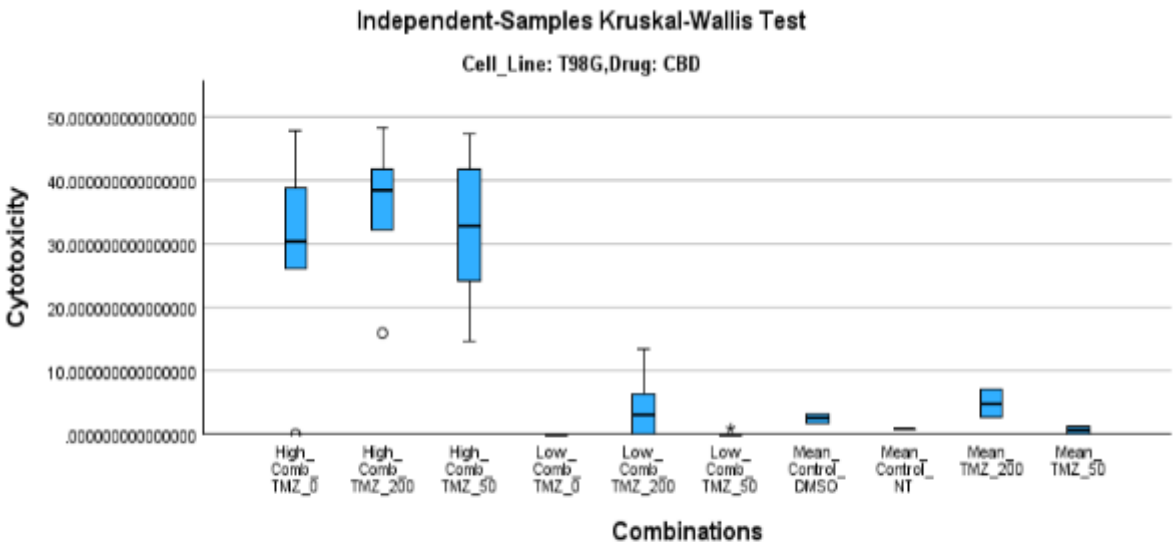
Independent-Samples Kruskal-Wallis Test
Cell_Line: T98G,Drug: CBD
Cytotoxicity
50.000000000000000
40.000000000000000
30.000000000000000
20.000000000000000
10.000000000000000
.000000000000000
High_ Comb_ TMZ_0
High_ Comb_ TMZ_200
High_ Comb_ TMZ_50
Low_ Comb_ TMZ_0
Low_ Comb_ TMZ_200
Low_ Comb_ TMZ_50
Mean_ Control_ DMSO
Mean_ Control_ NT
Mean_ TMZ_200
Mean_ TMZ_50
Combinations

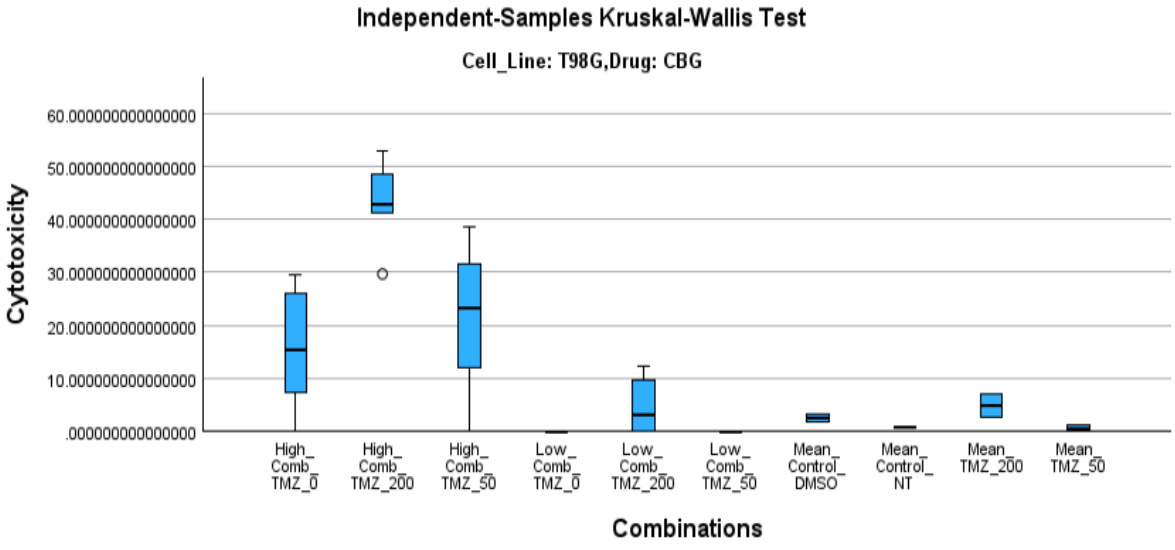
Independent-Samples Kruskal-Wallis Test
Cell_Line: T98G,Drug: CBG
Cytotoxicity
60.000000000000000
50.000000000000000
40.000000000000000
30.000000000000000
20.000000000000000
10.000000000000000
.000000000000000
High_ Comb_ TMZ_0
High_ Comb_ TMZ_200
High_ Comb_ TMZ_50
Low_ Comb_ TMZ_0
Low_ Comb_ TMZ_200
Low_ Comb_ TMZ_50
Mean_ Control_ DMSO
Mean_ Control_ NT
Mean_ TMZ_200
Mean_ TMZ_50
Combinations

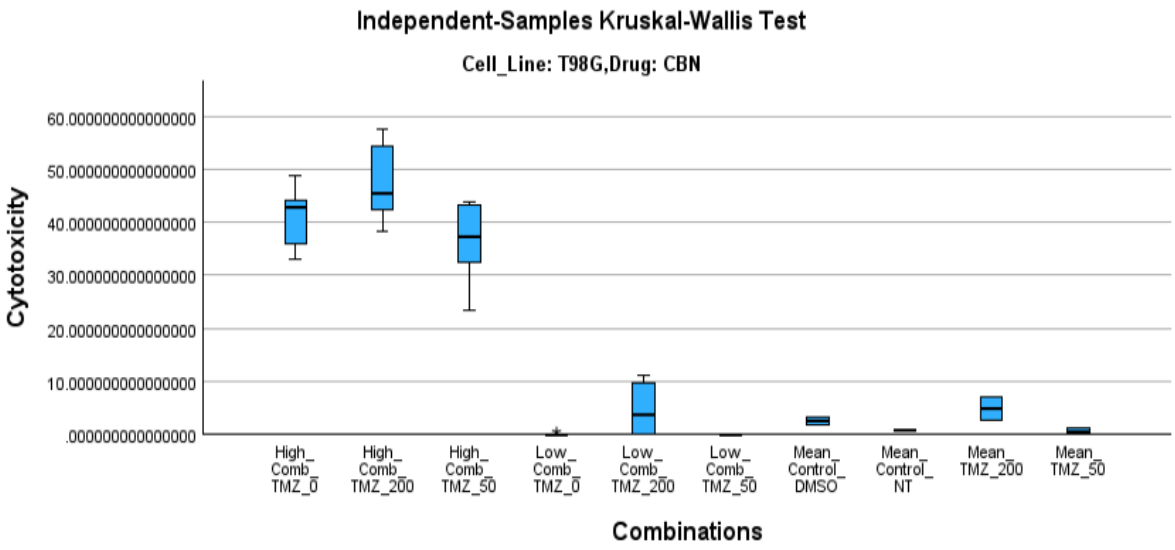
Independent-Samples Kruskal-Wallis Test
Cell_Line: T98G,Drug: CBN
Cytotoxicity
60.000000000000000
50.000000000000000
40.000000000000000
30.000000000000000
20.000000000000000
10.000000000000000
.000000000000000
High_ Comb_ TMZ_0
High_ Comb_ TMZ_200
High_ Comb_ TMZ_50
Low_ Comb_ TMZ_0
Low_ Comb_ TMZ_200
Low_ Comb_ TMZ_50
Mean_ Control_ DMSO
Mean_ Control_ NT
Mean_ TMZ_200
Mean_ TMZ_50
Combinations

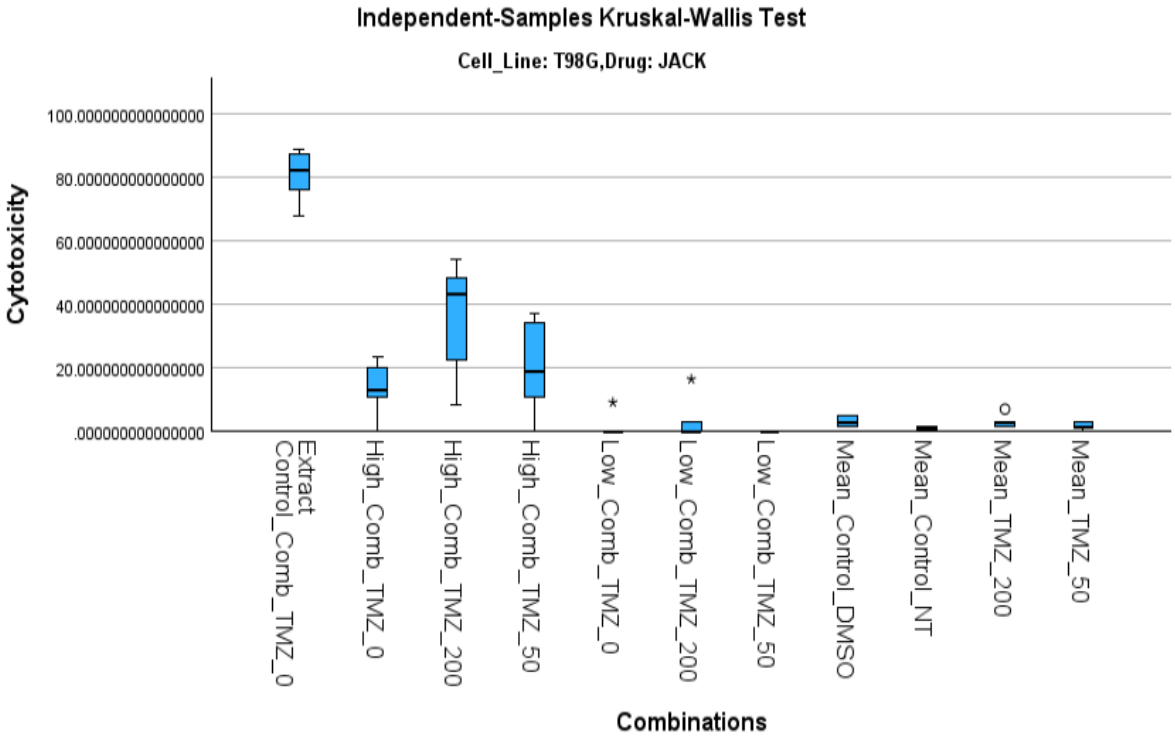
Independent-Samples Kruskal-Wallis Test
Cell_Line: T98G,Drug: JACK
Cytotoxicity
100.000000000000000
80.000000000000000
60.000000000000000
40.000000000000000
20.000000000000000
.000000000000000
Extract Control_Comb_TMZ_0
High_Comb_TMZ_0
High_Comb_TMZ_200
High_Comb_TMZ_50
Low_Comb_TMZ_0
Low_Comb_TMZ_200
Low_Comb_TMZ_50
Mean_Control_DMSO
Mean_Control_NT
Mean_TMZ_200
Mean_TMZ_50
Combinations

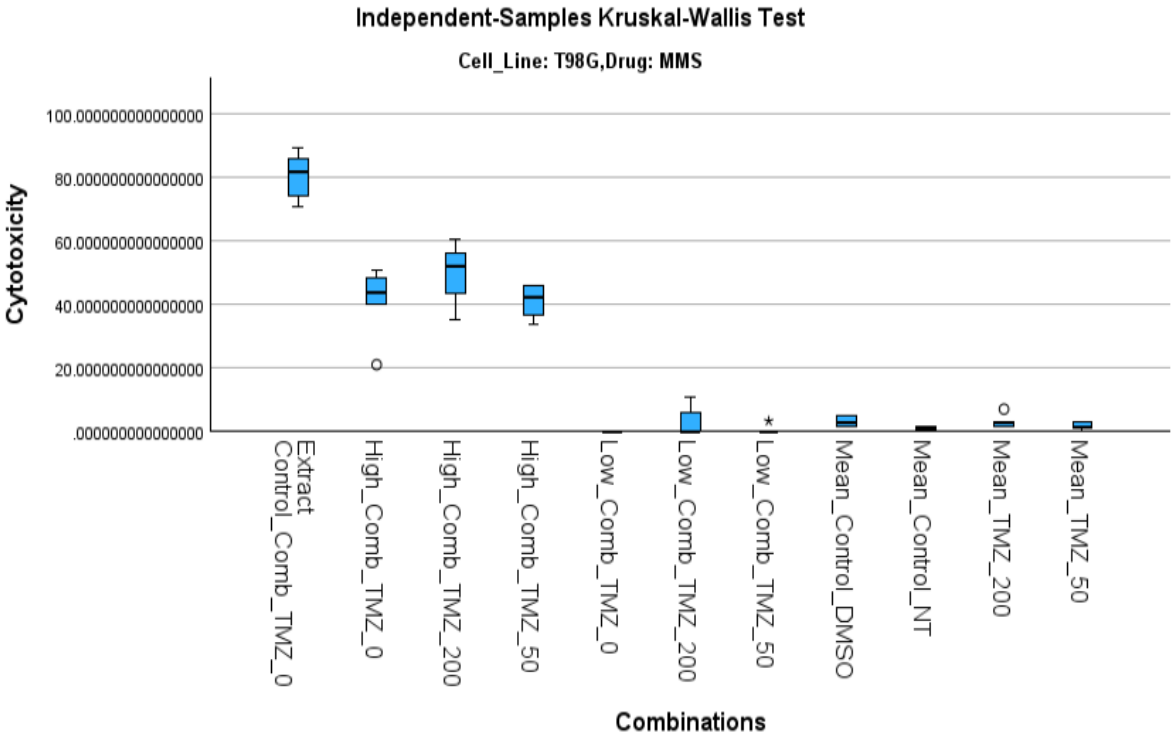
Independent-Samples Kruskal-Wallis Test
Cell_Line: T98G,Drug: MMS
Cytotoxicity
100.000000000000000
80.000000000000000
60.000000000000000
40.000000000000000
20.000000000000000
.000000000000000
Extract Control_Comb_TMZ_0
High_Comb_TMZ_0
High_Comb_TMZ_200
High_Comb_TMZ_50
Low_Comb_TMZ_0
Low_Comb_TMZ_200
Low_Comb_TMZ_50
Mean_Control_DMSO
Mean_Control_NT
Mean_TMZ_200
Mean_TMZ_50
Combinations

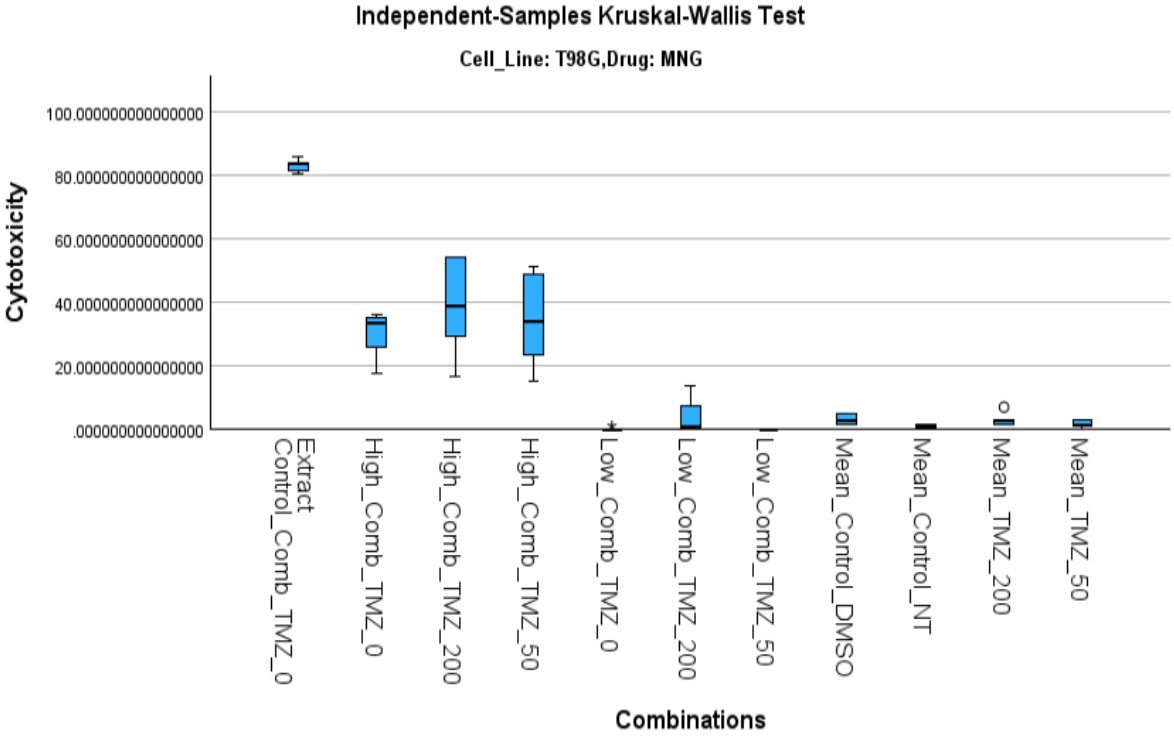
Independent-Samples Kruskal-Wallis Test
Cell_Line: T98G,Drug: MNG
Cytotoxicity
100.000000000000000
80.000000000000000
60.000000000000000
40.000000000000000
20.000000000000000
.000000000000000
Extract Control_Comb_TMZ_0
High_Comb_TMZ_0
High_Comb_TMZ_200
High_Comb_TMZ_50
Low_Comb_TMZ_0
Low_Comb_TMZ_200
Low_Comb_TMZ_50
Mean_Control_DMSO
Mean_Control_NT
Mean_TMZ_200
Mean_TMZ_50
Combinations

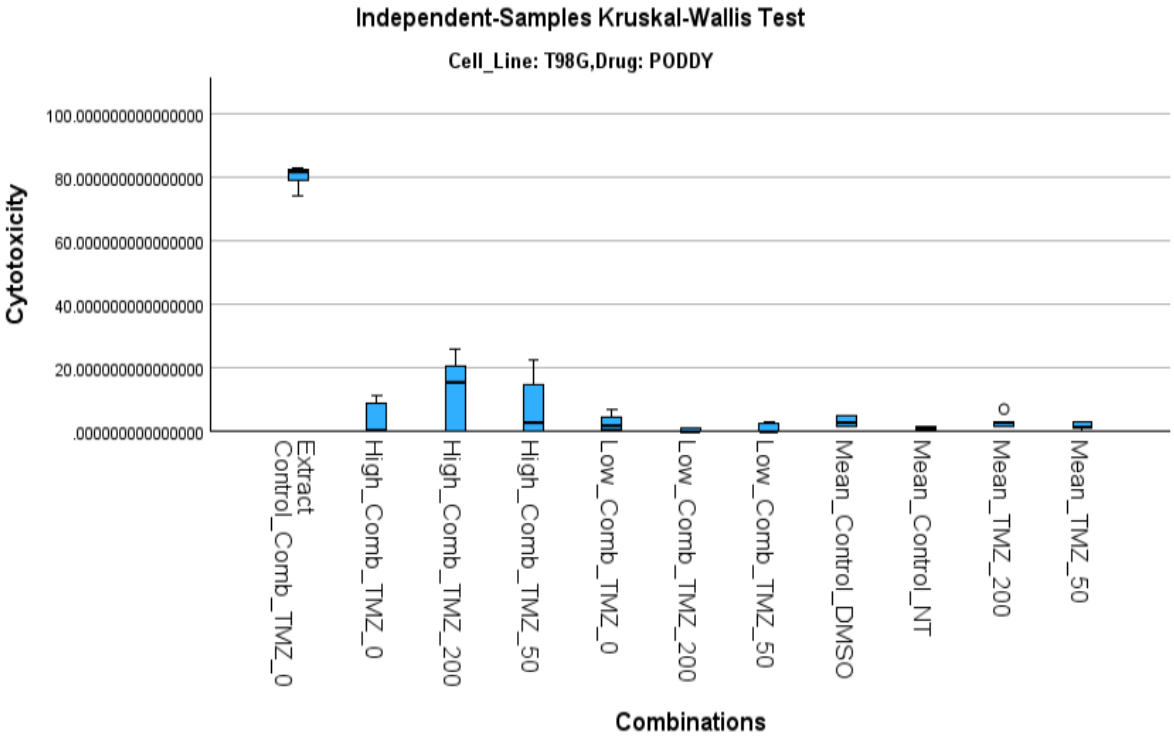
Independent-Samples Kruskal-Wallis Test
Cell_Line: T98G,Drug: PODDY
Cytotoxicity
100.000000000000000
80.000000000000000
60.000000000000000
40.000000000000000
20.000000000000000
.000000000000000
Extract Control_Comb_TMZ_0
High_Comb_TMZ_0
High_Comb_TMZ_200
High_Comb_TMZ_50
Low_Comb_TMZ_0
Low_Comb_TMZ_200
Low_Comb_TMZ_50
Mean_Control_DMSO
Mean_Control_NT
Mean_TMZ_200
Mean_TMZ_50
Combinations

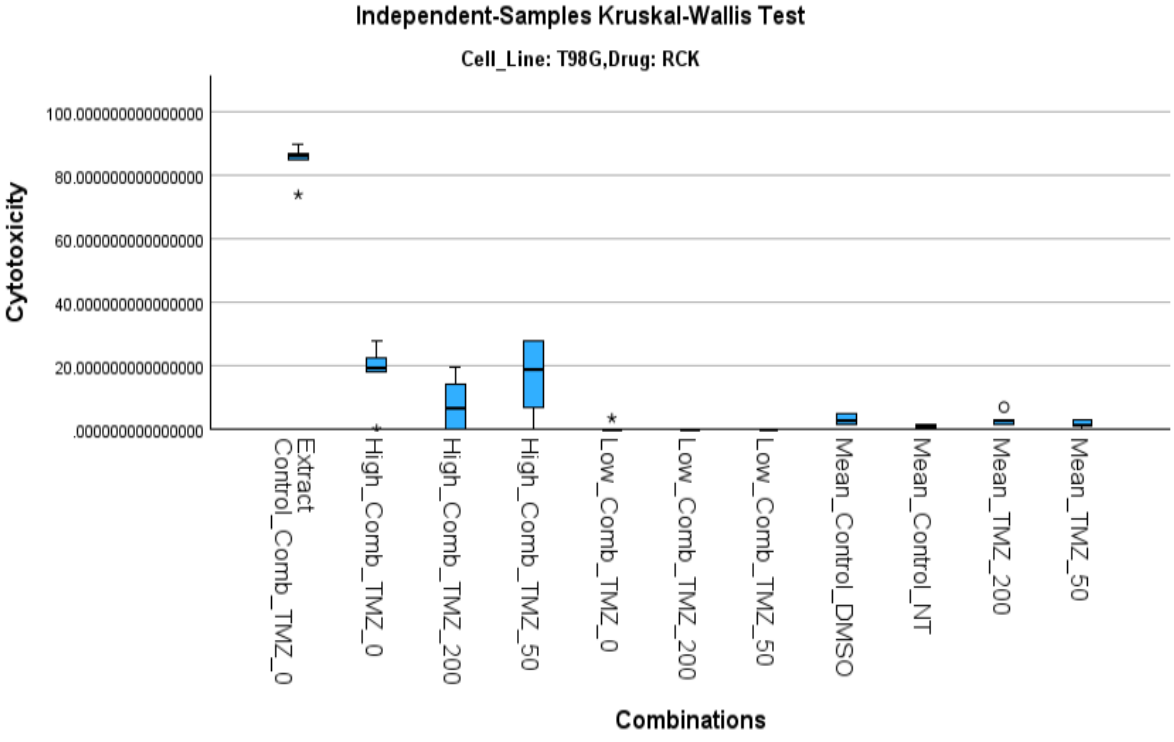
Independent-Samples Kruskal-Wallis Test
Cell_Line: T98G,Drug: RCK
Cytotoxicity
100.000000000000000
80.000000000000000
60.000000000000000
40.000000000000000
20.000000000000000
.000000000000000
Extract Control_Comb_TMZ_0
High_Comb_TMZ_0
High_Comb_TMZ_200
High_Comb_TMZ_50
Low_Comb_TMZ_0
Low_Comb_TMZ_200
Low_Comb_TMZ_50
Mean_Control_DMSO
Mean_Control_NT
Mean_TMZ_200
Mean_TMZ_50
Combinations

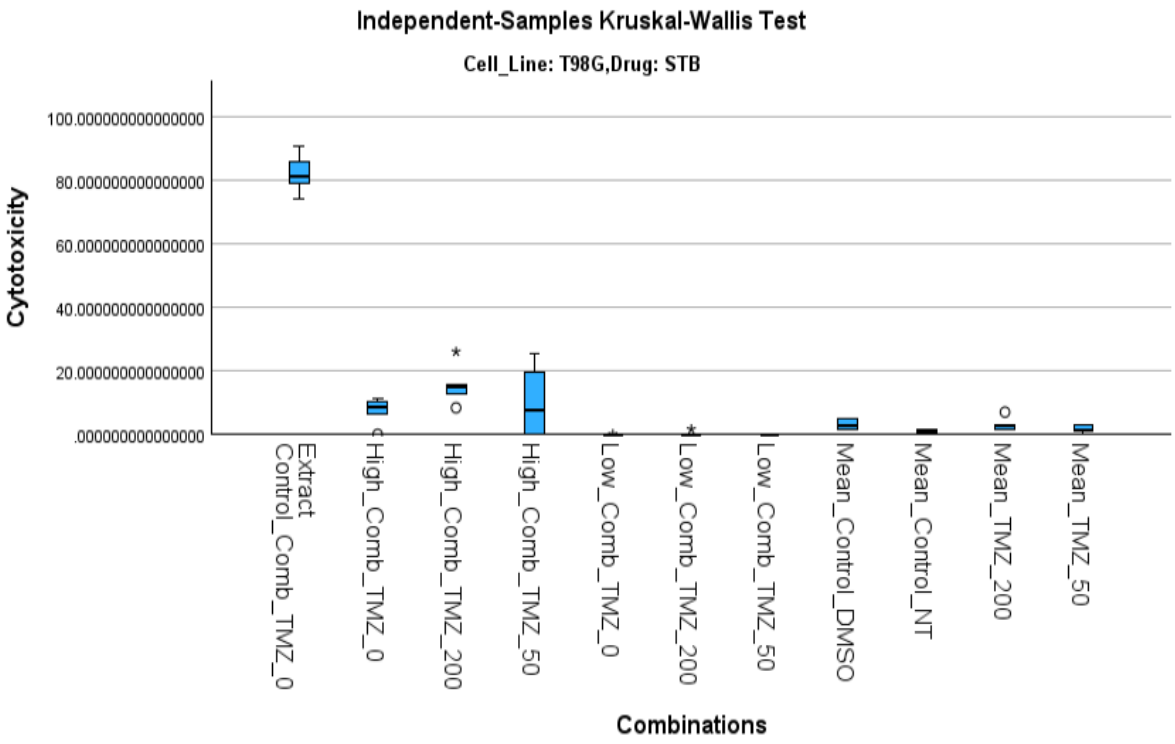
Independent-Samples Kruskal-Wallis Test
Cell_Line: T98G,Drug: STB
Cytotoxicity
100.000000000000000
80.000000000000000
60.000000000000000
40.000000000000000
20.000000000000000
.000000000000000
Extract Control_Comb_TMZ_0
High_Comb_TMZ_0
High_Comb_TMZ_200
High_Comb_TMZ_50
Low_Comb_TMZ_0
Low_Comb_TMZ_200
Low_Comb_TMZ_50
Mean_Control_DMSO
Mean_Control_NT
Mean_TMZ_200
Mean_TMZ_50
Combinations

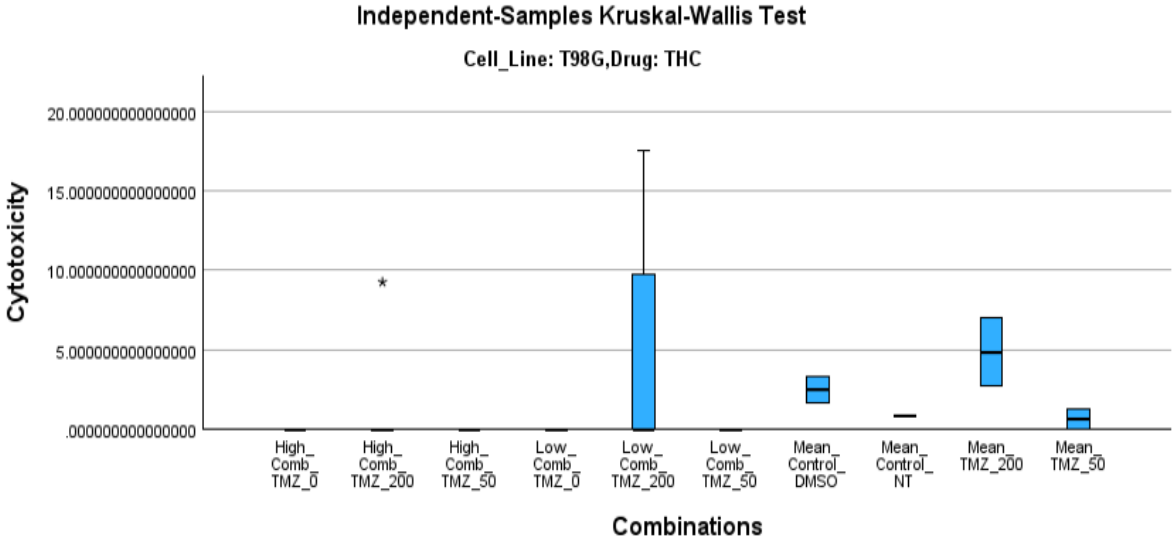
Independent-Samples Kruskal-Wallis Test
Cell_Line: T98G,Drug: THC
Cytotoxicity
20.000000000000000
15.000000000000000
10.000000000000000
5.000000000000000
.000000000000000
High_ Comb_ TMZ_0
High_ Comb_ TMZ_200
High_ Comb_ TMZ_50
Low_ Comb_ TMZ_0
Low_ Comb_ TMZ_200
Low_ Comb_ TMZ_50
Mean_ Control_ DMSO
Mean_ Control_ NT
Mean_ TMZ_200
Mean_ TMZ_50
Combinations

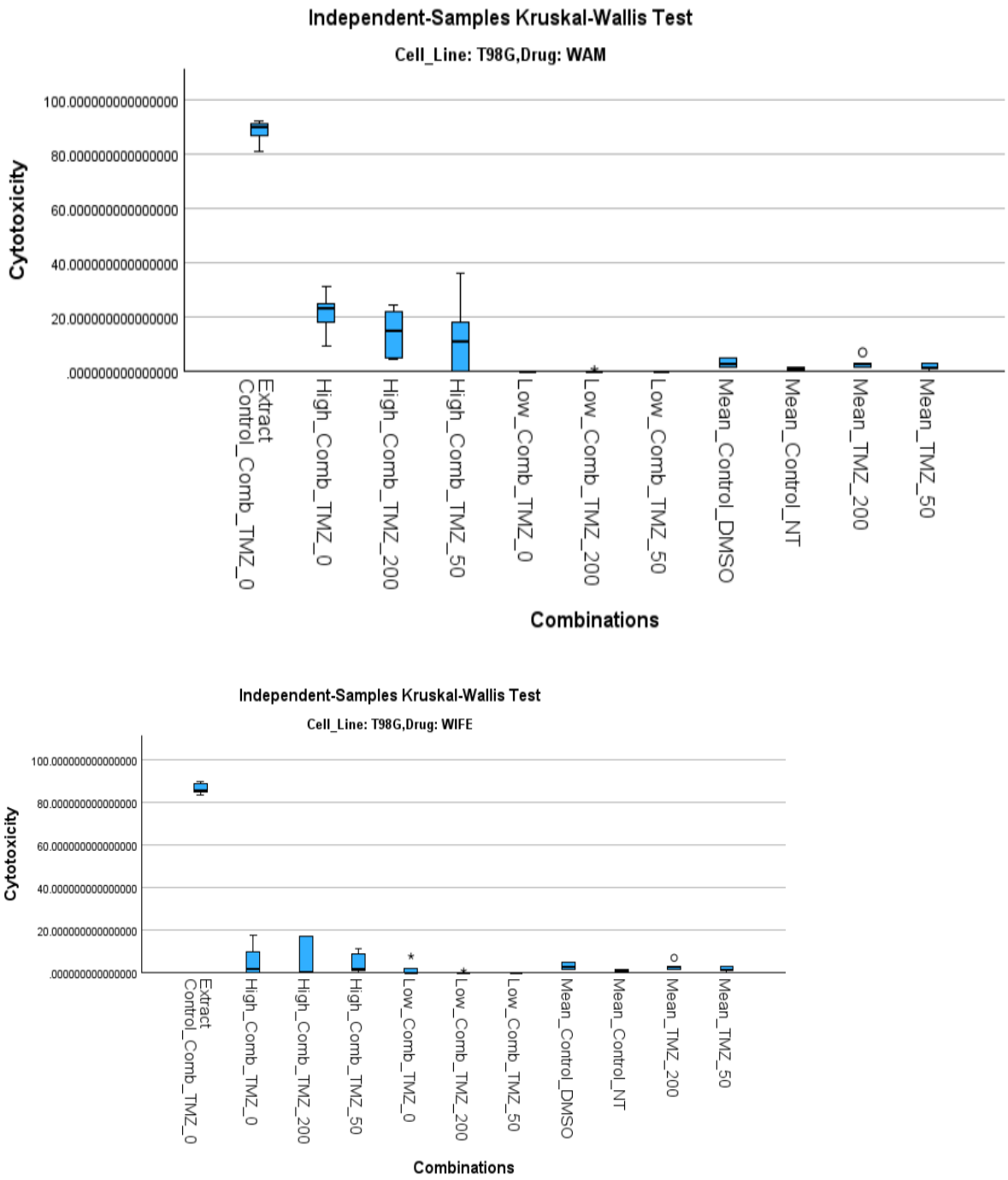

***Figure 4S**: **The Independent-samaples Kruskal Walis Test confirms that T98G is resistant to TMZ and that treatment combinations with TMZ increased cytotoxicity.** The bar graphs show the treatment combinations and the cytotoxicity levels for T98G from the statistical analysis test (n=6) using Kruskal-Wallis ANOVA with multiple sample comparison. The level of significance was 0.05.*

Supplementary figure 5

GPCR 119

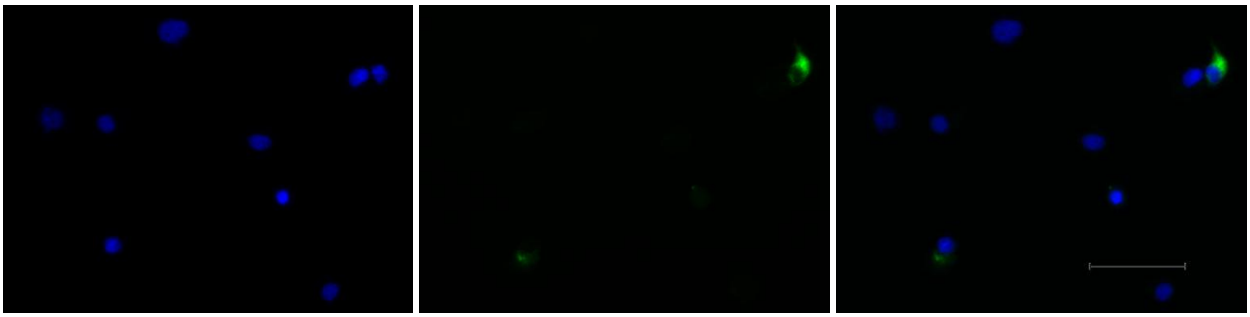

GPCR 3

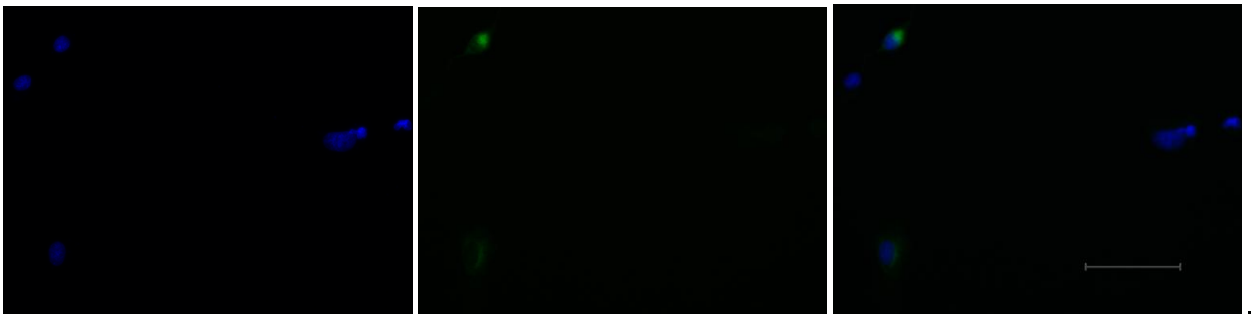

GPCR 18

GPR 12

CNR2

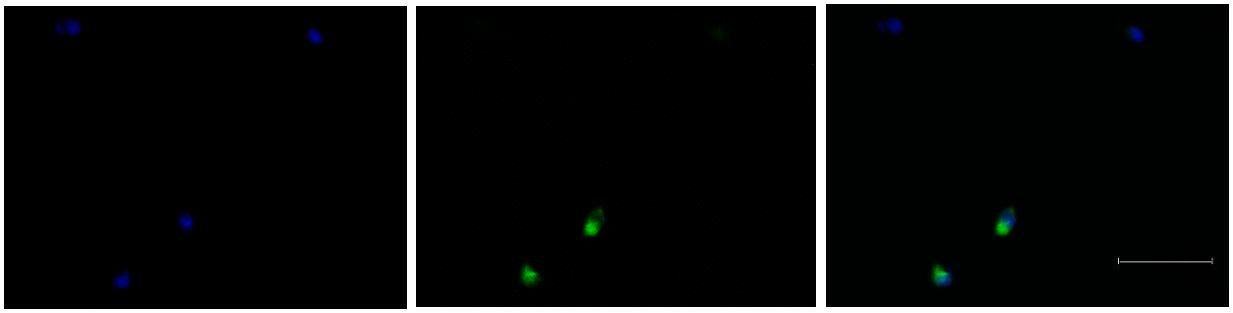

GPR55

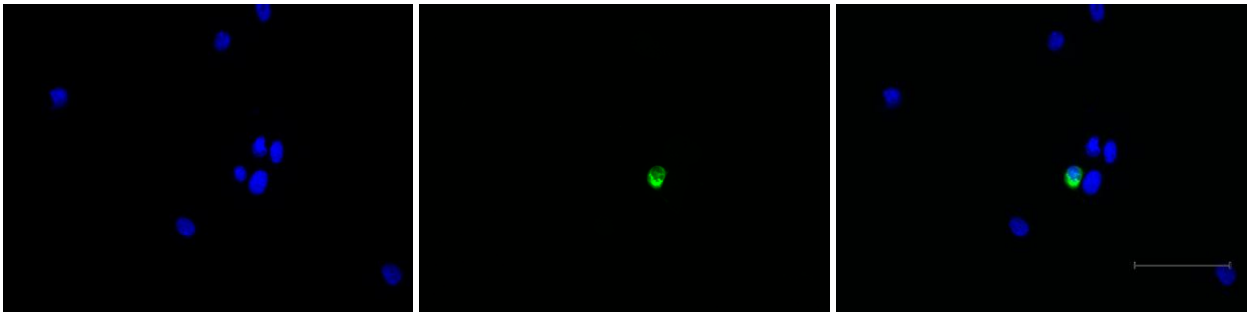

GPR6

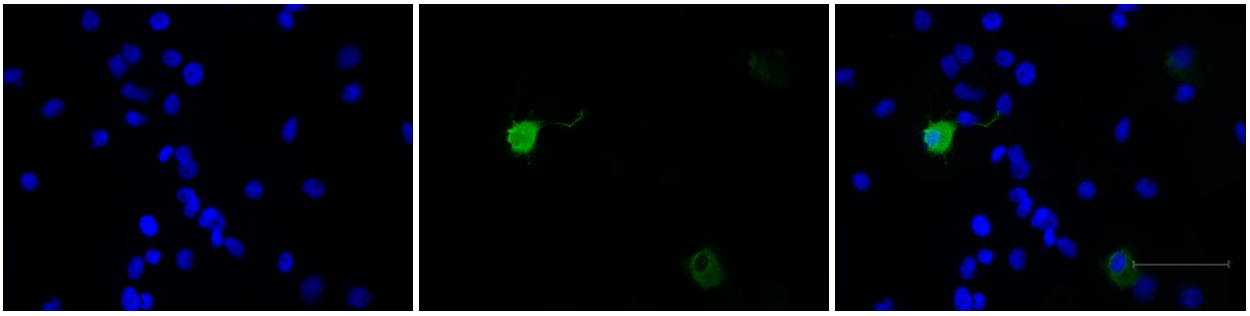

UNTRANSFECTED

NO PRIMARY ANTIBODY

Figure S5: Immunohistochemistry shows that the GPCR-Tango receptors are localized on the cell surface. *U251 Cells were transfected with GPCR-Tango plasmids that has a FLAG tag and immunolabeled using a rabbit anti-FLAG primary antibody followed by Alexa fluor 488-conjugated anti rabbit secondary antibody to visualize receptor expression (green). Nuclei were counterstained with DAPI (blue). The right panel shows the merged image of DAPI and GFP channels, demonstrating both nuclear and receptor fluorescence. the middle panel shows the Alexa fluor 488 signal corresponding to GPCR-Tango localized predominantly on the cell surface, while the left panel displays DAPI staining of cell nuclei. The receptors are labelled on each image.*

References

Abcam. (2022). *Annexin V-FITC staining for detecting apoptosis*. Retrieved 29 October from https://www.abcam.com/en-us/technical-resources/protocols/annexin-v-for-apoptosis

Alves, P., Amaral, C., Teixeira, N., & Correia-da-Silva, G. (2020). Cannabis sativa: Much more beyond Δ9-tetrahydrocannabinol. *Pharmacological Research*, *157*, 104822. https://doi.org/https://doi.org/10.1016/j.phrs.2020.104822

Andradas, C., Blasco-Benito, S., Castillo-Lluva, S., Dillenburg-Pilla, P., Diez-Alarcia, R., Juanes-García, A., García-Taboada, E., Hernando-Llorente, R., Soriano, J., Hamann, S., Wenners, A., Alkatout, I., Klapper, W., Rocken, C., Bauer, M., Arnold, N., Quintanilla, M., Megías, D., Vicente-Manzanares, M.,…Sánchez, C. (2016). Activation of the orphan receptor GPR55 by lysophosphatidylinositol promotes metastasis in triple-negative breast cancer. *Oncotarget*, *7*(30), 47565-47575. https://doi.org/10.18632/oncotarget.10206

Arthurs, A. L., Keating, D. J., Stringer, B. W., & Conn, S. J. (2020). The Suitability of Glioblastoma Cell Lines as Models for Primary Glioblastoma Cell Metabolism. *Cancers*, *12*(12), 3722. https://doi.org/10.3390/cancers12123722

Auffinger, B., Spencer, D., Pytel, P., Ahmed, A. U., & Lesniak, M. S. (2015). The role of glioma stem cells in chemotherapy resistance and glioblastoma multiforme recurrence. *Expert Review of Neurotherapeutics*, *15*(7), 741-752. https://doi.org/10.1586/14737175.2015.1051968

Ayakannu, T., Taylor, A. H., Bari, M., Mastrangelo, N., Maccarrone, M., & Konje, J. C. (2019). Expression and Function of the Endocannabinoid Modulating Enzymes Fatty Acid Amide Hydrolase and N-Acylphosphatidylethanolamine-Specific Phospholipase D in Endometrial Carcinoma [Original Research]. *Frontiers in Oncology*, *Volume 9 - 2019*. https://doi.org/10.3389/fonc.2019.01363

Baram, L., Peled, E., Berman, P., Yellin, B., Besser, E., Benami, M., Louria-Hayon, I., Lewitus, G. M., & Meiri, D. (2019). The heterogeneity and complexity of Cannabis extracts as antitumor agents. *Oncotarget*, *10*(41), 4091-4106. https://doi.org/10.18632/oncotarget.26983

Batistella, G. N. D. R., Santos, A. J., Paiva Neto, M. A. D., Ferrigno, R., Camargo, V. P. D., Stavale, J. N., & Maldaun, M. V. C. (2021). Approaching glioblastoma during COVID-19 pandemic: current recommendations and considerations in Brazil. *Arquivos de Neuro-Psiquiatria*, *79*(2), 167-172. https://doi.org/10.1590/0004-282x-anp-2020-0434

BOC. (2022). *MGC Pharmaceuticals Ltd. Announce Successful Glioblastoma Pre-clinical Trial Results*. Retrieved 25th April from https://businessofcannabis.com/mgc-pharmaceuticals-ltd-announce-successful-glioblastoma-pre-clinical-trial-results/

Bucevičius, J., Lukinavičius, G., & Gerasimaitė, R. (2018). The Use of Hoechst Dyes for DNA Staining and Beyond. *Chemosensors*, *6*(2).

Burdherd. (2020). *15 Popular High CBD Strains*. Retrieved October 29 from https://budherd.com.au/articles/15-popular-high-cbd-cannabis-strains

Carracedo, A., Lorente, M., Egia, A., Blázquez, C., García, S., Giroux, V., Malicet, C., Villuendas, R., Gironella, M., González-Feria, L., Piris, M. A., Iovanna, J. L., Guzmán, M., & Velasco, G. (2006). The stress-regulated protein p8 mediates cannabinoid-induced apoptosis of tumor cells. *Cancer Cell*, *9*(4), 301-312. https://doi.org/10.1016/j.ccr.2006.03.005

Cipriano, M., Häggström, J., Hammarsten, P., & Fowler, C. J. (2013). Association between Cannabinoid CB1 Receptor Expression and Akt Signalling in Prostate Cancer. *PLoS ONE*, *8*(6), e65798. https://doi.org/10.1371/journal.pone.0065798

Cordover, E., & Minden, A. (2020). Signaling pathways downstream to receptor tyrosine kinases: targets for cancer treatment. *Journal of Cancer Metastasis and Treatment*, *2020*. https://doi.org/10.20517/2394-4722.2020.101

Crispim Massuela, D., Hartung, J., Munz, S., Erpenbach, F., & Graeff-Hönninger, S. (2022). Impact of Harvest Time and Pruning Technique on Total CBD Concentration and Yield of Medicinal Cannabis. *Plants (Basel)*, *11*(1). https://doi.org/10.3390/plants11010140

Dasram, M. H., Naidoo, P., Walker, R. B., & Khamanga, S. M. (2024). Targeting the Endocannabinoid System Present in the Glioblastoma Tumour Microenvironment as a Potential Anti-Cancer Strategy. *International Journal of Molecular Sciences*, *25*(3), 1371. https://doi.org/10.3390/ijms25031371

Debela, D. T., Muzazu, S. G., Heraro, K. D., Ndalama, M. T., Mesele, B. W., Haile, D. C., Kitui, S. K., & Manyazewal, T. (2021). New approaches and procedures for cancer treatment: Current perspectives. *SAGE Open Med*, *9*, 20503121211034366. https://doi.org/10.1177/20503121211034366

Du, L., Zhang, Q., Li, Y., Li, T., Deng, Q., Jia, Y., Lei, K., Kan, D., Xie, F., & Huang, S. (2024). Research progress on the role of PTEN deletion or mutation in the immune microenvironment of glioblastoma. *Frontiers in Oncology*, *14*. https://doi.org/10.3389/fonc.2024.1409519

Dumitru, C. A., Sandalcioglu, I. E., & Karsak, M. (2018). Cannabinoids in Glioblastoma Therapy: New Applications for Old Drugs. *Frontiers in Molecular Neuroscience*, *11*. https://doi.org/10.3389/fnmol.2018.00159

Eckerdt, F., & Platanias, L. C. (2023). Emerging Role of Glioma Stem Cells in Mechanisms of Therapy Resistance. *Cancers*, *15*(13), 3458. https://doi.org/10.3390/cancers15133458

Faiz, M. B., Naeem, F., Irfan, M., Aslam, M. A., Estevinho, L. M., Ateşşahin, D. A., Alshahrani, A. M., Calina, D., Khan, K., & Sharifi-Rad, J. (2024). Exploring the therapeutic potential of cannabinoids in cancer by modulating signaling pathways and addressing clinical challenges. *Discover Oncology*, *15*(1). https://doi.org/10.1007/s12672-024-01356-8

Fellermeier, M., Eisenreich, W., Bacher, A., & Zenk, M. H. (2001). Biosynthesis of cannabinoids. *European Journal of Biochemistry*, *268*(6), 1596-1604. https://doi.org/https://doi.org/10.1046/j.1432-1327.2001.02030.x

Franco, R., Rivas-Santisteban, R., Reyes-Resina, I., Casanovas, M., Pérez-Olives, C., Ferreiro-Vera, C., Navarro, G., Sánchez de Medina, V., & Nadal, X. (2020). Pharmacological potential of varinic-, minor-, and acidic phytocannabinoids. *Pharmacol Res*, *158*, 104801. https://doi.org/10.1016/j.phrs.2020.104801

Grech, N., Dalli, T., Mizzi, S., Meilak, L., Calleja, N., & Zrinzo, A. (2020). Rising Incidence of Glioblastoma Multiforme in a Well-Defined Population. *Cureus*. https://doi.org/10.7759/cureus.8195

Grochans, S., Cybulska, A. M., Simińska, D., Korbecki, J., Kojder, K., Chlubek, D., & Baranowska-Bosiacka, I. (2022). Epidemiology of Glioblastoma Multiforme–Literature Review. *Cancers*, *14*(10), 2412. https://doi.org/10.3390/cancers14102412

Gularyan, S. K., Gulin, A. A., Anufrieva, K. S., Shender, V. O., Shakhparonov, M. I., Bastola, S., Antipova, N. V., Kovalenko, T. F., Rubtsov, Y. P., Latyshev, Y. A., Potapov, A. A., & Pavlyukov, M. S. (2020). Investigation of Inter- and Intratumoral Heterogeneity of Glioblastoma Using TOF-SIMS. *Molecular & Cellular Proteomics*, *19*(6), 960-970. https://doi.org/10.1074/mcp.ra120.001986

Guzmán, M., Duarte, M. J., Blázquez, C., Ravina, J., Rosa, M. C., Galve-Roperh, I., Sánchez, C., Velasco, G., & González-Feria, L. (2006). A pilot clinical study of Δ9-tetrahydrocannabinol in patients with recurrent glioblastoma multiforme. *British Journal of Cancer*, *95*(2), 197-203. https://doi.org/10.1038/sj.bjc.6603236

Hashemi, M., Bashi, S., & Zali, A. (2020). The expression level of cannabinoid receptors type 1 and 2 in the different types of astrocytomas. *Mol Biol Rep*, *47*(7), 5461-5467. https://doi.org/10.1007/s11033-020-05636-8

Held-Feindt, J., Dörner, L., Sahan, G., Mehdorn, H. M., & Mentlein, R. (2006). Cannabinoid receptors in human astroglial tumors. *Journal of Neurochemistry*, *98*(3), 886-893. https://doi.org/https://doi.org/10.1111/j.1471-4159.2006.03911.x

Hoxhaj, G., & Manning, B. D. (2020). The PI3K–AKT network at the interface of oncogenic signalling and cancer metabolism. *Nature Reviews Cancer*, *20*(2), 74-88. https://doi.org/10.1038/s41568-019-0216-7

Ivanov, V. N., Wu, J., & Hei, T. K. (2017). Regulation of human glioblastoma cell death by combined treatment of cannabidiol, γ-radiation and small molecule inhibitors of cell signaling pathways. *Oncotarget*, *8*(43), 74068-74095. https://doi.org/10.18632/oncotarget.18240

Jovčevska, I., Kočevar, N., & Komel, R. (2013). Glioma and glioblastoma - how much do we (not) know? *Molecular and Clinical Oncology*, *1*(6), 935-941. https://doi.org/10.3892/mco.2013.172

Kan, L. K., Drummond, K., Hunn, M., Williams, D., O'Brien, T. J., & Monif, M. (2020). Potential biomarkers and challenges in glioma diagnosis, therapy and prognosis. *BMJ Neurology Open*, *2*(2), e000069. https://doi.org/10.1136/bmjno-2020-000069

Kotecha, R., Odia, Y., Khosla, A. A., & Ahluwalia, M. S. (2023). Key Clinical Principles in the Management of Glioblastoma. *JCO Oncology Practice*, *19*(4), 180-189. https://doi.org/10.1200/op.22.00476

Kroeze, W. K., Sassano, M. F., Huang, X.-P., Lansu, K., McCorvy, J. D., Giguère, P. M., Sciaky, N., & Roth, B. L. (2015). PRESTO-Tango as an open-source resource for interrogation of the druggable human GPCRome. *Nature Structural & Molecular Biology*, *22*(5), 362-369. https://doi.org/10.1038/nsmb.3014

Kyriakou, I., Yarandi, N., & Polycarpou, E. (2021). Efficacy of cannabinoids against glioblastoma multiforme: A systematic review. *Phytomedicine*, *88*, 153533. https://doi.org/10.1016/j.phymed.2021.153533

Lah, T. T., Majc, B., Novak, M., Sušnik, A., Breznik, B., Porčnik, A., Bošnjak, R., Sadikov, A., Malavolta, M., Halilčević, S., Mlakar, J., & Zomer, R. (2022). The Cytotoxic Effects of Cannabidiol and Cannabigerol on Glioblastoma Stem Cells May Mostly Involve GPR55 and TRPV1 Signalling. *Cancers (Basel)*, *14*(23). https://doi.org/10.3390/cancers14235918

Lah, T. T., Novak, M., Pena Almidon, M. A., Marinelli, O., Žvar Baškovič, B., Majc, B., Mlinar, M., Bošnjak, R., Breznik, B., Zomer, R., & Nabissi, M. (2021). Cannabigerol Is a Potential Therapeutic Agent in a Novel Combined Therapy for Glioblastoma. *Cells*, *10*(2). https://doi.org/10.3390/cells10020340

Lai, S., Li, P., Liu, X., Liu, G., Xie, T., Zhang, X., Wang, X., Huang, J., Tang, Y., Liu, Z., Shen, G., Li, C., Lu, F., Wang, L., Jiang, F., Sun, C., Chen, Y., & Chen, M. (2024). Efficacy and safety of anlotinib combined with the STUPP regimen in patients with newly diagnosed glioblastoma: a multicenter, single-arm, phase II trial. *Cancer Biol Med*, *21*(5), 433-444. https://doi.org/10.20892/j.issn.2095-3941.2023.0373

Lakshmanan, I., & Batra, S. K. (2013). Protocol for Apoptosis Assay by Flow Cytometry Using Annexin V Staining Method. *Bio Protoc*, *3*(6). https://doi.org/10.21769/bioprotoc.374

Lee, S. (2016). Temozolomide resistance in glioblastoma multiforme. *Genes & Diseases*, *3*. https://doi.org/10.1016/j.gendis.2016.04.007

Lee, S. Y. (2016). Temozolomide resistance in glioblastoma multiforme. *Genes Dis*, *3*(3), 198-210. https://doi.org/10.1016/j.gendis.2016.04.007

Liguori, G. L. (2024). Challenges and Promise for Glioblastoma Treatment through Extracellular Vesicle Inquiry. *Cells*, *13*(4), 336. https://doi.org/10.3390/cells13040336

Likar, R., Koestenberger, M., Stutschnig, M., & Nahler, G. (2021). Cannabidiol May Prolong Survival in Patients With Glioblastoma Multiforme. *Cancer Diagn Progn*, *1*(2), 77-82. https://doi.org/10.21873/cdp.10011

Liu, Y. (2001). p53 protein at the hub of cellular DNA damage response pathways through sequence-specific and non-sequence-specific DNA binding. *Carcinogenesis*, *22*(6), 851-860. https://doi.org/10.1093/carcin/22.6.851

López-Valero, I., Saiz-Ladera, C., Torres, S., Hernández-Tiedra, S., García-Taboada, E., Rodríguez-Fornés, F., Barba, M., Dávila, D., Salvador-Tormo, N., Guzmán, M., Sepúlveda, J. M., Sánchez-Gómez, P., Lorente, M., & Velasco, G. (2018). Targeting Glioma Initiating Cells with A combined therapy of cannabinoids and temozolomide. *Biochem Pharmacol*, *157*, 266-274. https://doi.org/10.1016/j.bcp.2018.09.007

Louis, D. N., Perry, A., Reifenberger, G., Von Deimling, A., Figarella-Branger, D., Cavenee, W. K., Ohgaki, H., Wiestler, O. D., Kleihues, P., & Ellison, D. W. (2016). The 2016 World Health Organization Classification of Tumors of the Central Nervous System: a summary. *Acta neuropathologica*, *131*(6), 803-820. https://doi.org/10.1007/s00401-016-1545-1

Louis, D. N., Perry, A., Wesseling, P., Brat, D. J., Cree, I. A., Figarella-Branger, D., Hawkins, C., Ng, H. K., Pfister, S. M., Reifenberger, G., Soffietti, R., von Deimling, A., & Ellison, D. W. (2021). The 2021 WHO Classification of Tumors of the Central Nervous System: a summary. *Neuro-Oncology*, *23*(8), 1231-1251. https://doi.org/10.1093/neuonc/noab106

Lu, C., Kang, T., Zhang, J., Yang, K., Liu, Y., Song, K., Lin, Q., Dixit, D., Gimple, R. C., Zhang, Q., Shi, Z., Fan, X., Wu, Q., Li, D., Shan, D., Gao, J., Gu, D., You, H., Li, Y.,…Wang, X. (2025). Combined targeting of glioblastoma stem cells of different cellular states disrupts malignant progression. *Nature Communications*, *16*(1), 2974. https://doi.org/10.1038/s41467-025-58366-5

Luo, J. L. (2005). IKK/NF- B signaling: balancing life and death - a new approach to cancer therapy. *Journal of Clinical Investigation*, *115*(10), 2625-2632. https://doi.org/10.1172/jci26322

Marcu, J. P., Christian, R. T., Lau, D., Zielinski, A. J., Horowitz, M. P., Lee, J., Pakdel, A., Allison, J., Limbad, C., Moore, D. H., Yount, G. L., Desprez, P. Y., & McAllister, S. D. (2010). Cannabidiol enhances the inhibitory effects of delta9-tetrahydrocannabinol on human glioblastoma cell proliferation and survival. *Mol Cancer Ther*, *9*(1), 180-189. https://doi.org/10.1158/1535-7163.Mct-09-0407

Massi, P., Valenti, M., Solinas, M., & Parolaro, D. (2010). Molecular mechanisms involved in the antitumor activity of cannabinoids on gliomas: role for oxidative stress. *Cancers (Basel)*, *2*(2), 1013-1026. https://doi.org/10.3390/cancers2021013

McAllister, S. D., Abood, M. E., Califano, J., & Guzmán, M. (2021). Cannabinoid Cancer Biology and Prevention. *JNCI Monographs*, *2021*(58), 99-106. https://doi.org/10.1093/jncimonographs/lgab008

Michalski, C. W., Oti, F. E., Erkan, M., Sauliunaite, D., Bergmann, F., Pacher, P., Batkai, S., Müller, M. W., Giese, N. A., Friess, H., & Kleeff, J. (2008). Cannabinoids in pancreatic cancer: correlation with survival and pain. *Int J Cancer*, *122*(4), 742-750. https://doi.org/10.1002/ijc.23114

Morales, P., & Reggio, P. H. (2017). An Update on Non-CB1, Non-CB2 Cannabinoid Related G-Protein-Coupled Receptors. *Cannabis and Cannabinoid Research*, *2*(1), 265-273. https://doi.org/10.1089/can.2017.0036

Nabian, N., Ghalehtaki, R., Zeinalizadeh, M., Balaña, C., & Jablonska, P. A. (2024). State of the neoadjuvant therapy for glioblastoma multiforme—Where do we stand? *Neuro-Oncology Advances*, *6*(1). https://doi.org/10.1093/noajnl/vdae028

Nahler, G. (2023). Treatment of malignant diseases with phytocannabinoids: promising observations in animal models and patients. *Exploration of Medicine*, 847-877. https://doi.org/10.37349/emed.2023.00182

Ng, A. T., Steve, T., Jamouss, K. T., Arham, A., Kawtharani, S., & Assi, H. I. (2024). The challenges and clinical landscape of glioblastoma immunotherapy. *CNS Oncology*, *13*(1). https://doi.org/10.1080/20450907.2024.2415878

O'Brien, K. (2022). Cannabidiol (CBD) in Cancer Management. *Cancers (Basel)*, *14*(4). https://doi.org/10.3390/cancers14040885

Pennypacker, S. D., Cunnane, K., Cash, M. C., & Romero-Sandoval, E. A. (2022). Potency and Therapeutic THC and CBD Ratios: U.S. Cannabis Markets Overshoot [Original Research]. *Frontiers in Pharmacology*, *Volume 13 - 2022*. https://doi.org/10.3389/fphar.2022.921493

Perus, L. J. M., & Walsh, L. A. (2019). Microenvironmental Heterogeneity in Brain Malignancies. *Frontiers in Immunology*, *10*. https://doi.org/10.3389/fimmu.2019.02294

Petersen, G., Moesgaard, B., Schmid, P. C., Schmid, H. H., Broholm, H., Kosteljanetz, M., & Hansen, H. S. (2005). Endocannabinoid metabolism in human glioblastomas and meningiomas compared to human non-tumour brain tissue. *J Neurochem*, *93*(2), 299-309. https://doi.org/10.1111/j.1471-4159.2005.03013.x

Pinevich, A. A., Bode, I. I., Vartanyan, N. L., Kiseleva, L. N., Kartashev, A. V., & Samoilovich, M. P. (2022). Temozolomide-Resistant Human T2 and T98G Glioblastoma Cells. *Cell and Tissue Biology*, *16*(4), 339-351. https://doi.org/10.1134/S1990519X22040058

Poon, M. T. C., Bruce, M., Simpson, J. E., Hannan, C. J., & Brennan, P. M. (2021). Temozolomide sensitivity of malignant glioma cell lines - a systematic review assessing consistencies between in vitro studies. *BMC Cancer*, *21*(1), 1240. https://doi.org/10.1186/s12885-021-08972-5

Poon, M. T. C., Bruce, M., Simpson, J. E., Hannan, C. J., & Brennan, P. M. (2021). Temozolomide sensitivity of malignant glioma cell lines – a systematic review assessing consistencies between in vitro studies. *BMC Cancer*, *21*(1). https://doi.org/10.1186/s12885-021-08972-5

Purohit, M., Gupta, G., Afzal, O., Altamimi, A. S. A., Alzarea, S. I., Kazmi, I., Almalki, W. H., Gulati, M., Kaur, I. P., Singh, S. K., & Dua, K. (2023). Janus kinase/signal transducers and activator of transcription (JAK/STAT) and its role in Lung inflammatory disease. *Chemico-Biological Interactions*, *371*, 110334. https://doi.org/https://doi.org/10.1016/j.cbi.2023.110334

Reblin, M., Sahebjam, S., Peeri, N. C., Martinez, Y. C., Thompson, Z., & Egan, K. M. (2019). Medical Cannabis Use in Glioma Patients Treated at a Comprehensive Cancer Center in Florida. *Journal of Palliative Medicine*, *22*(10), 1202-1207. https://doi.org/10.1089/jpm.2018.0528

Reisenberg, M., Singh, P. K., Williams, G., & Doherty, P. (2012). The diacylglycerol lipases: structure, regulation and roles in and beyond endocannabinoid signalling. *Philos Trans R Soc Lond B Biol Sci*, *367*(1607), 3264-3275. https://doi.org/10.1098/rstb.2011.0387

Rieger, A. M., Nelson, K. L., Konowalchuk, J. D., & Barreda, D. R. (2011). Modified annexin V/propidium iodide apoptosis assay for accurate assessment of cell death. *J Vis Exp*(50). https://doi.org/10.3791/2597

Rodgers, L. T., Villano, J. L., Hartz, A. M. S., & Bauer, B. (2024). Glioblastoma Standard of Care: Effects on Tumor Evolution and Reverse Translation in Preclinical Models. *Cancers*, *16*(15), 2638. https://doi.org/10.3390/cancers16152638

Salazar, M., Carracedo, A., Salanueva, I. J., Hernández-Tiedra, S., Lorente, M., Egia, A., Vázquez, P., Blázquez, C., Torres, S., García, S., Nowak, J., Fimia, G. M., Piacentini, M., Cecconi, F., Pandolfi, P. P., González-Feria, L., Iovanna, J. L., Guzmán, M., Boya, P., & Velasco, G. (2009). Cannabinoid action induces autophagy-mediated cell death through stimulation of ER stress in human glioma cells. *J Clin Invest*, *119*(5), 1359-1372. https://doi.org/10.1172/jci37948

Scherma, M., Muntoni, A. L., Riedel, G., Fratta, W., & Fadda, P. (2020). Cannabinoids and their therapeutic applications in mental disorders. *Dialogues in Clinical Neuroscience*, *22*(3), 271-279. https://doi.org/10.31887/dcns.2020.22.3/pfadda

Seker-Polat, F., Pinarbasi Degirmenci, N., Solaroglu, I., & Bagci-Onder, T. (2022). Tumor Cell Infiltration into the Brain in Glioblastoma: From Mechanisms to Clinical Perspectives. *Cancers*, *14*(2), 443. https://doi.org/10.3390/cancers14020443

Seltzer, E. S., Watters, A. K., Mackenzie, D., Granat, L. M., & Zhang, D. (2020). Cannabidiol (CBD) as a Promising Anti-Cancer Drug. *Cancers*, *12*(11), 3203. https://doi.org/10.3390/cancers12113203

Seo, C., Jeong, M., Lee, S., Kim, E. J., Rho, S., Cho, M., Lee, Y. S., & Hong, J. (2022). Thermal decarboxylation of acidic cannabinoids in Cannabis species: identification of transformed cannabinoids by UHPLC-Q/TOF–MS. *Journal of Analytical Science and Technology*, *13*(1), 42. https://doi.org/10.1186/s40543-022-00351-4

Sepúlveda, J. M., Alonso, M., Velilla, G., Grove, C. G., Martínez-García, M., Foro, P., Gonzalez, C. G., Lopez, C. M., Luque, R., Luque, N., Stradella, A., Viltró, P. S., Martín, M. N., López, B. R., Guzmán, M., Tovar-Ambel, E., Velasco, G., Morillas, R. S., & Salva, J. F. (2024). 454P Tetrahydrocannabinol (THC) / cannabidiol (CBD) oral solution in combination with temozolomide (TMZ) and radiotherapy (RT) in patients with newly diagnosed glioblastoma: Phase Ib GEINO-1601 trial. *Annals of Oncology*, *35*, S411. https://doi.org/10.1016/j.annonc.2024.08.524

Shahani, A., Slika, H., Elbeltagy, A., Lee, A., Peters, C., Dotson, T., Raj, D., & Tyler, B. (2025). The epigenetic mechanisms involved in the treatment resistance of glioblastoma. *Cancer Drug Resistance*. https://doi.org/10.20517/cdr.2024.157

Shergalis, A., Bankhead, A., Luesakul, U., Muangsin, N., & Neamati, N. (2018). Current Challenges and Opportunities in Treating Glioblastoma. *Pharmacological Reviews*, *70*(3), 412-445. https://doi.org/10.1124/pr.117.014944

Soni, V., Adhikari, M., Simonyan, H., Lin, L., Sherman, J. H., Young, C. N., & Keidar, M. (2021). In Vitro and In Vivo Enhancement of Temozolomide Effect in Human Glioblastoma by Non-Invasive Application of Cold Atmospheric Plasma. *Cancers*, *13*(17).

Soubannier, V., & Stifani, S. (2017). NF-κB Signalling in Glioblastoma. *Biomedicines*, *5*(2), 29. https://doi.org/10.3390/biomedicines5020029

Strobel, H., Baisch, T., Fitzel, R., Schilberg, K., Siegelin, M. D., Karpel-Massler, G., Debatin, K.-M., & Westhoff, M.-A. (2019). Temozolomide and Other Alkylating Agents in Glioblastoma Therapy. *Biomedicines*, *7*(3), 69. https://doi.org/10.3390/biomedicines7030069

Stupp, R., Mason, W. P., Van Den Bent, M. J., Weller, M., Fisher, B., Taphoorn, M. J. B., Belanger, K., Brandes, A. A., Marosi, C., Bogdahn, U., Curschmann, J., Janzer, R. C., Ludwin, S. K., Gorlia, T., Allgeier, A., Lacombe, D., Cairncross, J. G., Eisenhauer, E., & Mirimanoff, R. O. (2005). Radiotherapy plus Concomitant and Adjuvant Temozolomide for Glioblastoma. *New England Journal of Medicine*, *352*(10), 987-996. https://doi.org/10.1056/nejmoa043330

Tamimi, A. F., & Juweid, M. (2017). Epidemiology and Outcome of Glioblastoma. In (pp. 143-153). Codon Publications. https://doi.org/10.15586/codon.glioblastoma.2017.ch8

Tang, Y., Wang, M., Yu, J., Lv, G., Wang, Y., & Yu, B. (2024). The antitumor action of endocannabinoids in the tumor microenvironment of glioblastoma. *Frontiers in Pharmacology*, *15*. https://doi.org/10.3389/fphar.2024.1395156

Terai, K., & Matsuda, M. (2005). Ras binding opens c-Raf to expose the docking site for mitogen-activated protein kinase kinase. *EMBO reports*, *6*(3), 251-255. https://doi.org/10.1038/sj.embor.7400349

Torres, S., Lorente, M., Rodríguez-Fornés, F., Hernández-Tiedra, S., Salazar, M., García-Taboada, E., Barcia, J., Guzmán, M., & Velasco, G. (2011). A Combined Preclinical Therapy of Cannabinoids and Temozolomide against Glioma. *Molecular Cancer Therapeutics*, *10*(1), 90-103. https://doi.org/10.1158/1535-7163.mct-10-0688

Torrisi, F., Alberghina, C., D'Aprile, S., Pavone, A. M., Longhitano, L., Giallongo, S., Tibullo, D., Di Rosa, M., Zappalà, A., Cammarata, F. P., Russo, G., Ippolito, M., Cuttone, G., Li Volti, G., Vicario, N., &

Parenti, R. (2022). The Hallmarks of Glioblastoma: Heterogeneity, Intercellular Crosstalk and Molecular Signature of Invasiveness and Progression. *Biomedicines*, *10*(4), 806. https://doi.org/10.3390/biomedicines10040806

Tutino, V., Caruso, M. G., De Nunzio, V., Lorusso, D., Veronese, N., Gigante, I., Notarnicola, M., & Giannelli, G. (2019). Down-Regulation of Cannabinoid Type 1 (CB1) Receptor and its Downstream Signaling Pathways in Metastatic Colorectal Cancer. *Cancers*, *11*(5).

Velasco, G., Carracedo, A., Blázquez, C., Lorente, M., Aguado, T., Haro, A., Sánchez, C., Galve-Roperh, I., & Guzmán, M. (2007). Cannabinoids and Gliomas. *Molecular Neurobiology*, *36*(1), 60-67. https://doi.org/10.1007/s12035-007-0002-5

Velasco, G., Sánchez, C., & Guzmán, M. (2016). Anticancer mechanisms of cannabinoids. *Curr Oncol*, *23*(2), S23-32. https://doi.org/10.3747/co.23.3080

Walker, S. B., Duarte, J. L., Di Filippo, L. D., & Chorilli, M. (2024). Improving the Biopharmaceutical Properties of Cannabinoids in Glioblastoma Multiforme Therapy With Nanotechnology: A Drug Delivery Perspective. *Drug Development Research*, *85*(8), e70023. https://doi.org/https://doi.org/10.1002/ddr.70023

Wang, D., Wang, H., Ning, W., Backlund, M. G., Dey, S. K., & DuBois, R. N. (2008). Loss of Cannabinoid Receptor 1 Accelerates Intestinal Tumor Growth. *Cancer Research*, *68*(15), 6468-6476. https://doi.org/10.1158/0008-5472.CAN-08-0896

Was, H., Borkowska, A., Bagues, A., Tu, L., Liu, J. Y. H., Lu, Z., Rudd, J. A., Nurgali, K., & Abalo, R. (2022). Mechanisms of Chemotherapy-Induced Neurotoxicity. *Frontiers in Pharmacology*, *13*. https://doi.org/10.3389/fphar.2022.750507

Weller, M., Cloughesy, T., Perry, J. R., & Wick, W. (2013). Standards of care for treatment of recurrent glioblastoma—are we there yet? *Neuro-Oncology*, *15*(1), 4-27. https://doi.org/10.1093/neuonc/nos273

Wright, M., Di Ciano, P., & Brands, B. (2020). Use of Cannabidiol for the Treatment of Anxiety: A Short Synthesis of Pre-Clinical and Clinical Evidence. *Cannabis Cannabinoid Res*, *5*(3), 191-196. https://doi.org/10.1089/can.2019.0052

Wu, X., Han, L., Zhang, X., Li, L., Jiang, C., Qiu, Y., Huang, R., Xie, B., Lin, Z., Ren, J., & Fu, J. (2012). Alteration of endocannabinoid system in human gliomas. *J Neurochem*, *120*(5), 842-849. https://doi.org/10.1111/j.1471-4159.2011.07625.x

Zhang, P., Xia, Q., Liu, L., Li, S., & Dong, L. (2020). Current Opinion on Molecular Characterization for GBM Classification in Guiding Clinical Diagnosis, Prognosis, and Therapy. *Frontiers in Molecular Biosciences*, *7*. https://doi.org/10.3389/fmolb.2020.562798

Zhu, W., Friedman, H., & Klein, T. W. (1998). Δ⁹-Tetrahydrocannabinol Induces Apoptosis in Macrophages and Lymphocytes: Involvement of Bcl-2 and Caspase-1¹. *The Journal of Pharmacology and Experimental Therapeutics*, *286*(2), 1103-1109. https://doi.org/10.1016/S0022-3565(24)37693-1

Zhu, Y., Pittella-Silva, F., Wang, Y., Wang, T., & Long, F. (2023). Editorial: Epigenetic regulation and therapy resistance in cancer. *Frontiers in Pharmacology*, *13*. https://doi.org/10.3389/fphar.2022.1119073